

FORMED PLATELET LINER
CONSTRUCTION FEASIBILITY

N93-16697

Unclas

G3/20 0136190

CONTRACT NAS 8-37456

PHASE A FINAL REPORT

September 1992

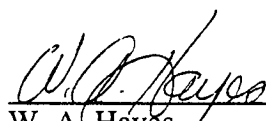
Prepared For:

National Aeronautics and Space Administration
George C. Marshall Space Flight Center
Marshall Space Flight Center, AL 35812

(NASA-CR-184506) FORMED PLATELET
COMBUSTOR LINER CONSTRUCTION
FEASIBILITY, PHASE A Final Report
(Aerojet-General Corp.) 169 p

Prepared By:

Approved By:


W. A. Hayes
Platelet Devices
Research and Engineering


W. M. Burkhardt
Program Manager

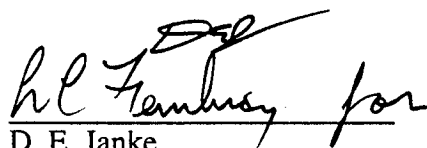

D. E. Janke
Platelet Devices
Research and Engineering

TABLE OF CONTENTS

	<u>Page</u>
1.0 Introduction	1
2.0 Summary and Conclusions	3
3.0 Benefits Analysis	5
4.0 Platelet Stack Forming	17
5.0 Platelet Stack Joining	84
6.0 Fabrication Process Definition	126
7.0 Silver Aided Bonding	130
Appendix A – Platelet Design and Fabrication Processes	A-1

PRECEDING PAGE BLANK NOT FILMED

LIST OF TABLES

<u>Table No.</u>		<u>Page</u>
3.1	SSME, STBE and STME Baseline Geometry and Operating Conditions	6
3.2	Cycle Life Benefits - SSME	10
3.3	Cycle Life Benefits - STBE	10
3.4	Cycle Life Benefits - STME	11
3.5	Cycle Life Benefits - SSME With Bi-Metallic Wall	11
3.6	Cycle Life Benefits - STBE With Bi-Metallic Wall	12
3.7	Cycle Life Benefits - STBE With Nickel Liner	12
4.1	Regeneratively Cooled Thrust Chamber Parameters	19
4.2	Formed Platelet Liner Forming	39
4.3	Section Testing Results - ZrCu Coarse Pattern	68
5.1	Identified Joining Issues	85
5.2	Joining Parameters Investigated Using Simple/Linear Samples	90
5.3	Flat Joining Sample Configurations	91
5.4	Critical Processes For Diffusion Bond Joining	100
7.1	Silver Aided Bond Experiment – Taguchi Array	132
7.2	Factor's and Levels For Taguchi Array	133
7.3	Sample Processing Matrix, Bonding Post-Bond	136
7.4	Sample Processing Matrix, Post-Bond Age	137
7.5	Tensile Test Results	138

LIST OF FIGURES

<u>Figure No.</u>		<u>Page</u>
3.1	Formed Platelet Liners Substantially Increase SSME Combustion Chamber Thermal Margins	8
3.2	Formed Platelet Liners Substantially Increase STME Combustion Chamber Thermal Margins	9
3.3	Formed Platelet Liners Have 25% Pressure Drop Savings Over Conventional Milled Slot Combustor Liner	13
4.1	Thrust Chamber Geometric Parameters	26
4.2	Geometric Throat Station Parameters of Milled Slot Thrust Chambers Superimposed on Formed Platelet Devices	27
4.3	40K Combustion Chamber Contour For Platelet Stack Forming	29
4.4	Single Step Forming Die	31
4.5	Two-Dimensional Forming Die	32
4.6	First Series Throat and Barrel Cross Sections of Panel Designs	34
4.7	First Series Coarse Pattern Platelet	35
4.8	Platelet Gas Side Wall 0.033 THK ZrCu	37
4.9	Two-Step Forming Process	42
4.10	OD Cracking Due to Use of Throat Springs, S/N 015	43
4.11	Removing Throat Springs From the Die Eliminated Cracking of Part SN 002	44
4.12	Tooling Modifications Were Necessary to Prevent Tearing of the Part	45
4.13	Parts Formed in 2 Steps Cracked the Close Out of the Part	46
4.14	Parts Formed in a Single Operation Remained Intact	47
4.15	Material Outside of 90° Chamber Section Was Removed to Study the Effect on Channel Deformation	49
4.16	Fine Pattern Artwork Was Modified For T/R Study	50
4.17	Second Series Panel Designs T/R Ratio Studies	51
4.18	Second Iteration Panel Design	53
4.19	Second Iteration Platelet Design	54
4.20	Second Iteration Channel Design	55
4.21	Flow Data Results ZrCu Coarse Pattern Panels	58
4.22	ZrCu Fine and Stepped Patterns and Flow Results	58
4.23	Cold Flow Results ZrCu Stepped Pattern	58
4.24	Cold Flow Results Cres 304L Coarse Pattern	59
4.25	Cold Flow Results Cres 304L Fine Pattern	59
4.26	Cold Flow Results Cres 304L Stepped Pattern	59

LIST OF FIGURES (CONT)

<u>Figure No.</u>		<u>Page</u>
4.27	Spring Back in the Throat Section Increases With Panel Thickness	60
4.28	Results of Contour Measurements, 1st and 2nd Panel Design	61
4.29	Die Gap Varies Along the Chamber Axis	63
4.30	Second Iteration Design Showed Improved Edge Location After Forming	64
4.31	Skew of the Channel Along the Chamber Axis Increases With Part Thickness	66
4.32	Section Testing Results	67
4.33	Panel Joining Demonstration Platelet Design	74
4.34	Seam Channel Land Location Results	75
4.35	Formed Platelet Edge Deviation 3D Joining Demo Panels	77
4.36	Restrain Anneal Fixture	79
4.37	Radial Contour Comparison	80
4.38	Axial Contour Comparison	81
5.1	Task 1.4 Phase A Test Logic For Joining	86
5.2	Panel Joining Samples - Flat Samples	88
5.3	Weld Joint Configurations	92
5.4	Channel Weld Results	94
5.5	Land Weld Results	95
5.6	Photomicrographs of HIP Processed Samples	97
5.7	Comparison of As-EDM's and Hand Polished Surfaces	98
5.8	Process Flow of Diffusion Bond Joining of Formed Platelet Panels	99
5.9	Two Interfaces in the Chemically Machined Sample Achieved 100% Bonding	103
5.10	Diffusion Bond Edge Joining Process	104
5.11	Comparison of Wire EDM Processes	106
5.12	Etch Parameter Optimization Provided Complete Recast Removal	107
5.13	Initial 2D Sample Configuration	109
5.14	EBW Bead Dimensions	111
5.15	Sample Configuration	111
5.16	Photomicrographs of 2D Bond Samples	112
5.17	Bond Sample Radiograph	113
5.18	2D HIP Bond Samples W/Leak Test Capability	115
5.19	2D HIP Bond Sample Sections	116
5.20	Laser Welding of 3D Demo Panels	118

LIST OF FIGURES (CONT)

<u>Figure No.</u>		<u>Page</u>
5.21	Joining Study - 3D Sample	119
5.22	Photomicrographs of 3D Demo SN 01 Joint, Forward End	121
5.23	3D Demo S/N 01 Assy - Throat Land Cross Section	122
5.24	Photomicrographs of Weld Sample of S/N 02 Closeout	124
6.1	Process Definition - 40K Liner 1/2	127
6.2	Process Definition - 40K Liner 2/2	128
6.3	Flowchart Legend	129
7.1	Bond Block Sample Identification	134
7.2	Comparison of Bond Aid Performance	139

1.0 INTRODUCTION

Environments generated in high pressure liquid rocket engines impose severe requirements on regeneratively cooled combustor liners. Liners fabricated for use in high chamber pressures using conventional processes suffer from limitations that can impair operational cycle life and can adversely affect wall compatibility.

Chamber liners fabricated using formed platelet technology provide an alternative to conventional regeneratively cooled liners; an alternative that has many attractive benefits. A formed platelet liner is made from a stacked assembly of platelets with channel features. The assembly is diffusion bonded into a flat panel and then three-dimensionally formed into a section of a chamber.

Platelet technology permits the liner to have very precisely controlled and thin hot gas walls and therefore increased heat transfer efficiency. Further cooling efficiencies can be obtained through enhanced design flexibility. These advantages translate into increased cycle life and enhanced wall compatibility. The increased heat transfer efficiency can alternately be used to increase engine performance or turbopump life as a result of pressure drop reductions within the regeneratively cooled liner. Other benefits can be obtained by varying the materials of construction within the platelet liner to enhance material compatibility with operating environment or with adjoining components.

Manufacturing cost savings are an additional benefit of a formed platelet liner. This is because of reduced touch labor and reduced schedule when compared to conventional methods of manufacture.

The formed platelet technology is not only compatible with current state-of-the art combustion chamber structural support and manifolding schemes, it is also an enabling technology that allows the use of other high performance and potentially low cost methods of construction for the entire combustion chamber assembly.

The contract under which this report is submitted contains three phases. These are: Phase A, feasibility study and technology development; Phase B, sub-scale fabrication feasibility; and Phase C, large scale fabrication validation. This report covers the Phase A activities, which began in December of 1988.

This contract activity was contracted by the NASA Marshall Space Flight Center under sponsorship of the NASA Office of Aeronautics and Space Technology Earth to Orbit Propulsion Technology Program.

The NASA/MSFC Program Manager for this program was Mr. Fred Braam. The Aerojet Propulsion Division Program Manager was Mr. Wendel M. Burkhardt. Mr. W. A. (Bill) Hayes was the Project Engineer and Mr. D. E. (Dave) Janke was the Lead Design Engineer. Significant contributions were made by Ms. Sarah Tobin, the original Project Engineer and Lead Designer; by Mr. Harry Mueggenburg, Platelet Design Section Manager; and by Mr. A. R. Scott, Development Operations Producibility. Other key people who contributed to the success of this program are too numerous to mention; their efforts are greatly appreciated.

2.0 SUMMARY AND CONCLUSIONS

The Phase A activities studied the feasibility of using platelet technology for the construction of regeneratively cooled combustion chamber liners. Results of the study show that such an approach is feasible and has many attractive benefits.

The study produced numerous technical achievements and technology demonstrations. Included in these were:

- 1) Development and demonstration of liner panel forming techniques that produce repeatable, consistent hardware. Also demonstrated were the functional characteristics of this hardware via destructive and non-destructive examinations.
- 2) Design techniques to allow the correlation of feature location in the formed vs. flat panel states.
- 3) Application and demonstration of an APD-developed channel filling polymer that allows forming of platelet panels with minimal internal passage deformation.
- 4) Analysis of the benefits obtainable through the application of formed platelet technology to regeneratively cooled combustor liners. These benefits include significant cycle life, wall compatibility, pressure drop, and manufacturing cost and schedule improvements over conventional technology.
- 5) Exploration of present, applicable platelet technology limits. Coolant channels with 15:1 aspect ratios and hot gas walls as thin as 0.008 inch were demonstrated.
- 6) Techniques for joining of formed platelet panels. A process in which the panel mating edges can be diffusion bonded together to form an essentially monolithic structure was demonstrated. This process, though successfully demonstrated, does require further development to make it a repeatable process.
- 7) A study of the use of silver as a diffusion bond aid to increase the thermal conductivity of ZrCu platelet structures. The study showed that, at its current level of development, the silver aided bond system is not a viable substitute for the standard bond system.
- 8) Development of a baseline plan for the fabrication of a 40K sized functional formed platelet liner.

At the successful completion of the Phase A study a recommendation was made, and accepted, to proceed into Phase B of the program. Phase B will demonstrate the developed technology through the design, fabrication, and hot fire testing of a 40K combustion chamber employing a formed platelet liner.

3.0 BENEFITS ANALYSIS

3.1 INTRODUCTION

An analysis of a Formed Platelet Combustor Liner compared to conventional milled-slot liners was made to identify potential performance and cost benefits.

3.2 OBJECTIVE

Thermal, structural and cost analysis were performed comparing the Formed Platelet Liner to the existing SSME Main Combustion Chamber (MCC), the proposed Space Transportation Booster Engine (STBE) chamber, and the Space Transportation Main Engine (STME) chamber. The specific objectives were to quantify the following items:

Performance benefits, including:

- Chamber cycle life improvements
- Potential chamber coolant pressure drop savings

Manufacturing benefits, including:

- Cost savings
- Schedule savings

3.3 APPROACH, PERFORMANCE BENEFITS

A thermal analysis was conducted first to establish a channel geometry for platelet liners for SSME, STBE and STME. Several different geometries were studied, including varying hot gas wall thickness, number of coolant channels and materials. The resultant temperature profiles were then used in a structural analysis to find strains and predict the number of cycles to failure. As the goal of this effort was to determine the relative reduction in wall temperature and resultant cycle life improvement for preliminary designs, the predictions should be viewed as a reference value only.

3.4 DISCUSSION, PERFORMANCE BENEFITS

The baseline SSME, STBE and STME chamber geometries and performance characteristics are listed in Table 3.1. The total coolant flow rate was held constant for the

studies; pressure drop was allowed to vary. Limits on channel geometry were made to simplify the analysis as follows:

Land width = Channel width

Channel aspect ratio (height/width) < 15

TABLE 3.1

SSME, STBE AND STME GEOMETRY BASELINE AND OPERATING CONDITIONS

<u>Existing Geometry (1989)</u>	<u>SSME</u>	<u>STBE</u>	<u>STME</u>
Number of Channels	390	406	451
Channel Width, Throat (in.)	.040	.060	.050
Channel Land; Throat (in.)	.013	.040	.040
Channel Depth, Throat (in.)	.113	.147	.187
Hot Gas Wall, Throat (in.)	.028	.032	.030
Liner Material	Narloy Z	ZrCu	ZrCu
<u>Operating Conditions (1989)</u>			
Chamber Pressure (psia)	3006	3150	2250
Recovery Temperture (°F)	5925	6167	4732
hg (Btu/(in. ² -sec-°F)	0.01668	0.01170	0.0178
Coolant Bulk Temperature (°F)	-254.3	-133.6	-261.7
Coolant Toal Pressure (psia)	5703	4241	2885
Total Coolant Flow Rate (lbm/sec)	26.1	347.5	64.70
Coolant	Hydrogen	Methane	Hydrogen
Maximum Wall Temperature (°F)	1200	1030	920
Maximum Delta Temperature (°F)	1436	1174	1176

Wall thicknesses evaluated vary from 0.0025 to 0.040 inch. Land/channel widths from 0.007 to 0.025 inch were evaluated. Configurations beyond the current capability of platelet technology were analyzed to establish performance trends.

The use of materials other than ZrCu for SSME and STBE liners was also investigated. Materials investigated include:

SSME MCC:

ZrCu

CRES

ZrCu with a thin (0.001 or 0.002) CRES barrier platelet

STBE Liner:

ZrCu

Nickel

ZrCu with CRES barrier platelet

A parametric thermal analyses evaluated different materials and channel geometries to obtain temperature predictions for the SSME MCC, STBE and STME chambers. Pressure drop savings were also predicted for the STBE chamber.

The thermal analysis used an APD-developed thermal channel code to predict maximum throat temperatures. The STBE and STME temperatures were based on predicted chamber boundary conditions as of early 1989. The thermal conductivity values of bonded ZrCu used were reduced approximately 11 to 20% to account for the presence of the diffusion bond aid. The nickel and CRES thermal conductivities used were that of wrought materials, as any bond aid used would be of a conductivity equal to or greater than the base material.

A structural analysis was conducted to determine cycle life. The approach was to conduct a Finite Element Method (FEM) plane strain analysis on a throat cross-section. Temperature profiles from the thermal analysis were used to determine strains at various points in the thermal cycle of a liner. Manson-Halford low cycle fatigue curves were used to obtain N_f , and the number of cycles to failure predicted by $N_f/10$.

A complete description of constraints, assumptions and analysis methodology can be found in references 1 and 2. The predicted thermal margins and life increase for both SSME and STME chambers are shown in Figures 3.1 and 3.2 for ZrCu platelets. Tables 3.2, 3.3 and 3.4 list the maximum wall temperature and resultant cycle life as a function of gas side wall thickness and number of coolant channels.

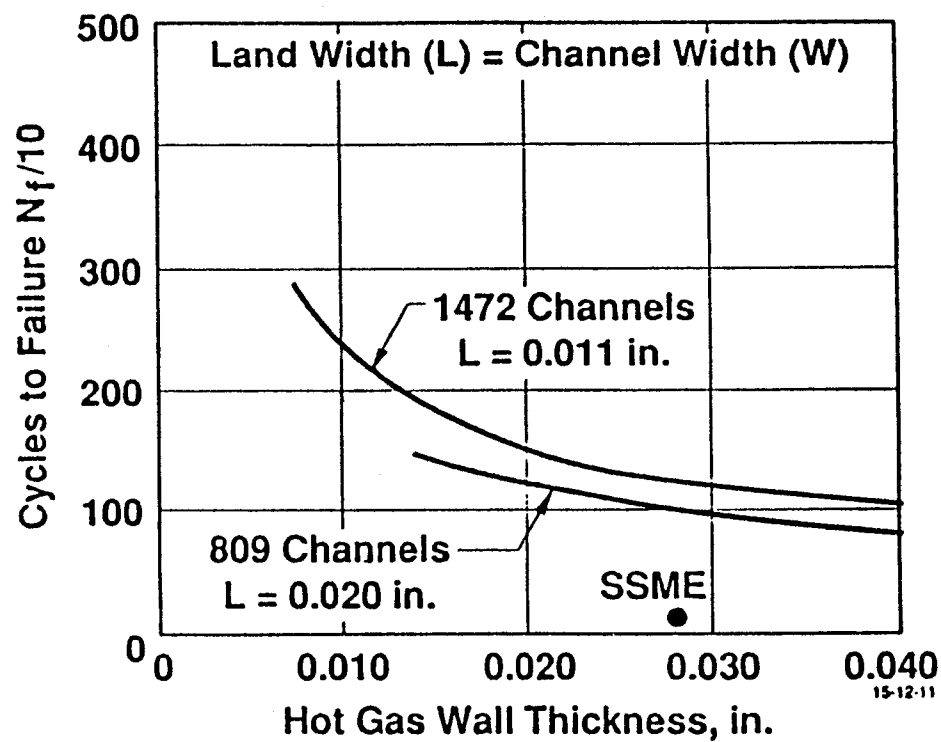
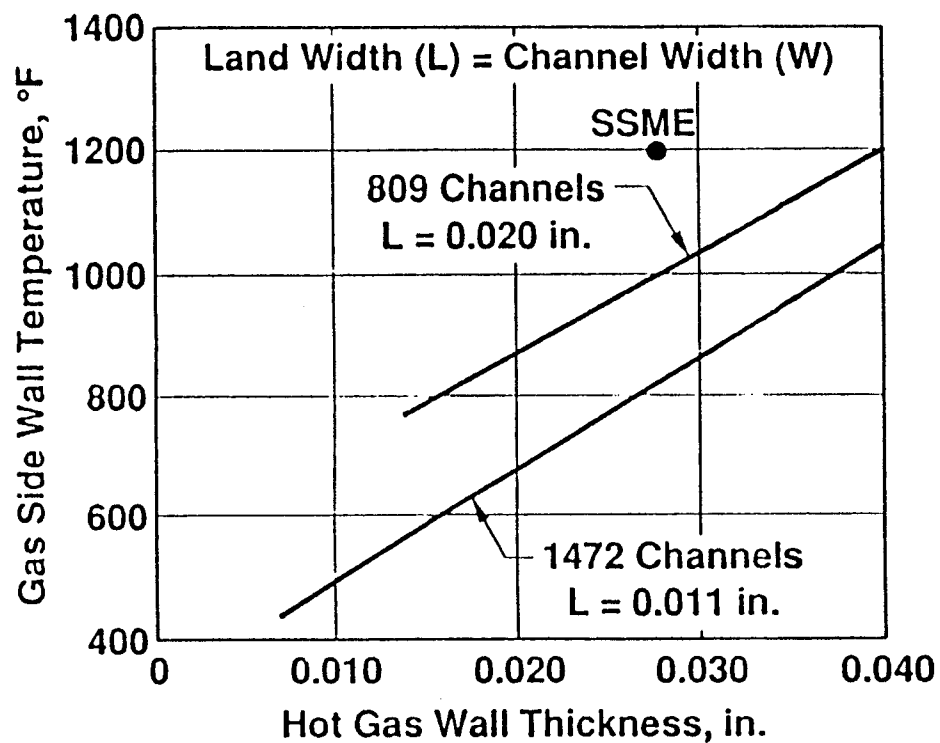
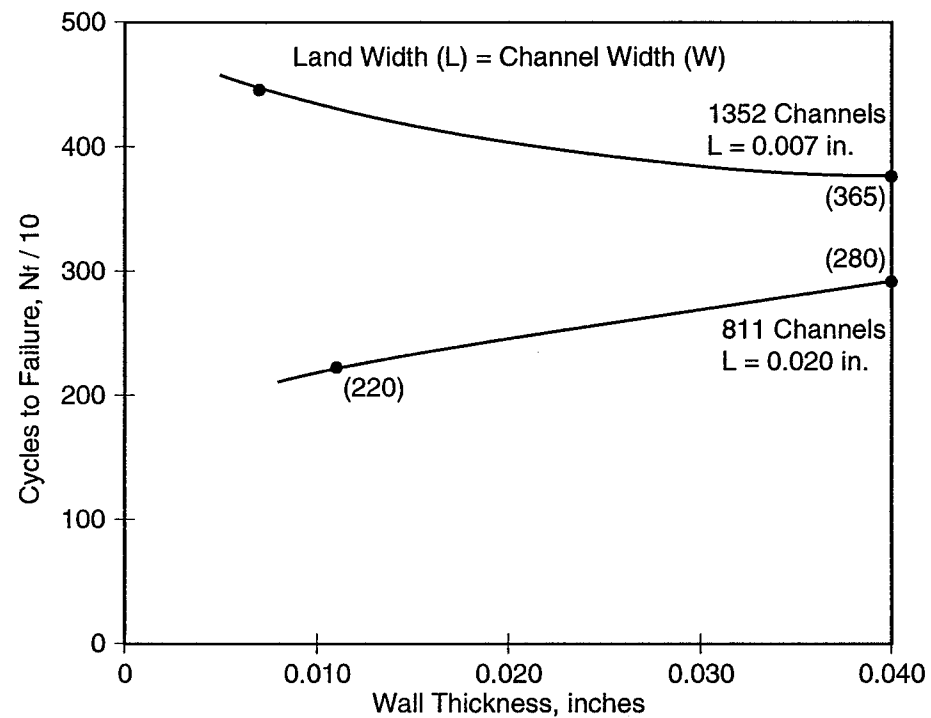
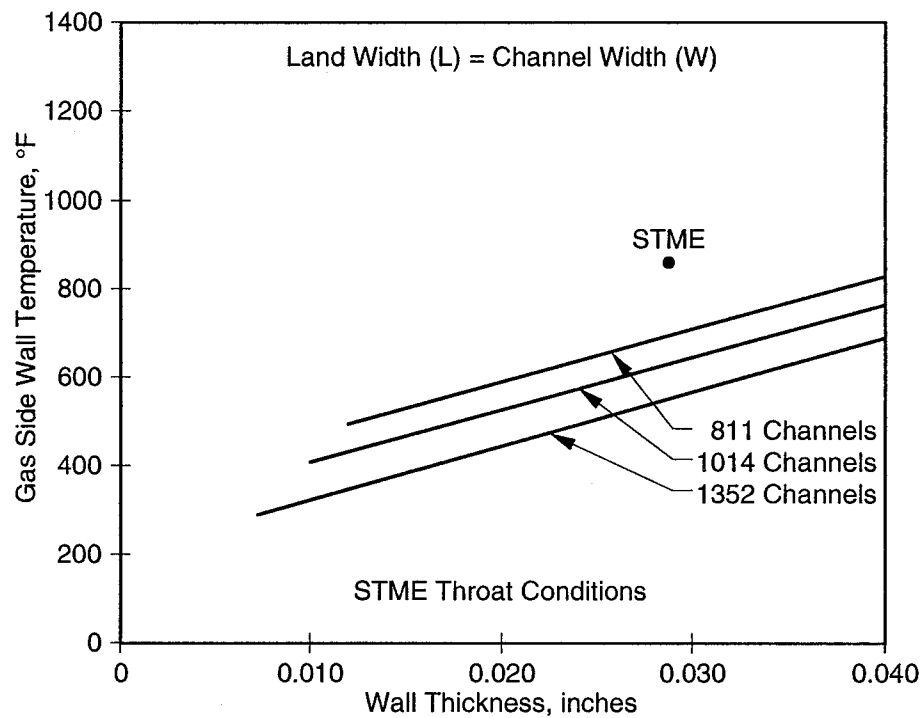


Figure 3.1 Formed Platelet Liners Substantially Increase SSME Combustion Chamber Thermal Margins



1.12.2.15

Figure 3.2. Formed Platelet Liners Substantially Increase STME Combination Chamber Thermal Margins

TABLE 3.2**CYCLE LIFE BENEFITS – SSME**

SSME Throat Conditions
ZrCu Platelets/STD Bond Aid

<u>Gas Side Wall Thickness, in.</u>	<u>No. Channels</u>	<u>T_{max}, °F</u>	<u>Delta T_{max}, °F</u>	<u>Maximum Strain in./in.</u>	<u>Cycles to Failure N_f/10</u>
*0.028	390	1183	1397	0.0285	14
0.020	809	871	1123	0.030	83
0.020	1470	689	942	0.0186	150
0.020	2229	583	827	0.0162	195
0.0135	809	754	1007	0.0200	145
0.0075	1470	441	693	0.0134	280
0.005	2229	265	477	0.0116	365

*SSME Baseline

TABLE 3.3**CYCLE LIFE BENEFITS – STBE**

STBE Throat Conditions
ZrCu Platelets/STD Bond Aid

<u>Gas Side Wall Thickness, in.</u>	<u>No. Channels</u>	<u>T_{max}, °F</u>	<u>Delta T_{max}, °F</u>	<u>Maximum Strain in./in.</u>	<u>Cycles to Failure N_f/10</u>
*0.032	406	1004	1155	0.0212	160
0.016	1122	639	772	0.0153	215
0.016	1683	534	664	0.013	300
0.0145	808	709	842	0.0167	200
0.0105	1122	555	688	0.0136	270
0.0064	1683	380	507	0.0097	500

*STBE Baseline

TABLE 3.4**CYCLE LIFE BENEFITS – STME**

STME Throat Conditions
ZrCu Platelets/STD Bond Aid

<u>Gas Side Wall Thickness, in.</u>	<u>No. Channels</u>	<u>T_{max} °F</u>	<u>Delta T_{max}, °F</u>	<u>Maximum Strain in./in.</u>	<u>Cycles to Failure N_f/10</u>
0.012	811	499	750	0.150	220
0.040	811	796	1050	0.0140	280
0.0072	1352	280	540	0.0106	440
0.040	1352	668	930	0.0122	365

Thermal analysis of the alternate materials show reasonable wall temperatures, as summarized in Tables 3.5, 3.6 and 3.7. The alternate materials could provide better propellant compatibility than ZrCu. However, as a structural analysis was performed on the ZrCu configurations only, it is not known how the cycle life of the other materials would compare.

TABLE 3.5**CYCLE LIFE BENEFITS – SSME WITH BIMETALLIC WALL**

SSME Throat Conditions
ZrCu/CRES 347 Gas Side Wall

<u>Gas Side Wall Thickness</u>	<u>No. Channels</u>	<u>T_{max}, °F</u>	<u>Delta T_{max}, °F</u>	<u>Maximum Strain in./in.</u>	<u>Cycles to Failure N_f/10</u>
0.020/0.002	2229	1127	1381	0.0286	32
0.020/0.001	2229	869	1118	0.0224	62
0.010/0.002	1470	1052	1306	0.0267	36
0.010/0.001	1470	788	1042	0.0206	73
0.010/0.001	2229	686	931	0.0182	94
0.005/0.002	2229	872	1125	0.0197	76

TABLE 3.6**CYCLE LIFE BENEFITS – STBE WITH BIMETALLIC WALL**

STBE Throat Conditions
ZrCu Platelets/STD Bond Aid

<u>Gas Side Wall Thickness, in.</u>	<u>No. Channels</u>	<u>T_{max}, °F</u>	<u>Delta T_{max}, °F</u>	<u>Maximum Strain in./in.</u>	<u>Cycles to Failure N_f/10</u>
0.020/0.002	1683	1016	1150	0.0234	56
0.020/0.001	1683	813	944	0.0188	84
0.010/0.002	1122	973	1107	0.0224	60
0.010/0.001	1122	768	901	0.0177	94
0.010/0.001	1683	671	800	0.0156	125
0.005/0.002	1683	811	944	0.0189	83
0.005/0.001	1683	592	719	0.0139	160

TABLE 3.7**CYCLE LIFE BENEFITS – STBE WITH NICKEL LINER**

STBE Throat Conditions
Ni 200 Platelets

<u>Gas Side Wall Thickness, in.</u>	<u>No. Channels</u>	<u>T_{max}, °F</u>	<u>Delta T_{max}, °F</u>	<u>Maximum Strain in./in.</u>	<u>Cycles to Failure N_f/10</u>
0.016	1683	1436	1567	0.028	11
0.008	1683	988	1118	0.0168	150
0.0055	1683	820	949	0.0158	250

Analyses were conducted to investigate possible savings in coolant pressure drop for formed platelet liners. The pressure drop for various coolant channel designs was calculated using the May 1989 STME chamber contour and operating conditions. ZrCu platelets and H₂ coolant were used for analysis. Figure 3.3 compares the pressure drop for platelet liners to the conventionally slotted liners, assuming a constant 0.030 width channel (baseline STME design) and maximum temperature of 1000°F, 100°F below the STME baseline design. Using variable width channels results in a pressure drop savings of up to 47% of the STME baseline value. A constant width design was chosen for the baseline STME chamber design to simplify the

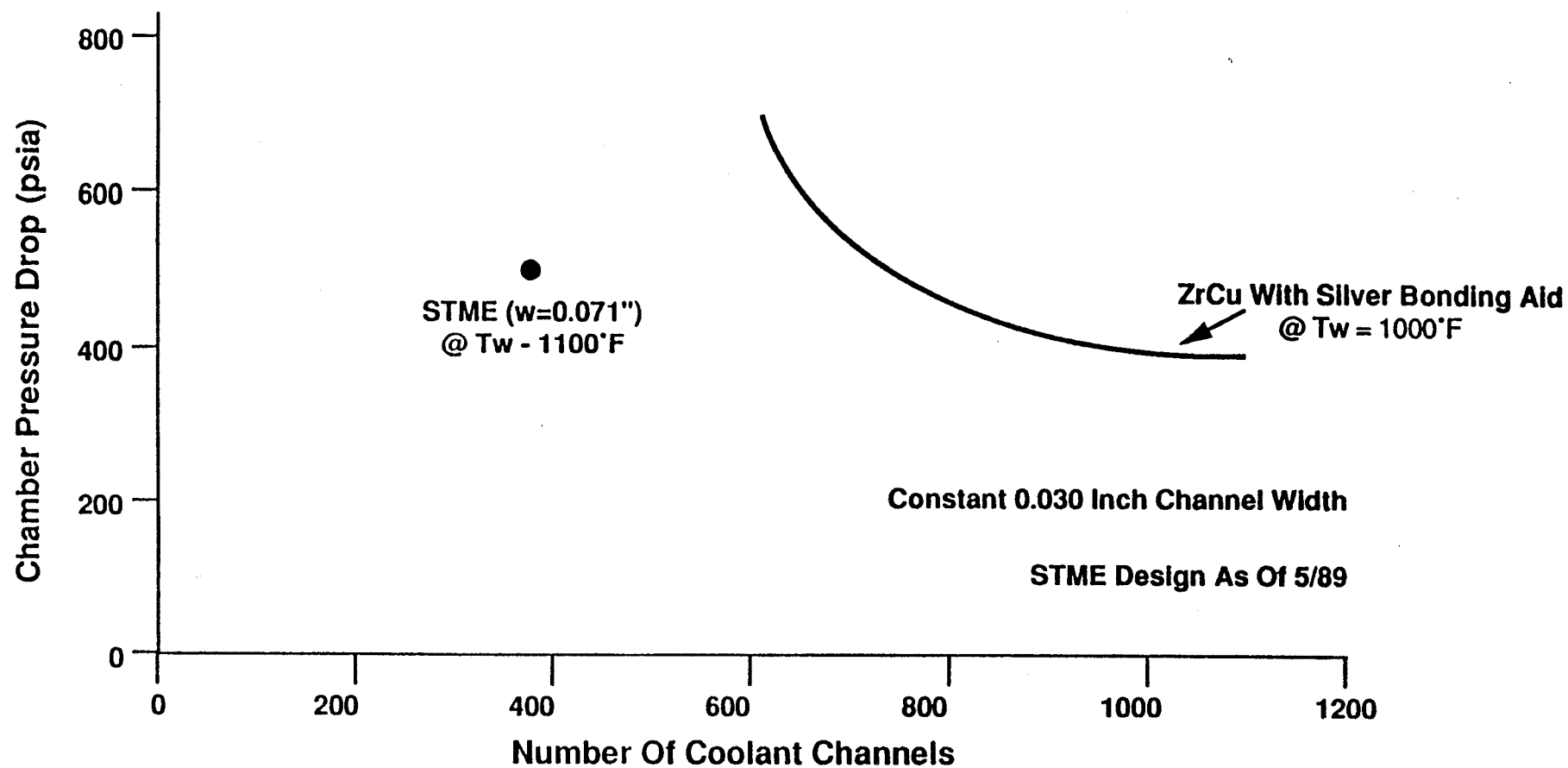


Figure 3.3. Formed Platelet Liners Have 25% Pressure Drop Savings Over Conventional Milled Slot Combustor Liner

conventional liner fabrication. The use of variable width channel design when fabricated with a formed platelet liner does not present any increase in fabrication cost.

3.5 APPROACH, MANUFACTURING BENEFITS

The manufacturing benefits analysis compared the cost and schedule of producing a SSME combustor liner using formed platelet technology to the current manufacturing approach. The cost of the support structure and manifolding are assumed identical for the two fabrication approaches. Additional assumptions were made for analysis of the formed platelet liner:

- A free-standing liner is constructed from four platelet panels.
- 25% manufacturing attrition of individual platelets.
- 25% manufacturing attrition of platelet panels.
- A single step forming process would be used.
- Platelet etching and plating facilities exist, thus requiring no additional capital.

Data and experience from similar Aerojet programs was used wherever applicable to estimate costs and schedule. The cost per liner is based on manufacture of 22 units.

3.6 DISCUSSION, MANUFACTURING BENEFITS

The manufacturing costs were established from an estimate of touch labor hours for recurring and non-recurring costs. Cost factors were applied to these hours to account for supervision, inspection and quality engineering. These cost factors, which are based upon Aerojet's SSME Low Cost Study (NAS8-37503), are listed below:

- Supervision = $1.65 * \text{Touch labor hours} * \$75/\text{hr}$
- Inspection = $0.40 * \text{Touch labor hours} * \$75/\text{hr}$
- Quality engineering = $1.41 * \text{Inspection} * \$75/\text{hr}$

Material costs were then established, and total recurring and non-recurring costs calculated. A summary of costs is as follows:

Non-recurring costs:

- | | |
|----------------------------------|---------|
| • Platelet artwork | 100 hrs |
| • Forming tooling (design & fab) | 760 hrs |
| • Machining & welding fixtures | 720 hrs |
| • Material costs | \$10 K |

Recurring costs, First unit:

Etch, stack & bond platelets	275 hrs
Forming	50 hrs
Machining & welding	210 hrs
Platelet Material	\$2 K

Using the cost factors, the above costs are then broken into a first unit cost, and a cost per unit, assuming 22 units and a 95% learning curve:

First unit cost:

Non-recurring cost	\$539 K	
Recurring cost	<u>\$181 K</u>	
Total		\$720 K

For 22 units, cost per unit:

Non-recurring cost	\$ 25 K	
Recurring cost	<u>\$128 K</u>	
Total		\$153 K

The present cost of an SSME MCC liner, based upon Low cost SSME studies and Rocketdyne data, is approximately 18% of the \$4.3 M cost per MCC, or \$770 K. The cost of a formed platelet liner is then 20% of the cost of a conventionally machined liner.

Fabrication time for the machining, slotting and close-out of a SSME MCC liner, from fabrication schedules provided by NASA/MSFC, is approximately 19 months. Estimates for the fabrication of a formed platelet liner are as follows:

Platelet etching, stacking & bonding	1.5 months
Platelet stack forming	1.0 months
Machining of formed panels	1.0 months
Welding of panels and HIP bonding	<u>1.0 months</u>
Total fabrication time	4.5 months

3.7 CONCLUSIONS

Combustor chambers made with conventional technologies operate with relatively thick side walls resulting in high hot gas wall temperatures and limited cycle life. Design improvements are difficult to make to conventionally machined channel geometry because of tolerance control.

Substantial decreases in wall temperatures, as much as 400°F for the SSME MCC, can be realized with an increased number of channels and thinner hot gas walls, which can be fabricated using current platelet technology. Decreased wall temperatures result in order-of-magnitude life cycle improvements. Using platelets, channel geometries can be tailored to achieve 25% (STME) pressure drop savings, while still maintaining lower wall temperatures than conventional technologies.

The cost of a formed platelet liner for the SSME is estimated to be 20% of the cost of a conventionally machined liner. Fabrication time of a liner is reduced by two-thirds, from more than 1.5 years to less than 5 months.

4.0 PLATELET STACK FORMING

4.1 INTRODUCTION

The platelet panel forming related tasks are described in this section. These tasks are as follows:

- 1.1 Combustor Liner Sizing
- 1.3 Platelet Stack Forming Experiments
- 1.7 Panel Joining Demonstration, panel forming tasks only
- 1.9 Contour Forming Experiments.

Task numbers refer to contract WBS activities. The various tasks described involve all aspects of the panel forming accomplished in Phase I, including the panel and die designs and fabrication, panel forming and subsequent panel testing.

4.2 OBJECTIVE

The primary objective of the Platelet Stack Forming task was to establish a basic forming process for platelet panels intended for cooled combustion chamber liners. This included investigating various die configurations and panel designs in order to define the behavior of complex panel forming. An additional goal was to develop a geometry prediction technique to allow panel designs to compensate for the effect of forming on the channel placement.

4.3 APPROACH

A three-step approach was taken to characterize platelet panel forming. The first step, Task 1.1, was to evaluate combustor liner geometries from existing rocket engines and select the contour to use for experimentation. Forming experiments were then performed in Tasks 1.3 and 1.9 to determine the method for forming and the tooling features required in panel and die designs. The forming effects that different panel configurations have on the internal panel geometry was also characterized in the second step. The third step, Task 1.7, was to demonstrate the feasibility of fabricating a free-standing liner by joining two panel segments.

The result of the platelet stack forming tasks was a basic characterization of how different panel and die designs affect the forming of platelet combustor liners.

4.4 TASK 1.1 COMBUSTOR LINER SIZING ANALYSIS

The first task was to determine the range of geometric forming parameters to investigate. Parameters critical to forming were determined, and tabulated in Table 4.1 for 24 existing rocket engines combustor liners. Figure 4.1 illustrates the geometric parameters tabulated in Table 4.1. The engines evaluated in the study included staged combustion, gas generator and expander cycles. The engines varied in chamber pressure from 300 to 5000 psia, and varied in thrust from about 3000 lbs to 1,500,000 lbs. Of greatest interest were the 11 rocket engines with milled slot coolant channels. The pertinent design data from these engines include chamber contours, wall thicknesses, and channel geometries. The remaining engines use tubes for the coolant channels. Only the chamber contour data from these engines were used. The table is not complete for every engine. This is due to the difficulty in obtaining some of the data for the older rocket engine designs.

Aerojet analytical studies performed on platelet stack designs have confirmed that an important variable in the forming process is the ratio of the thickness (t) of the platelet stack to the smallest bend radius (R), or t/R , of the finished part. The data from Table 4.1 shows that the smallest bend radius is usually just aft of the throat leading into the nozzle. As the t/R ratio becomes larger, the forming process increases in difficulty.

The smallest bend radius data from Table 4.1 for engines using slotted cooling channels is plotted in Figure 4.2 along with previous Aerojet forming experience. The ease of forming a part increases when moving toward the upper left hand corner of the graph. The range of bend radii and t/R ratios encountered in milled slot chamber engines vary as follows:

<u>Variable</u>	<u>Lower Bound</u>	<u>Upper Bound</u>
Minimum Radius, in.	0.65	5.0
t/R	0.05	6.25

Other variables affecting forming include the coolant channel design, hot gas wall thicknesses, and material of construction. The tooling design and any filler materials used in the channels also affect formability. The most important forming issues are as follows:

TABLE 4.1

REGENERATIVELY COOLED THRUST CHAMBER PARAMETERS, SHEET 1 OF 7

		F-1 (Rocketdyne)	M-1	ATC Proposed STBE	SSME (Rocketdyne)
Pc N/M ² (psia)		7.58 x 10 ⁶ (1100)	6.89 x 10 ⁶ (1000)	21.7x 10 ⁶ (3150)	20.7 x 10 ⁶ (300)
Thrust N (lbf)		6.67 x 10 ⁶ (1,500,000)	6.67 x 10 ⁶ (1,500,000)	3.34 x 10 ⁶ (750,000)	2.22 x 10 ⁶ (500,000)
Propellants Oxidizer Fuel		LOX/RP-1	LOX/H ₂	LOX/CH ₄	LOX/H ₂
Coolant		RP-1	H ₂	H ₂ or CH ₄	H ₂
Chamber Liner Mat'l		Inconel X	CRES 347		NARLOY-Z
Type Chamber		Brazed Tube	Brazed Tube	Milled Slot	Milled Slot
L'	cm (in)		74.93 (29.5)	38.1 (15.00)	35.56 (14.00)
C _R		1.306	1.74	2.8	2.966
D _{Chamber}	cm (in)	101.6 (40)	107.2 (42.2)	53.34 (21.0)	45.06 (17.74)
R _l	cm (in)			15.875 (6.25)	22.53 (8.87)
θ ₁		13°	10° 56'	30°	25° 25'
R _u	cm (in)			15.875 (6.25)	13.09 (5.153)
D _{Throat}	cm (in)	88.9 (35)	81.23 (31.982)	31.75 (12.5)	26.18 (10.306)
θ ₂			8° 4'	33°	25° 25'
Max. Regen Cooled Expansion Area Ratio		10:1	14:1		5:1
Gas Side Wall Thickness	Barrel cm (in)			.089 (.035)	.089 (.035)
	Throat			0.71 (.028)	.071 (.028)
	Nozzle			1 (.063)	.089 (.035)
Channel W x D	Barrel	178 @ 1 3/32 OD		.1 x .381 (.040 x .150)	.157 x .419 (.062 x .165)
	Throat			.1 x .353 (.040 x .139)	.1 x .335 (.040 x .132)
	Nozzle	3:1 10:1 356 1" OD		.1 x .762 (.040 x .300)	.15 x .483 (.062 x .190)
Land	B			.239 (.094)	.204 (.0802)
	T			.10 (.040)	.109 (.0430)
	N			.251 (.099)	
No Channels		178 to 3:1	300 Tubes	492	390
Formed Platelet Liner	t			.978 (.385)	.635 (.250)
	t/R _{Throat}			.0616	.0485
	Barrel				2.66
	Throat				3.3
	Nozzle				3.06

TABLE 4.1

REGENERATIVELY COOLED THRUST CHAMBER PARAMETERS, SHEET 2 OF 7

		RS27-01A (Rocketdyne)	H - 1 (Rocketdyne)	THOR MB -1 (Rocketdyne)
Pc N/M (psia)		4.8×10^6 (700)	4.8×10^6 (700)	4.1×10^6 (600)
Thrust N (lbf)		9.96×10^5 (224,000)	9.11×10^5 (205,000)	7.56×10^5 (170,000)
Propellants Oxidizer/Fuel		LOX/RP-1	LOX/RP-1	LOX/RP-1
Coolant		RP-1	RP-1	RP-1
Chamber Mat'l				Type "A" Ni
Type Chamber		Brazed Tube	Brazed Tube	
L'	cm (in)		79.12 (31.15)	71.5 (28.15)
CR				
DChamber	cm (in)	52.22 (20.56)	52.22 (20.56)	53.07 (20.9)
R _l	cm (in)			
θ_1				10°
R _u	cm (in)			
DThroat	cm (in)	40.97 (16.13)	41.15 (16.2)	41.15 (16.2)
θ_2		9.75°		
Max. Regen Cooled Expansion Area Ratio				
Gas Side Wall Thickness	Barrel cm (in)			
	Throat			
	Nozzle			.102 (.040)
Channel W x D	Barrel			
	Throat			
	Nozzle			
Land	B			
	T			
	N			
No Channels		292	292	
Formed Platelet Liner	t			
	t/R Throat			
	Channel Aspect Ratio			
	Barrel			
	Throat			
	Nozzle			

TABLE 4.1

REGENERATIVELY COOLED THRUST CHAMBER PARAMETERS, SHEET 3 OF 7

		ATLAS MA -5 (Rocketdyne)	LE - 7 (MHI)	Titan II	J - 2 (Rocketdyne)
Pc N/M (psia)		3.6×10^6 (550)	14.7×10^6 (2130)	5.4×10^6 (785)	5.4×10^6 (780)
Thrust N (lbf)		1.33×10^6 (300,000)	1.07×10^6 (240,000)	1.05×10^6 (235,000)	1.02×10^6 (230,000)
Propellants Oxidizer/Fuel		LOX/RP-1	LOX/H ₂	N ₂ O ₄ /AEROZINE 50	LOX/LH ₂
Coolant		RP-1	H ₂	AEROZINE 50	H ₂
Chamber Mat'l		Type "A" Ni	Cu Alloy	Nicro Braze/347SS	CRES 347
Type Chamber		Brazed Tube	Milled Slot	Brazed Tube	Brazed Tube
L'	cm (in)			51.3 (20.2)	46.94 (18.48)
C _R				2.57	1.72
D _{Chamber}	cm (in)	53.2 (20.95)	9.1 (3.58)	55.32 (21.78)	46.99 (18.5)
R _I	cm (in)				22.35 (8.80)
θ ₁				25°	13.7°
R _u	cm (in)		3.45 (1.36)		28.02 (11.03)
D _{Throat}	cm (in)	41.15 (16.2)		38.74 (15.25)	37.34 (14.7)
θ ₂				23°	4.2°
Max. Regen Cooled Expansion Area Ratio				6:1	
Gas Side Wall Thickness	Barrel cm (in)				
	Throat				
	Nozzle				
Channel W x D	Barrel				
	Throat				
	Nozzle				
Land	B				
	T				
	N				
No Channels			288	Barrel 160 THT/Nozzle 320	Barrel 360 540 Braze
Formed Platelet Liner	P/W				
	t				
	t/R Throat				
	Channel Aspect Ratio				
	Barrel				
	Throat				
	Nozzle				

TABLE 4.1

REGENERATIVELY COOLED THRUST CHAMBER PARAMETERS, SHEET 4 OF 7

		Titan I	LR - 105	MSFC 40K (Rocketdyne)	Aerojet Proposed 40K
Pc N/M (psia)		4.0×10^6 (585)	4.8×10^6 (700)	20.7×10^6 (3000)	20.7×10^6 (3000)
Thrust N (lbf)		6.67×10^5 (150,000)	3.56×10^5 (80,000)	1.78×10^5 (40,000)	1.78×10^5 (40,000)
Propellants Oxidizer/Fuel		LOX/RP-1	LOX/RP-1	LOX/H ₂	LOX/LH ₂
Coolant		RP-1	RP-1	H ₂	H ₂
Chamber Mat'l		CRES 347	CRES 347	NARLOY-Z	ZR-Cu
Type Chamber		Brazed Tube	Brazed Tube	Milled Slot	Formed Platelet
L'	cm (in)			35.56 (14.00)	
C _R		2.0	1.77	2.924	2.924
D _{Chamber}	cm (in)	55.3 (21.78)	31.12 (12.25)	14.38 (5.660)	14.38 (5.660)
R ₁	cm (in)			7.13 (2.808)	4.20 (1.655)
θ ₁		15°		25° 25'	30°
R _u	cm (in)			13.09 (5.153)	4.20 (1.655)
D _{Throat}	cm (in)	38.74 (15.25)	23.42 (9.22)	8.41 (3.31)	8.42 (3.31)
θ ₂		17.5°		25° 25'	30°
Max. Regen Cooled Expansion Area Ratio					5:1
Gas Side Wall Thickness	Barrel cm (in)			.089 (.035)	
	Throat			.071 (.028)	
	Nozzle			.089 (.035)	
Channel W x D	Barrel			.157 x .419 (.062 x .165)	
	Throat			.102 x .335 (.040 x .132)	
	Nozzle			.157 x .483 (.062 x .190)	
Land	B			.1996 (.0786)	
	T			.1082 (.0426)	
	N				
No Channels		250		128	
Formed Platelet Liner	t			.635 (.250)	.635 (.250)
	t/R Throat			.151	.151
	Channel Aspect Ratio				
	Barrel			2.66	
	Throat			3.3	
	Nozzle			3.06	

TABLE 4.1

REGENERATIVELY COOLED THRUST CHAMBER PARAMETERS, SHEET 5 OF 7

		BO 320 (MBB-Rocketdyne)	AGENA (Bell)	RL - 10 (Pratt-Whitney)
Pc N/M (psia)		20.7×10^6 (3000)	3.4×10^6 (500)	2.1×10^6 (300)
Thrust N (lbf)		1.33×10^5 (30,000)	7.12×10^4 (16,000)	6.67×10^4 (15,000)
Propellants Oxidizer/Fuel		LOX/LH ₂	IRFNA/UDMH	LOX/LH ₂
Coolant		H ₂	IRFNA	H ₂
Chamber Mat'l		OFHC	Aluminum	CRES 347
Type Chamber		Milled Slot	Drilled	Brazed Tube
L'	cm (in)		59.72 (23.54)	50.8 (20)
CR		6.95	5.34	2.95
D _{Chamber}	cm (in)	18.2 (7.17)	27.41 (10.79)	26.06 (10.26)
R _l	cm (in)			11.68 (4.6)
θ_1		45°		11°
R _u	cm (in)			13.46 (5.3)
D _{Throat}	cm (in)	6.9 (2.72)	11.86 (4.67)	15.18 (5.975)
θ_2		15°	25.7°	32.05°
Max. Regen Cooled Expansion Area Ratio			13:1	
Gas Side Wall Thickness	Barrel cm (in)	.25 (.098)		
	Throat	.1 (.0394)		
	Nozzle	.3 (.118)		
Channel W x D	Barrel	.370 x .36 (.146 x .142)		
	Throat	.12 x .21 (.047 x .083)		
	Nozzle	.38 x .35 (.150 x .138)		
Land	B			
	T	.128 (.0504)		
	N			
No Channels		90		360
Formed Platelet Liner	t	.699 .275		
	t/R Throat	.202		
	Channel Aspect Ratio			
	Barrel	.97		
	Throat	1.77		
	Nozzle	.92		

TABLE 4.1

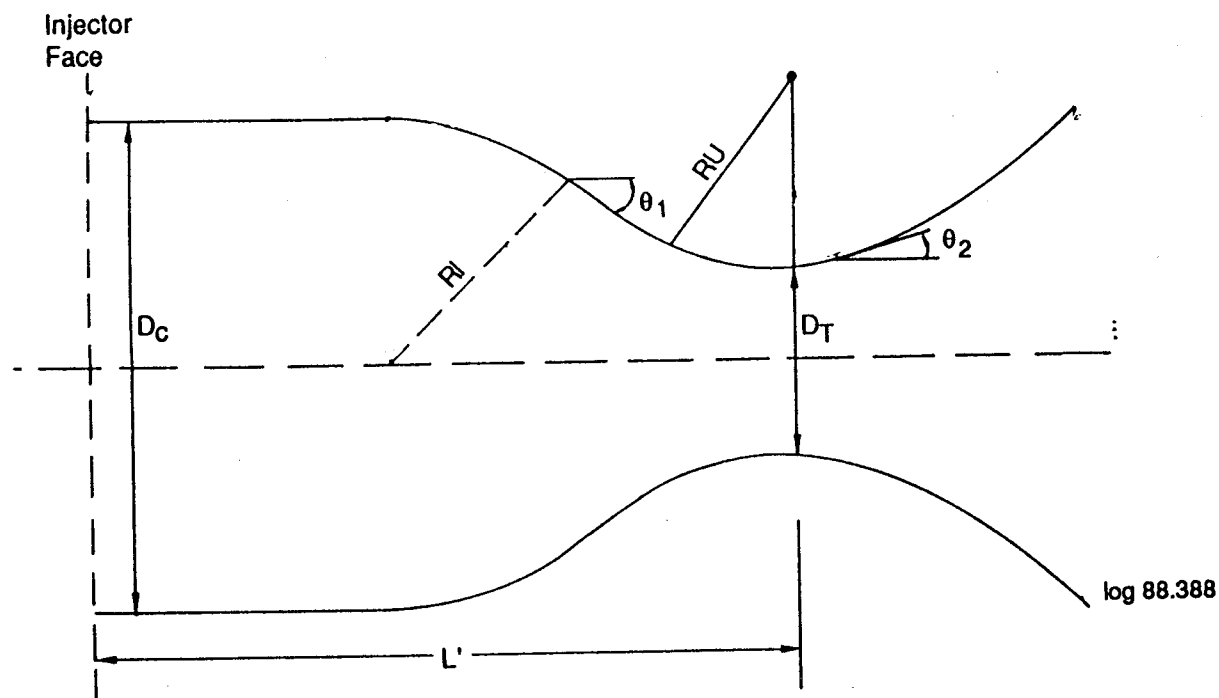
REGENERATIVELY COOLED THRUST CHAMBER PARAMETERS, SHEET 6 OF 7

	PC N/M (psia)	Thrust N (lbf)	Propellants Oxidizer/Fuel	Coolant	Chamber Mat'l	Type Chamber	L* cm (in)	CR	D Chamber cm (in)	R1 cm (in)	θ1 °	Ru cm (in)	D Throat cm (in)	θ2 °	Max. Regen Cooled Expansion Area Ratio	Gas Side Wall Thickness			Channel W x D			Land			No Channels			Formed Platelet Liner P/W									
																Barrel cm (in)	Throat	Nozzle	Barrel	Throat	Nozzle	B	T	N	233	104	t					t/R Throat	Channel Aspect Ratio	Barrel	Throat	Nozzle	
OTV	13.8 x 10 ⁶ (2000)	1.33 x 10 ⁴ (7500)	LOX/H ₂	H ₂	NASA-Z	Milled Slot	26.67 (10.5)	24.9	19.41 (7.64)	8.54 (3.364)	37°	3.81 (1.5)	3.86 (1.52)	35°			.152 (.06)	.051 (.02)	.152 (.06)	.234 x .119 (.092 x .047)	.165 x .267 (.065 x .105)	.0254 x .211 (.01 x .083)	.152 x .119 (.060 x .047)	.254 x .119 (.100 x .047)	.203 (.080)	.102 (.04)	.028 (.011)	.142 (.056)	233	104	.965 (.38)	.424 (.167)	.5	1.615	8.3	10	
	2.4 x 10 ⁶ (350)	2.67 x 10 ⁴ (6,000)	N2O4/MMH	MMH	NI 200	Milled Slot	35.56 (14 in)	2.7	14.01 (5.516)	8.54 (3.364)	30°	4.27 (1.682)	8.54 (3.364)	33°			.152 (.060)	.254 (.06/.10)	.254 (.06/.10)	.363 x .107 (.143 x .042)	.279 x .216 (.110 x .085)	.279 x .216 (.110 x .085)	.203 (.080)	.114 (.045)	.203 (.080)	.028 (.011)	.142 (.056)	233	104	.965 (.38)	.424 (.167)	.1	1.615	.783	.47		
	8.6 x 10 ⁶ (125)	2.67 x 10 ⁴ (6,000)	N2O4/MMH	MMH	CRES 304L	Milled Slot	40.39 (15.9)	1.95	20.6 (8.11)	7.38 (2.905)	30°	2.38 (2.905)	14.76 (5.81)	15°			.097 (.038)	.084 (.033)	.089 (.035)	.363 x .107 (.143 x .042)	.279 x .216 (.110 x .085)	.279 x .216 (.110 x .085)	.203 (.080)	.114 (.045)	.203 (.080)	.028 (.011)	.142 (.056)	233	120	.965 (.38)	.424 (.167)	.048	1.615	.293	.904		
Upated OME																																					
OMS																																					

TABLE 4.1

REGENERATIVELY COOLED THRUST CHAMBER PARAMETERS, SHEET 7 OF 7

Pc N/M (psia)	10.3 x 10 ⁶ (1500)	2.4 x 10 ⁶ (350)	13.8 x 10 ⁶ (2000)
	Thrust N (lbf)	1.67 x 10 ⁴ (3750)	1.67 x 10 ⁴ (3750)
	Propellants Oxidizer/Fuel	N2O4/MMH	N2O4/MMH
	Coolant	N2O4	MMH
Chamber Mat'l	Pt Liner/NI Channel	CRES 304L	NASA-Z
Type Chamber	Milled Slot	Milled Slot	Milled Slot
L	cm (in)	10.16 (4.0)	20.32 (8.0)
C R		2.38	4.23
D Chamber	cm (in)	5.00 (1.97)	13.97 (5.5)
R _l	cm (in)	2.97 (1.17)	6.79 (2.675)
θ ₁		26° 45'	30°
R _u	cm (in)	1.66 (.652)	3.40 (1.337)
D Throat	cm (in)	3.24 (1.276)	6.79 (2.674)
θ 2			15°
Max. Regen Cooled Expansion Area Ratio			
Gas Side Wall Thickness	Barrel cm (in)	.111 (.0437)	.127 (.050)
Throat	Throat	.084 (.0329)	.058 (.023)
	Nozzle	.127/.47 (.05/.185)	.094/.203 (.037/.080)
	Barrel	.096 x .114 (.038 x .045)	.198 x .251 (.078 x .099)
Channel W x D	Barrel	.064 x .090 (.025 x .0355)	.102 x .084 (.040 x .033)
	Throat	.064 x .254 (.025 x .100)	.218 x .254 (.086 x .100)
	Nozzle	.141 9.0557	.178 (.070)
Land	B		
	T	.093 (.0367)	.107 (.042)
	N		.178 (.070)
No Channels			
P/W	1	.775 (.305)	.508 (.20)
	t/R Throat	.478	.15
	Channel Aspect Ratio		
	Barrel	1.184	1.27
Formed Platelet Liner	Throat	1.42	.825
	Nozzle	4	1.16
XLR - 132	Transstar I	OTV	



D_C = Chamber

D_T = Throat Diameter

RI = Throat Inlet Radius

RU = Upstream Throat Radius

L' = Chamber Length

θ_1 = Convergent Angle

θ_2 = Divergent Angle

Figure 4.1. Thrust Chamber Geometric Parameters

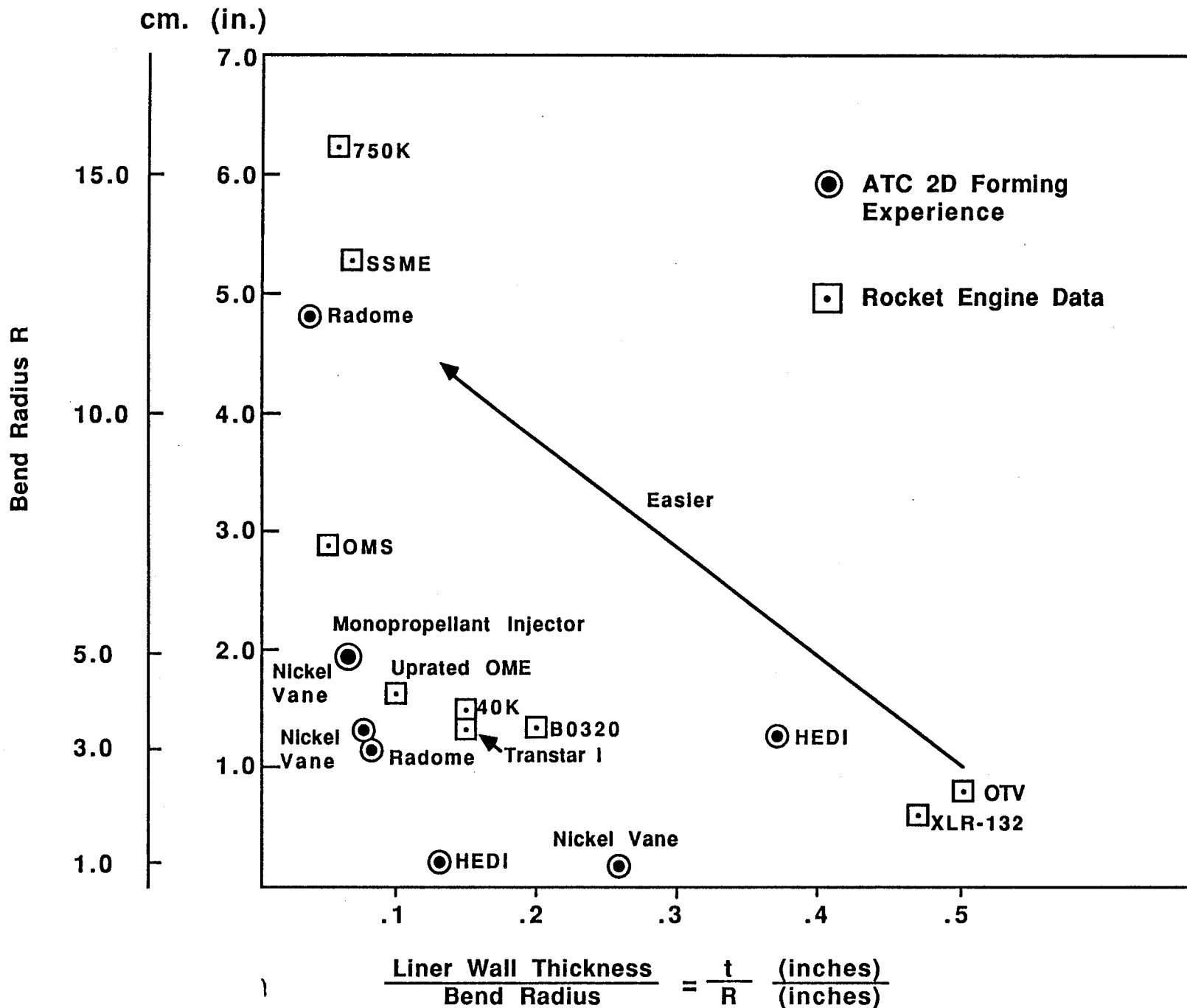


Figure 4.2 Geometric Throat Station Parameters of Milled Slot Thrust Chambers Superimposed on Formed Platelet Devices

- Gas side wall thickness
- Channel geometry
 - Channel width
 - Channel depth
 - Land width
- Panel land geometry
- Platelet stack thickness vs. minimum bend radius
- Secondary bend radii
- Forming die design
- Channel filler material
- Metal movement characteristics - prediction techniques
- Channel geometry changes along chamber axis
- Platelet panel material
- Chamber section arc-segment (number of panels per liner)

A comprehensive evaluation investigating all variables was not possible within program constraints. Simple coupon experiments were considered as a means of evaluating some forming parameters, such as t/R ratios. However, because simple coupons could not reproduce the effects of forming panels with internal geometries into complex three-dimensional shapes, the simple coupon experiments were rejected. The effort was focused on forming fully three dimensional panels complete with coolant channels.

The decision was made to narrow the investigation to a single die contour and several panel designs. The platelets within the panels could be re-arranged to provide different wall thickness and channel geometries, as well as different panel thicknesses.

The contour selected for the die set and panel design, shown in Figure 4.3, can be used at the Marshall Space Flight Center 40K test facility. This contour was a simplified version of previous 40K contours. The die contour was symmetrical about the throat plane. A non-symmetrical contour complicates the die design, platelet panel design, and the actual panel forming.

4.5 TASK 1.3 PLATELET STACK FORMING EXPERIMENTS

The basic process for forming panels was established in this task. Two forming dies were designed and fabricated. Two series of platelet panels were designed, fabricated and formed.

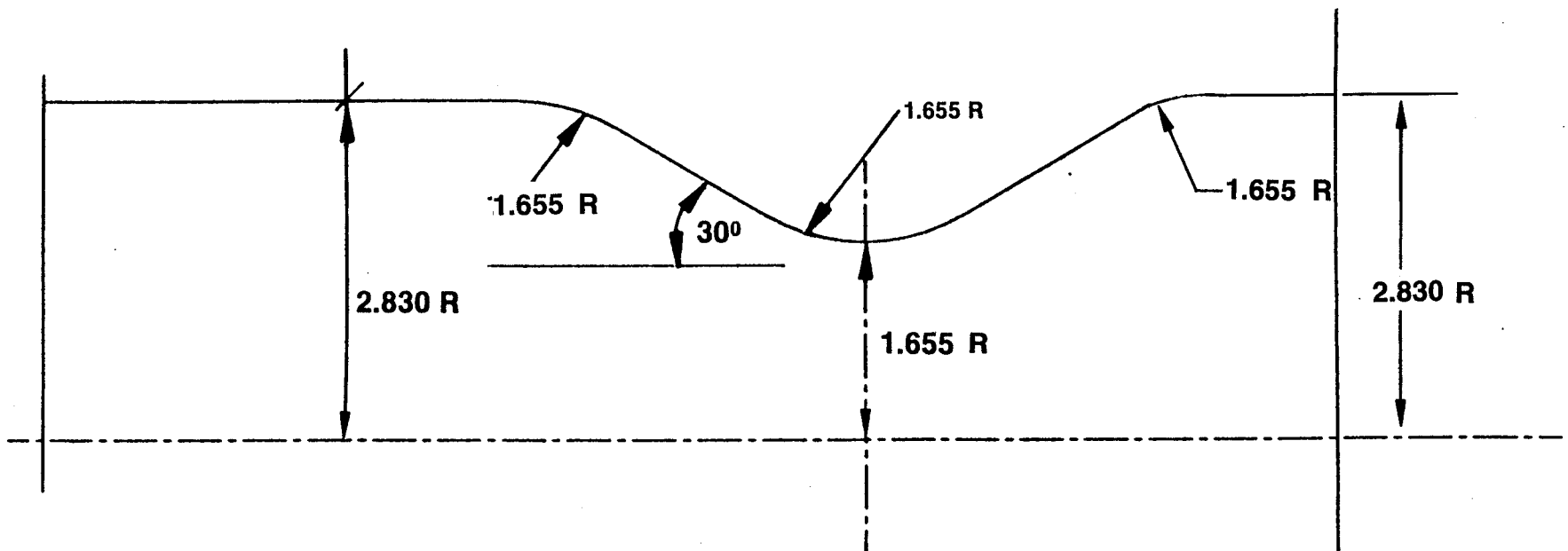


Figure 4.3. 40K Combustion Chamber Contour for Platelet Stack Forming

4.5.1 Forming Die Design

The first task performed in establishing a die design was to look at similar experiences in industry. Although a large variety of textbooks and articles on forming processes exist, little information could be found on forming panels with internal passages into three-dimensional shapes. The best reference material was found at Aerojet, since we have had previous experience forming "porous" platelet structures, such as the Radome and the HEDI forebody, into simple two-dimensional shapes.

The original forming tool design offered several options for panel forming methods. The first method was a single step process, taking the flat bonded panel to the formed condition with one movement of the die. The single step forming die is shown in Figure 4.4. The advantages of single-step forming were that only one die set is required, and no additional processing is required between forming steps that may require removal and replacement of channel filler material.

A two-step forming process was devised to provide constant support to the throat section during forming. The first step uses another die, shown in Figure 4.5, which allows only two-dimensional (2-D) forming of the panel to take place. Tooling pins hold a panel at the throat plane and the first point of contact for the punch is the throat. The barrel and nozzle ends of the panel are allowed to move toward the throat.

The second step is to complete the forming to the three-dimensional shape with the same die used for the one step forming process. The two-step process did not produce acceptable panels, as will be discussed later. Both forming processes were intended to restrain the panel outer edges by using spring-loaded pressure plates at the panel sides. This restrained outer edge was intended to prevent wrinkling of the hot-gas wall.

4.5.2 First Series Platelet Panel Design

Three platelet stacks designs and two different materials were established for the first series of forming experiments. The designs included a coarse and fine channel pattern, and a stepped fine pattern with changing channel depths. All three designs were nominally 0.250 inch thick, and made from ZrCu and 304L stainless steel. Thus several panel-design-related forming issues could be evaluated with the first series designs:

Channel geometry, channel widths

Channel geometry, channel depths

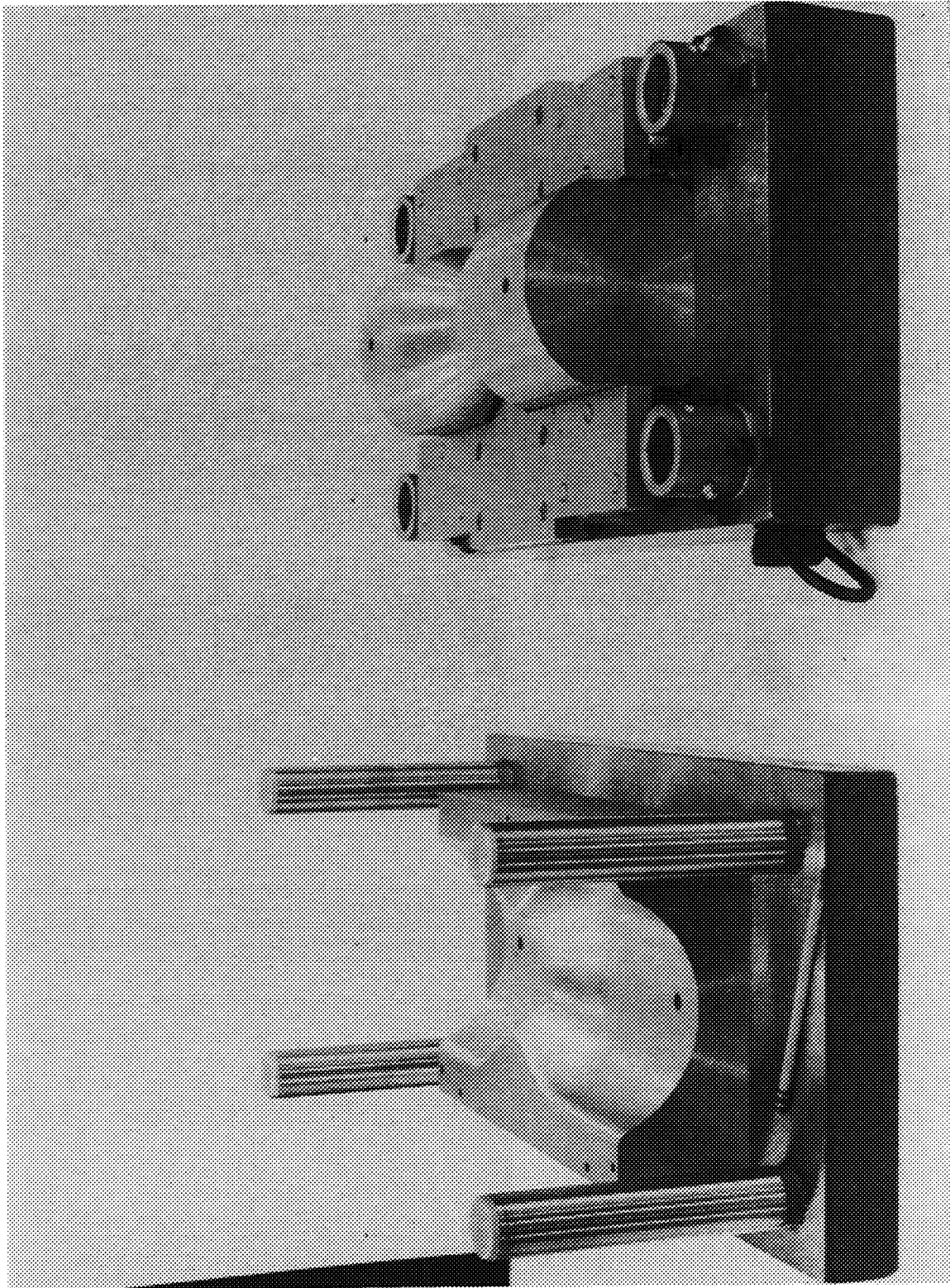


Figure 4.4 Single-Step Forming Die

ORIGINAL PAGE
BLACK AND WHITE PHOTOGRAPH

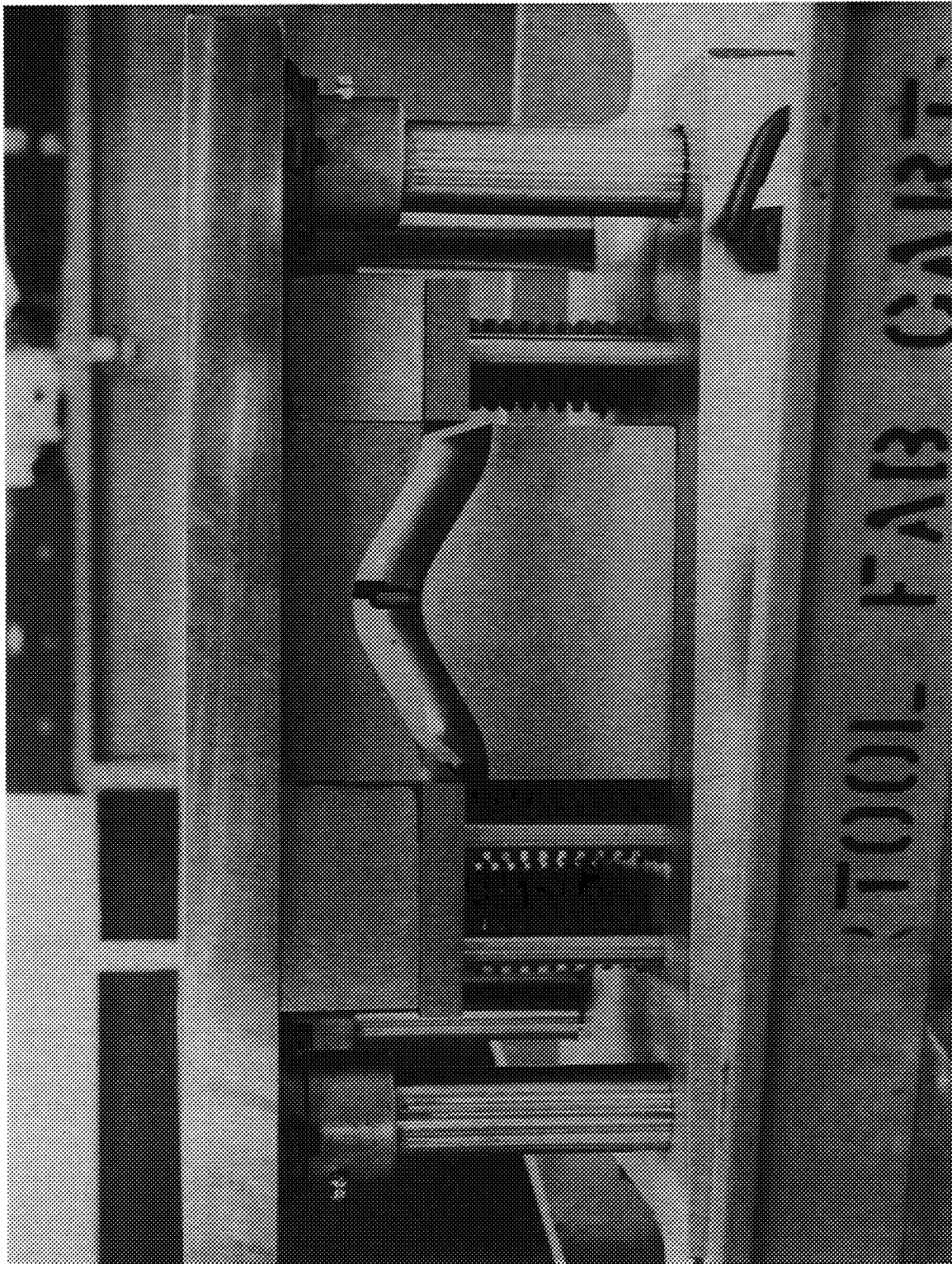


Figure 4.5 Two-Dimensional Forming Die

Changing channel geometry

Platelet panel materials

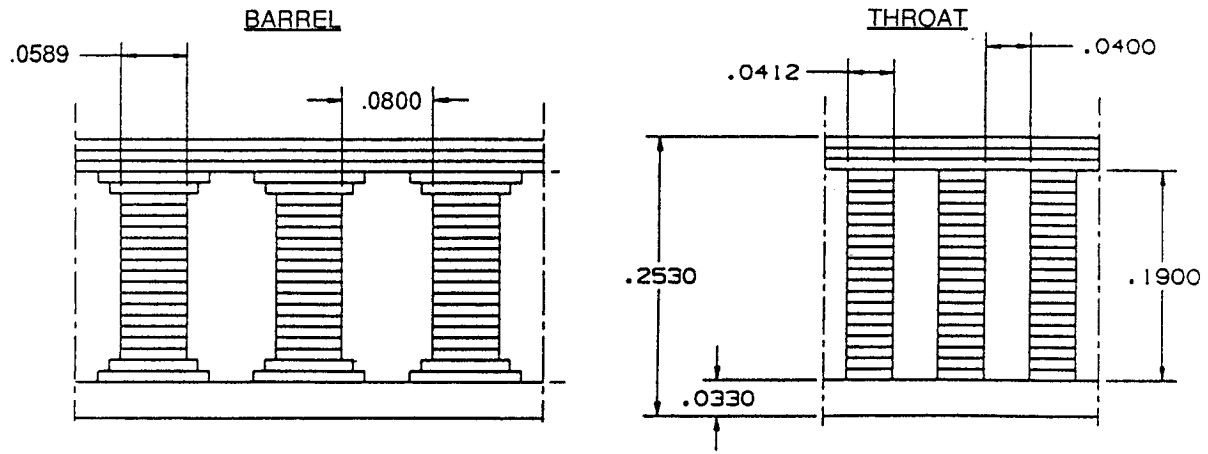
Twenty-five different platelet designs were used to make the panels. Key design features of the panels were the channel widths, channel manifolding, and tabs across the channels. Additional panel features included channels in the panel located outside the finished part, a grid pattern on both sides of the panel, and tooling holes.

The coarse pattern design had 32 channels in a panel (128 channels per combustion chamber), and a 0.033 inch hot gas wall. Each panel was one quarter, or 90° segment of a liner. The fine pattern and the stepped channel designs had 62 channels per panel with a 0.012 hot gas wall. Cross-sections of the channels are illustrated in Figure 4.6. A plan view of a coarse pattern platelet is shown in Figure 4.7. The minimum channel widths and land widths were based on previous Aerojet platelet experience; 0.020 inch lands and channels had been used successfully in other designs.

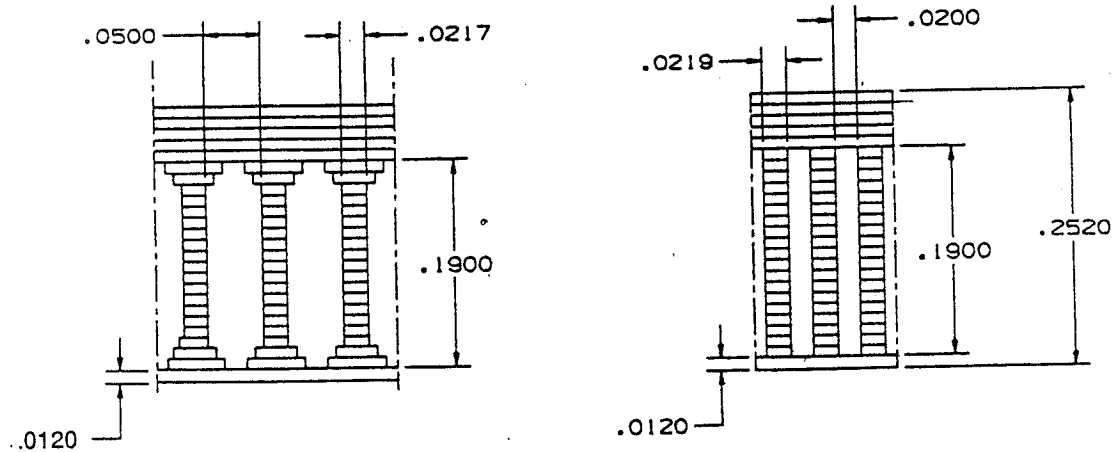
The coolant channels were manifolded into groups to simplify water flow testing. The coarse pattern grouped the channels for manifolding in sets of three. This allowed for flowing each set of channels separately, providing valuable data on flow distribution across the panel. Manifolds for the fine and stepped channel designs fed five channels each. The inlet of the manifolds alternated from the forward to the aft end in adjacent channel sets, allowing space for flow tooling to seal against the panel.

Because individual platelets required handling during the fabrication process and there were many long, small lands, tabs were placed about every two inches along the channel. The tabs, which were approximately one-half the thickness of the platelet, connected the lands together, prevented land bending and distortion during handling of the individual platelets. While tabs in the experimental panels are often aligned platelet to platelet, an operative chamber would stagger tabs to minimize pressure drop. Tabs have been used successfully in similar platelet designs including Radome. Tabs may even be beneficial to the design; i.e., thermal analysis indicates that correct placement of tabs may enhance local heat transfer by affecting coolant velocities.

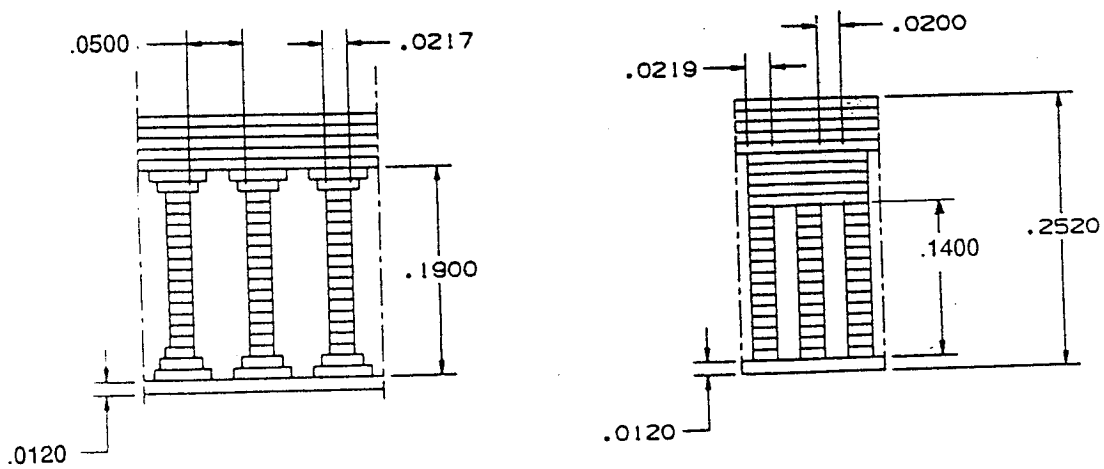
Additional channels are placed in the panel outboard of the final part shape. The extra channels provided a uniform mass density throughout the part, in an attempt to prevent excess stretching in the throat. It was thought that these channels would also ensure uniform deformation across the platelet stack, as a restraining force was to be applied to the sides of the panel during forming.



Coarse Pattern



Fine Pattern



Stepped Channel

Figure 4.6. First Series Throat and Barrel Cross Sections of Panel Designs

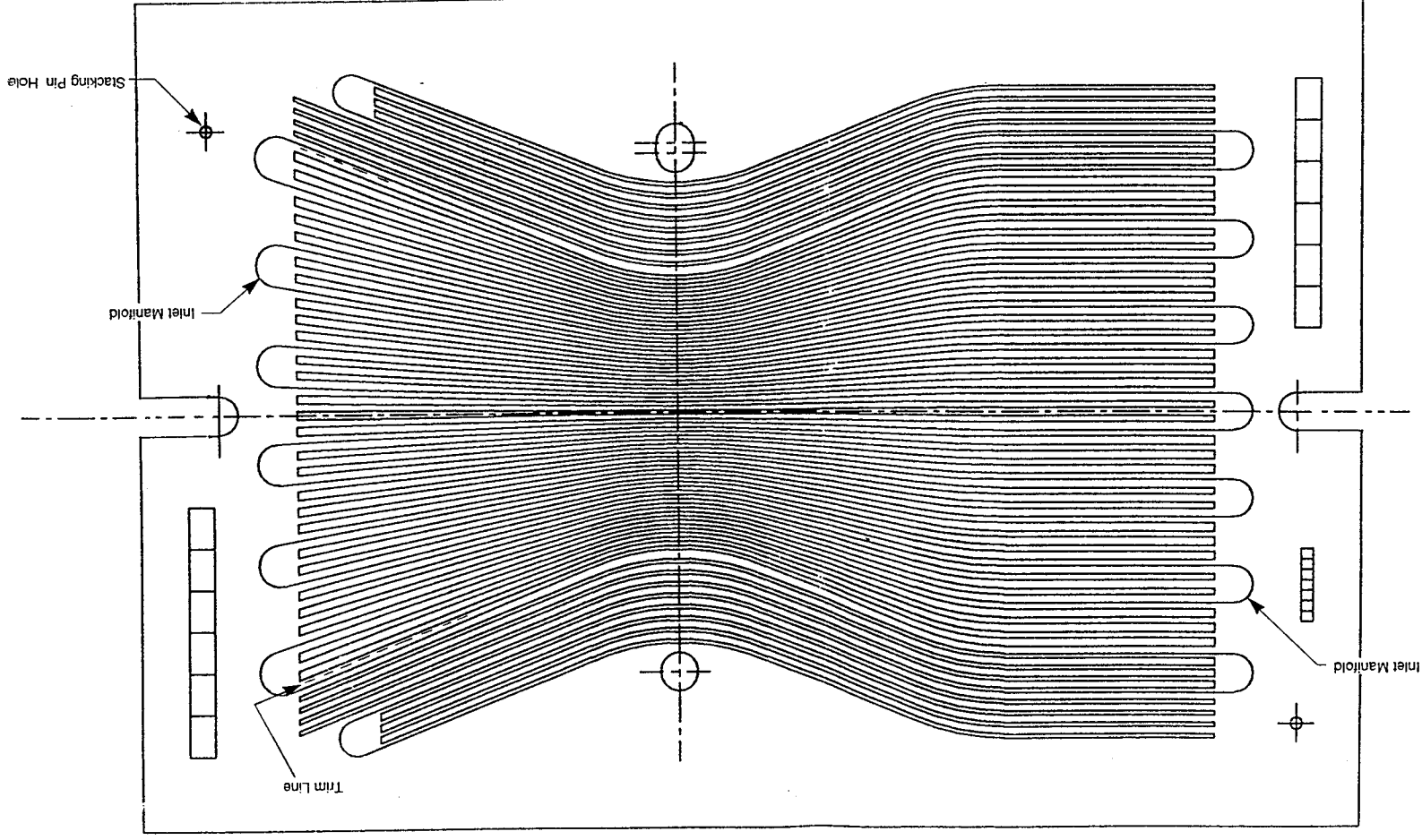


Figure 4.7. First Series Coarse Pattern Platelet

A grid pattern was placed onto the outer surface of the outer platelets of each panel, as shown in Figure 4.8, to allow measurement of metal movement on the panel. The grid was etched less than 0.003 deep and did not affect the forming process. The grid pattern is used on experimental panels only; operational panels will have smooth hot gas walls and close-out surfaces.

The platelet design also included tooling holes for stacking and forming. The two holes at the throat were to be used during the first forming operation and the slots along the chamber axis were used during the final contouring.

4.5.3 Channel Filler Material

An objective of the forming task was to evaluate the need for a filler material in the channels to prevent land deformation during forming. The following filler materials were considered:

Fine-Grain Sand

"Sera-Bend"

Paraffin

"Rigid-Ax" wax

Aerojet developed, proprietary polymer

After evaluating the candidate materials for possible channel contamination, previous experiences, and ease of use, the Aerojet polymer was selected. The material is water soluble with a melting point of 140°F, thus hot water can be used for removal. The polymer is also fluorescent, meaning illumination by blacklight can be used to verify complete removal. Panels were formed both with and without the polymer to evaluate its effectiveness.

4.5.4 First Series Panel Fabrication

Sixteen ZrCu coarse-pattern test panels were bonded, of which thirteen were subjected to bond densification and aging in a HIP furnace in order to increase the material structural properties. The three panels not HIP processed were used to evaluate the necessity for the process. The coarse panels were 0.240 inch thick, not 0.250 inch thick as planned due to a close-out platelet inadvertently omitted during platelet stacking. Six ZrCu fine pattern panels and four ZrCu stepped channel panels were bonded and HIP densified and aged. Due to material availability, the stepped channel design used 0.008 instead of 0.010 inch thick platelets. The

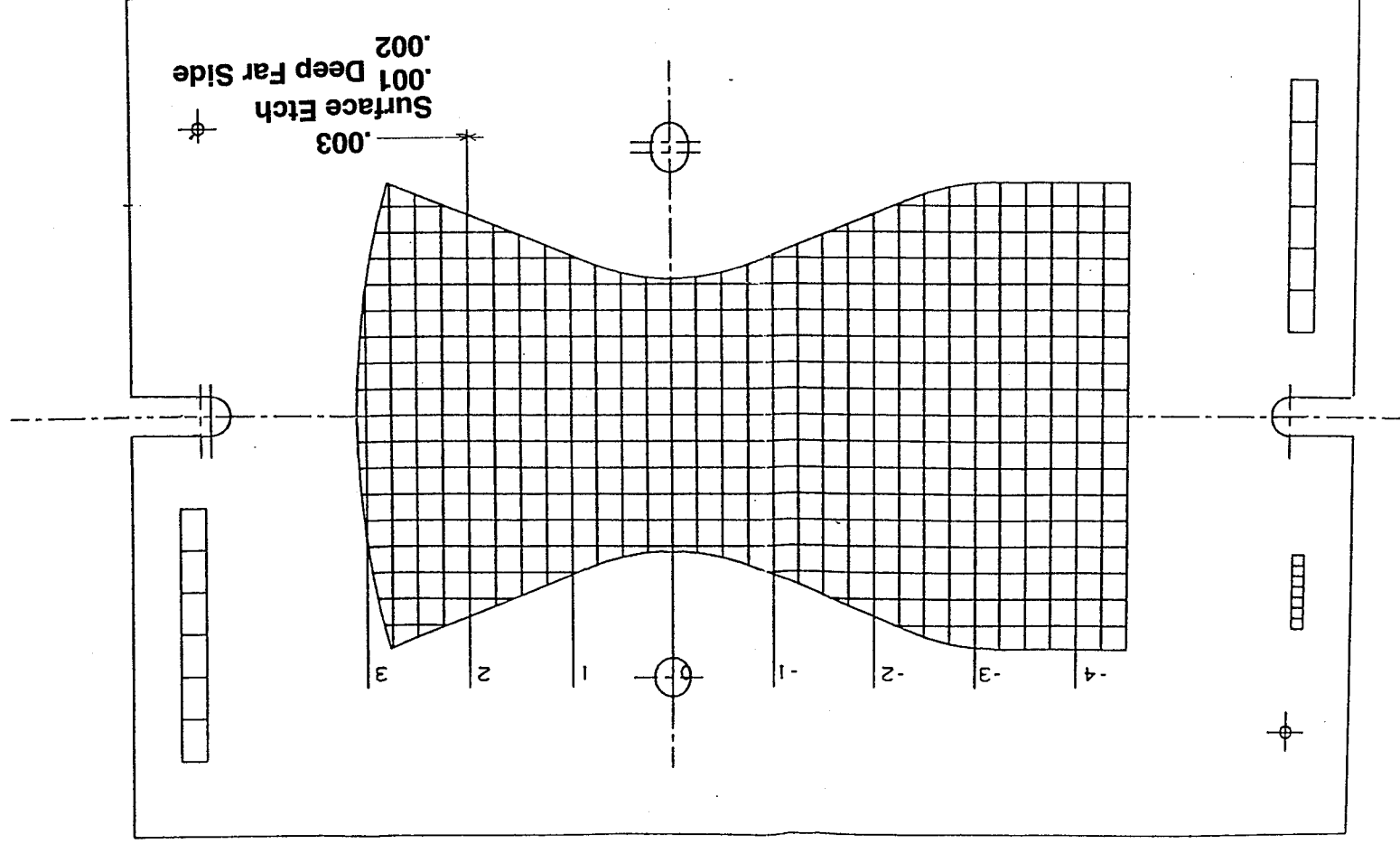


Figure 4.8. Platelet Gas Side Wall .033 Thick Zr-Cu

thirty 0.008 inch platelets used in place of the twenty-four 0.010 inch platelets appeared not to have affected the outcome of the experiment.

Thirteen CRES 304L panels were bonded and HIP densified. Four panels of each of the coarse, fine, and stepped pattern design were fabricated. One additional coarse pattern panel, 1204190-69 was fabricated. The panel had the platelet tabs between the quarter liner and frame in the converging and diverging sections removed. The tabs were removed to compare the effect of tabs on channel deformation during forming.

4.5.5 First Series Forming Experiments

4.5.5.1 Introduction

The forming experiments began with the forming of four solid copper panels to proof the tooling. Coarse pattern ZrCu panels were then used to evaluate the one-step and two step processes. The one step forming process was preferred because it was believed the liner was workhardened after the first forming operation of the two step process causing the second forming operation to be more difficult and resulting in tearing of the closeout wall near both axial panel edges. After selecting the one-step forming process using no restraining springs, modifications to the panels were found necessary to achieve repeatable panel throat location. Once the forming process and required panel tooling features were established, panels of various thicknesses and channel designs were then formed to evaluate the effects of forming various panel designs. Water cold flows of panels before and after forming were also performed, as well as sectioning to look at channel deformations. Results of the forming experiments are summarized in Table 4.2.

4.5.5.2 Tooling Proof

The first forming took place with four 0.250 inch thick solid OFHC copper plates. Both forming processes were performed, proofing both the 2D and the 3D die sets. The forming results are listed in Table 4.2. Three plates were formed using the single step procedure, all three exhibited undesirable coining in the throat area. One panel was formed with the two-step procedure, and no coining was visible in the throat area.

4.5.5.3 Die and Forming Process Evaluation

Coarse pattern ZrCu panels were then formed to evaluate the forming procedure. The first two panels formed, S/N 015 and S/N 002, were formed with the two-step

TABLE 4.2

Formed Platelet Liner Forming Summary

Panel S/N	Part Number	Material	Channel Pattern	Design Number	Hot Gas Wall Thickness	Stack Height	Post-Bond HIP	Leak Test Flat	Leak Test 2-D	Leak Test 3-D	Cold Flow Flat	Cold Flow 2-D	Cold Flow 3-D	Filler	Springs (3-D)	Forming Steps	3-D Die Used	Comments
DIE VERIFICATION PANELS																		
01		OFHC	None	Solid Plate	w/ Grid	0.250									Yes	1	Org 1-Step	Coining in Throat
02		OFHC	None	Solid Plate	w/ Grid	0.250									Yes	1	Org 1-Step	Coining in Throat
03		OFHC	None	Solid Plate	w/ Grid	0.250									Yes	1	Org 1-Step	Coining in Throat
04		OFHC	None	Solid Plate	w/ Grid	0.250									Yes	2	Org 2D-3D	No throat coining
FIRST SERIES FORMING EXPERIMENTS																		
001	1204190-9	ZrCu	Coarse	1	0.033	0.244	No	Y	Y	N	Y	Y	N	Y	N	2	Mod II	
002	1204190-9	ZrCu	Coarse	1	0.033	0.244	Yes	Y	N	N	Y	N	N	Y/N *	Y	2	Org 2D-3D	Ripped at panel perimeter
003	1204190-9	ZrCu	Coarse	1.1	0.033	0.242	Yes	Y	N	N	Y	N	N	Y	N	1	Mod II	.010 slip sheet tore and wrinkled, damaged part
004	1204190-9	ZrCu	Coarse	1	0.033	0.243	Yes	Y	Y	N	Y	Y	N	Y	Y	2	Mod II	Split close-out down centerline, sectioned
005	1204190-9	ZrCu	Coarse	1.1	0.033	0.242	Yes	Y	-	Y	Y	-	Y	Y	N	1	Mod II	Excess channels removed before forming, improved channel tip
006	1204190-9	ZrCu	Coarse	1	0.033	0.242	Yes	Y	-	Y	Y	-	Y	Y	N	1	Mod II	No Tearing or cracking
007	1204190-9	ZrCu	Coarse	1	0.033	0.242	No	Y	-	Y	Y	-	Y	N	N	1	Mod II	Sectioned
008	1204190-9	ZrCu	Coarse	1	0.033	0.242	Yes	Y	Y	N	Y	Y	N	Y	N	2	Mod II	Split close-out down centerline, sectioned
009	1204190-9	ZrCu	Coarse	1.1	0.033	0.242	Yes	Y	-	N	Y	-	N	Y	N	1	Org 3D	
010	1204190-9	ZrCu	Coarse	1	0.033	0.242	Yes	L	-	N	N	-	N	Y	N	1	Mod II	No Tearing or cracking, sectioned
011	1204190-9	ZrCu	Coarse	1	0.033	0.242	Yes	Y	-	Y	Y	-	Y	Y	N	1	Mod II	
012	1204190-9	ZrCu	Coarse	1	0.033	0.242	Yes	Y	Y	N	Y	Y	N	N	-	2	-	Forming not completed
013	1204190-9	ZrCu	Coarse	1	0.033	N/A	No	Y	-	-	-	-	-	Y	-	-	-	Sectioned to verify filling process
014	1204190-9	ZrCu	Coarse	1	0.033	0.242	Yes	L	-	N	N	-	N	Y	Y	1	Mod II	No Tearing or cracking
015	1204190-9	ZrCu	Coarse	1	0.033	0.242	Yes	Y	N	N	Y	N	N	N	Y	2	Org 2D-3D	Ripped at panel perimeter, cracks on O.D.
016	1204190-9	ZrCu	Coarse	1	0.033	0.244	Yes	Y	N	N	Y	N	N	Y	Y	2	Mod I	Ripped at panel perimeter
SECOND SERIES FORMING EXPERIMENTS																		
017	1204190-19	ZrCu	Fine	1	0.012	0.254	Yes	Y	-	N	Y	-	N	Y	N	1	Mod II	Ripped at perimeter of part
018	1204190-19	ZrCu	Fine	1.1	0.012	0.254	Yes	Y	-	N	Y	-	N	Y	N	1	Org 3D	
019	1204190-19	ZrCu	Fine	1.1	0.012	0.255	Yes	Y	-	Y	Y	-	Y	Y	N	1	Mod II	Excess channels removed before forming
020	1204190-19	ZrCu	Fine	1	0.012	N/A	Yes	Y	-	-	Y	-	-	N	-	-	-	Not formed
021	1204190-19	ZrCu	Fine	1.1	0.012	0.254	Yes	Y	-	N	Y	-	N	N	N	1	Mod II	
022	1204190-19	ZrCu	Fine	1	0.012	N/A	Yes	N	-	-	N	-	-	-	-	-	-	Damaged during fabrication
023	1204190-29	ZrCu	Stepped	1.1	0.012	0.256	Yes	Y	-	Y	Y	-	Y	Y	N	1	Mod II	Excess channels removed before forming
024	1204190-29	ZrCu	Stepped	1.1	0.012	0.255	Yes	Y	-	N	Y	-	N	Y	N	1	Mod II	Reformed in original 3D die
025	1204190-29	ZrCu	Stepped	1	0.012	N/A	Yes	L	-	-	N	-	-	N	-	-	-	Not formed
026	1204190-29	ZrCu	Stepped	1	0.012	0.255	Yes	Y	-	N	Y	-	N	Y	N	1	Mod II	Ripped at perimeter of part
027	1204190-39	CRES 304L	Coarse	1.1	0.030	0.250	Yes	Y	-	Y	Y	-	Y	Y	N	1	Mod II	
028	1204190-39	CRES 304L	Coarse	1.1	0.030	0.250	Yes	Y	-	N	Y	-	N	Y	N	1	Mod II	
029	1204190-39	CRES 304L	Coarse	1.1	0.030	N/A	Yes	N	-	-	N	-	-	N	-	-	-	Not Formed
030	1204190-39	CRES 304L	Coarse	1.1	0.030	N/A	Yes	N	-	-	N	-	-	N	-	-	-	Not Formed
031	1204190-49	CRES 304L	Fine	1.1	0.010	0.250	Yes	Y	-	N	Y	-	N	Y	N	1	Mod II	
032	1204190-49	CRES 304L	Fine	1.1	0.010	0.251	Yes	Y	-	Y	Y	-	Y	Y	N	1	Mod II	
033	1204190-49	CRES 304L	Fine	1.1	0.010	N/A	Yes	N	-	-	N	-	-	N	-	-	-	Not Formed
034	1204190-49	CRES 304L	Fine	1.1	0.010	N/A	Yes	N	-	-	N	-	-	N	-	-	-	Not Formed
035	1204190-59	CRES 304L	Stepped	1.1	0.010	0.250	Yes	Y	-	N	Y	-	N	Y	N	1	Mod II	
036	1204190-59	CRES 304L	Stepped	1.1	0.010	0.250	Yes	Y	-	N	Y	-	N	Y	N	1	Mod II	
037	1204190-59	CRES 304L	Stepped	1.1	0.010	N/A	Yes	N	-	-	N	-	-	N	-	-	-	Not Formed
038	1204190-59	CRES 304L	Stepped	1.1	0.010	N/A	Yes	N	-	-	N	-	-	N	-	-	-	Not Formed
039	1204190-69	CRES 304L	Coarse	1.1	0.030	0.250	Yes	Y	-	N	Y	-	N	Y	N	1	Mod II	Tabs removed from conv. & div. sections

FOLDOUT FRAME

FOLDOUT FRAME

2.

TABLE 4.2
Formed Platelet Liner Forming Summary
(Cont.)

Panel S/N	Part Number	Material	Channel Pattern	Design Number	Hot Gas Wall Thickness	Stack Height	Post-Bond HIP	Leak Test Flat	Test 2-D	3-D	Cold Flow Flat	2-D	3-D	Filler	Springs (3-D)	Forming Steps	3-D Die Used	Comments
040	1204435-19	ZrCu	Fine	1.2	0.012	0.142	Yes	N	-	N	Y	-	Y	Y	N	1	MOD III/Shim	t/R Study
041	1204435-19	ZrCu	Fine	1.2	0.012	0.142	Yes	N	-	N	Y	-	Y	Y	N	1	MOD III/Shim	t/R Study
042	1204435-19	ZrCu	Fine	1.2	0.012	0.142	Yes	N	-	N	Y	-	Y	Y	N	1	MOD III/Shim	t/R Study
043	1204435-9	ZrCu	Fine	1.2	0.012	0.372	Yes	N	-	N	Y	-	Y	Y	N	1	MOD III/ 3/8	t/R Study
044	1204435-9	ZrCu	Fine	1.2	0.012	0.372	Yes	N	-	N	Y	-	Y	Y	N	1	MOD III/ 3/8	t/R Study
045	1204435-9	ZrCu	Fine	1.2	0.012	0.372	Yes	N	-	N	Y	-	Y	Y	N	1	MOD III/ 3/8	t/R Study
046	1204796-9	ZrCu	Fine	2	0.008	0.262	Yes	Y	-	N	Y	-	Y	Y	N	1	MOD III	3-D Joining Attempt
047	1204796-9	ZrCu	Fine	2	0.008	0.262	Yes	Y	-	N	Y	-	Y	Y	N	1	MOD III	3-D Joining Attempt
048	1204796-9	ZrCu	Fine	2	0.008	0.262	Yes	Y	-	N	Y	-	Y	Y	N	1	MOD III	3-D Joining Attempt
049	1204796-9	ZrCu	Fine	2	0.008	0.262	Yes	Y	-	N	Y	-	Y	Y	N	1	MOD III	3-D Joining Attempt
050	1204796-9	ZrCu	Fine	2	0.008	0.262	Yes	Y	-	N	Y	-	Y	Y	N	1	MOD III	3-D Joining Attempt
051	1204796-9	ZrCu	Fine	2	0.008	0.262	Yes	Y	-	N	Y	-	Y	Y	N	1	MOD III	3-D Joining Attempt
3-D JOINING DEMO																		
052	1206530-9	ZrCu	Fine	2.1	0.008	0.258	Yes	Y	-	N	Y	-	Y	Y	N	1	MOD III	Panel Joining Assembly No 1
053	1206530-9	ZrCu	Fine	2.1	0.008	0.257	Yes	Y	-	N	Y	-	Y	Y	N	1	MOD III	
054	1206530-9	ZrCu	Fine	2.1	0.008	0.257	Yes	Y	-	N	Y	-	Y	Y	N	1	MOD III	Panel Joining Assembly No 2
055	1206530-9	ZrCu	Fine	2.1	0.008	0.257	Yes	Y	-	N	Y	-	Y	Y	N	1	MOD III	Panel Joining Assembly No 2
056	1206530-9	ZrCu	Fine	2.1	0.008	0.257	Yes	Y	-	N	Y	-	Y	Y	N	1	MOD III	Panel Joining Assembly No 1
057	1206530-9	ZrCu	Fine	2.1	0.008	0.257	Yes	Y	-	N	Y	-	Y	Y	N	1	MOD III	
058	1206530-9	ZrCu	Fine	2.1	0.008	0.257	Yes	Y	-	N	Y	-	Y	Y	N	1	MOD III	
059	1206530-9	ZrCu	Fine	2.1	0.008	0.257	Yes	Y	-	N	Y	-	Y	Y	N	1	MOD III	

process, illustrated in Figure 4.9, in the as-designed tooling. Panel S/N 015, shown in Figure 4.10, cracked on the close-out wall of the part at the edge of a quarter panel chamber section and tore at the perimeter of the part in the throat area during the final contouring operation. The part was held around the entire perimeter with spring-loaded pads in the die. To eliminate the cracking on the O.D. of the part, the springs were removed from the throat area for the next test panel. Panel S/N 002 is shown in Figure 4.11. There is no cracking of the part within the useable 90 degree sector but the part still tore in the throat region.

To correct the tearing at the edge of the parts the tooling was modified. Figure 4.12 illustrates the rework of the die. The tooling modification was evaluated by forming ZrCu panel S/N 016 using the two-step process. This part cracked in the same area as the previous parts, indicating that further modification was required.

Two ZrCu panels were formed in the single step process to evaluate the second die modification. Panel S/N 014 was formed with the restraining springs and panel S/N 010 was formed without springs in the die set. Both panels formed without any tearing or cracking of the part indicating that the dies were satisfactory for continued forming experiments.

Three more ZrCu panels were formed to evaluate the two-step versus the one-step processes, and the use of restraining springs. Panels S/N 004 and S/N 008 were formed in the two-step process without springs. Both panels split the channel close-out wall down the centerline of the part as shown in Figure 4.13. Panel S/N 006 was successfully formed in one step without any tearing or cracking as shown in Figure 4.14.

After evaluating the panels formed to date, the single step forming process with no springs was selected as the superior process. Panels formed in 2 steps had repeatedly cracked the channel close-out wall. Use of springs to restrain the panels also caused close-out wall cracking. Channel deformation studies showed that panels formed in a single step resulted in channels that were more true to the desired contour than with panels formed in two steps. Measurements of channel 'tip' are discussed in Section 4.5.7.6.

4.5.5.4 Panel Modifications

Inspection of parts formed with extra material around the perimeter show that the outside channel, which was designed to be radial, is slightly skewed from radial. In order to investigate the effect of excess material outboard of the last channel, a ZrCu coarse

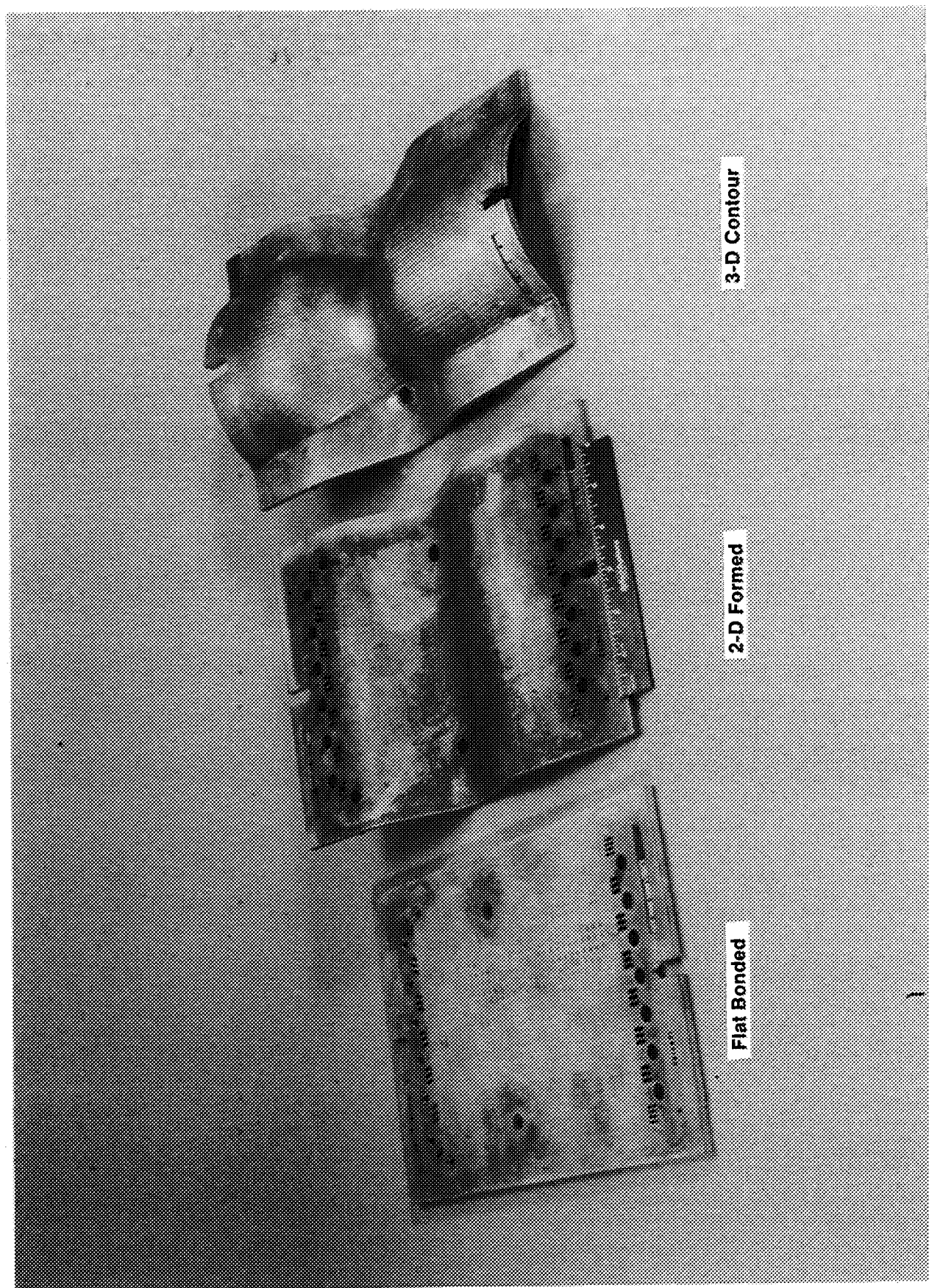


Figure 4.9 Two-Step Forming Process

ORIGINAL PAGE
BLACK AND WHITE PHOTOGRAPH

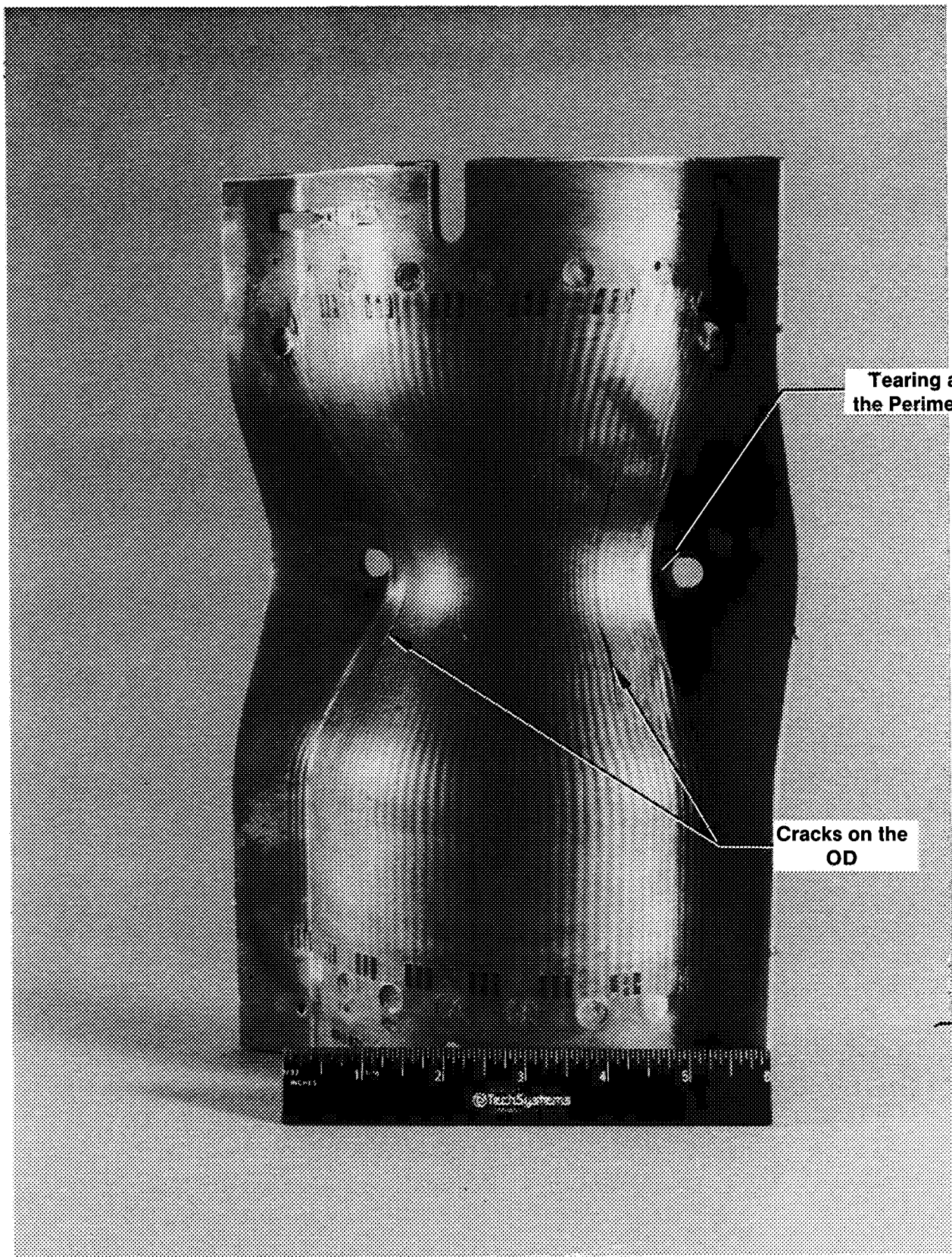


Figure 4.10 OD Cracking Due to Use of Throat Springs S/N 015

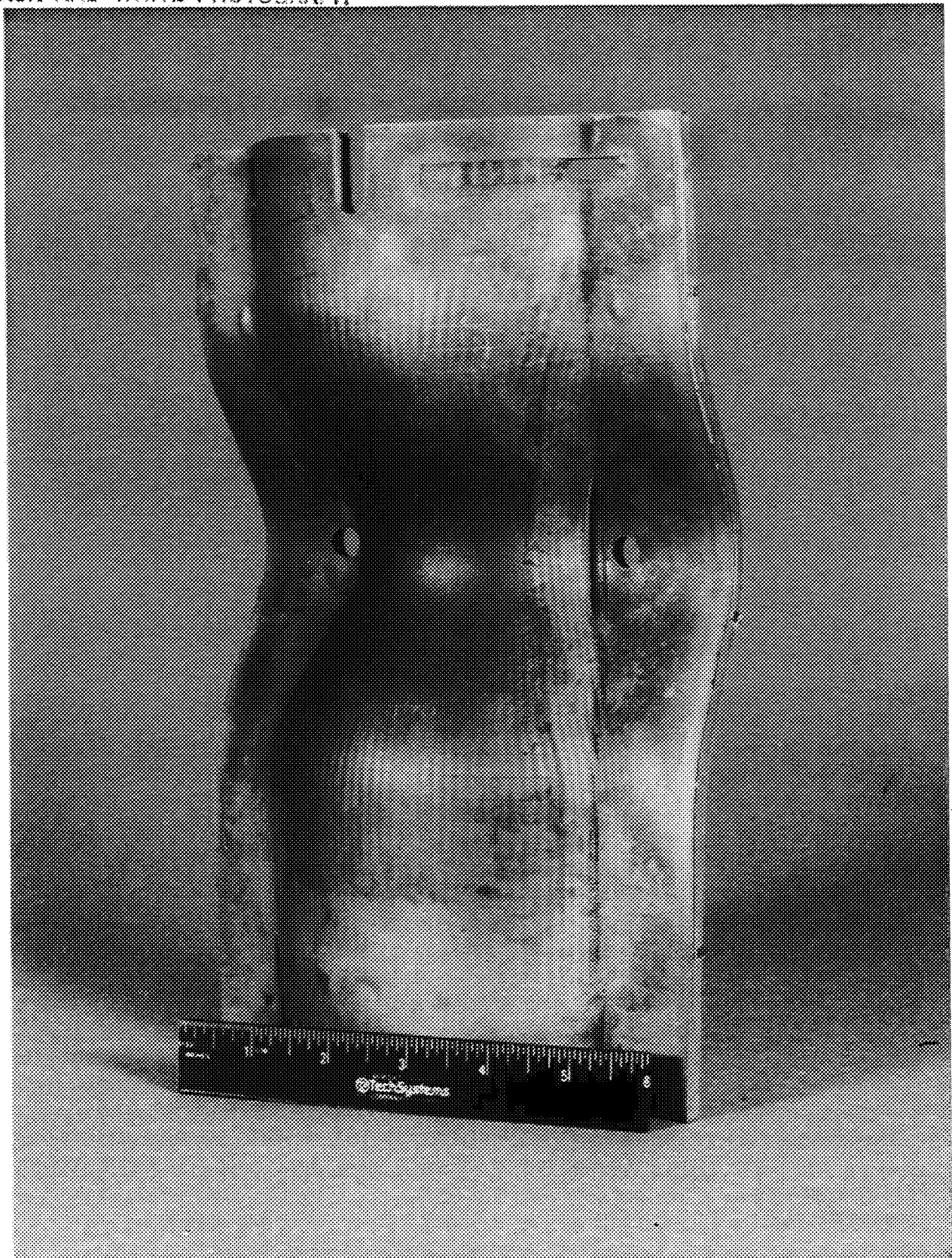


Figure 4.11. Removing Throat Springs From the Die Eliminated Cracking of Part SN 002

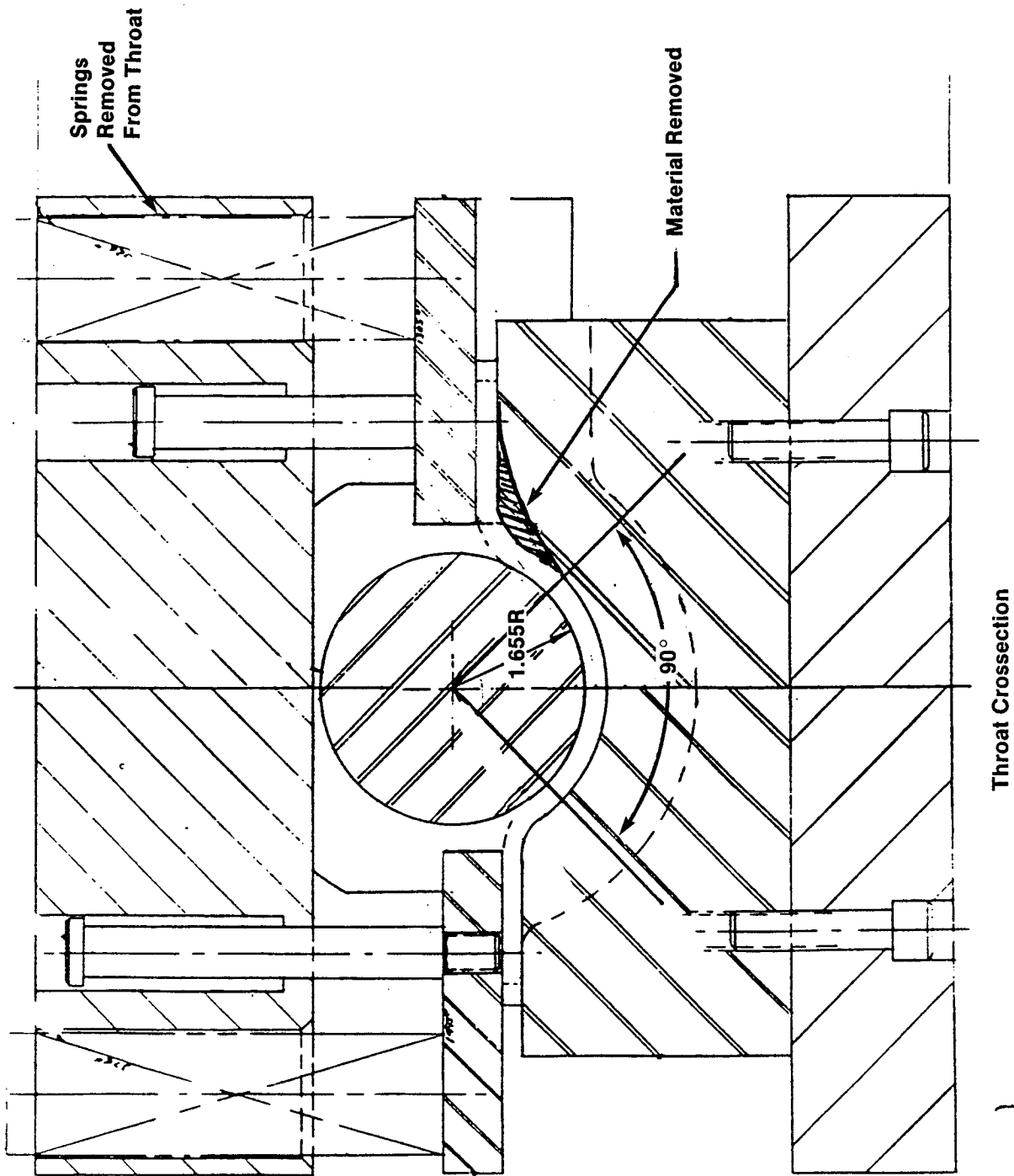


Figure 4.12. Tooling Modifications Were Necessary to Prevent Tearing of the Part

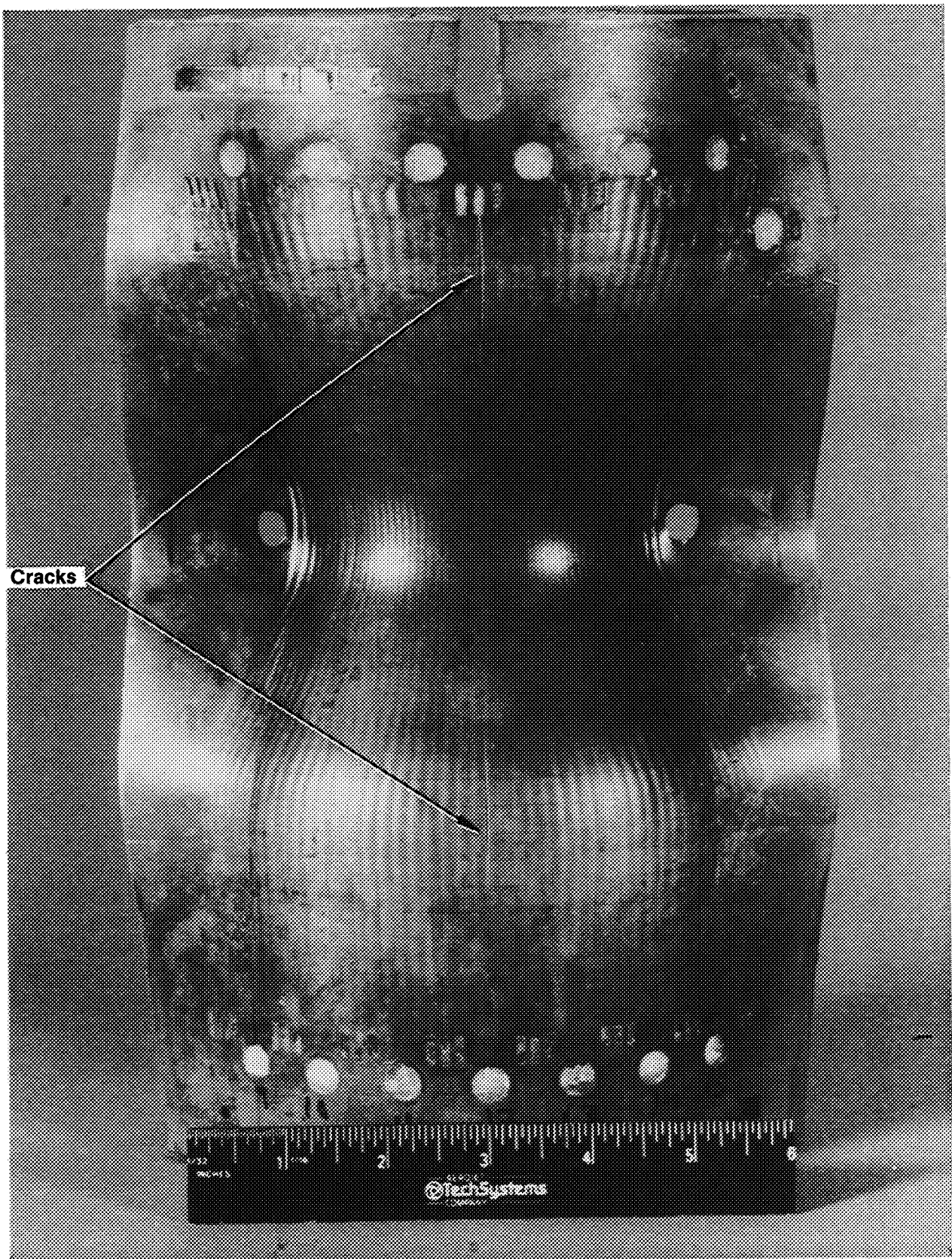


Figure 4.13. Parts Formed in 2 Steps Cracked the Close Out of the Part

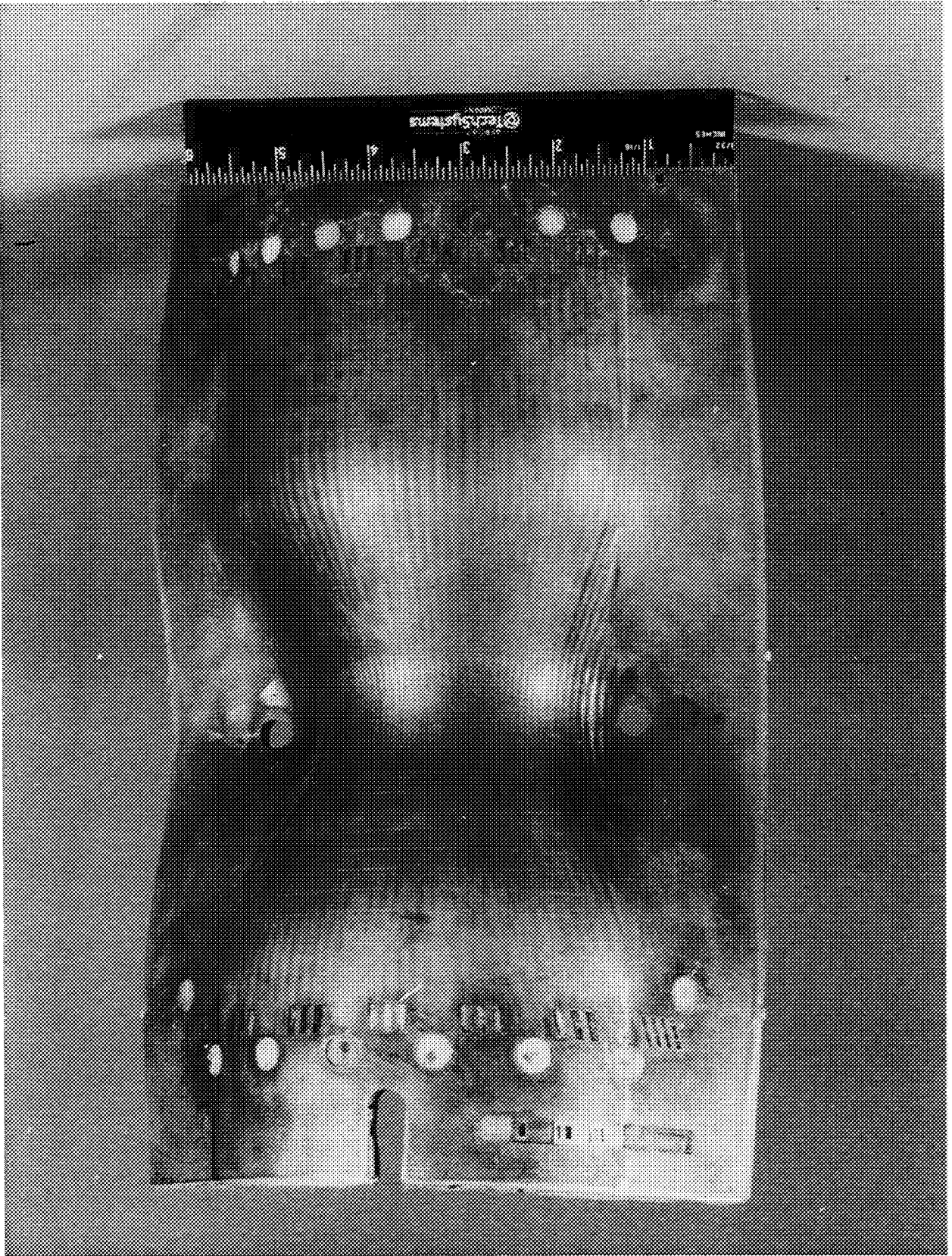


Figure 4.14 Parts Formed in a Single Operation Remained Intact

pattern panel, S/N 005 was machined to remove the excess material as shown in Figure 4.15. The panel was successfully formed and found to have less channel skewing.

Four more panels were formed to further evaluate the modified panel design. Two panels, fine pattern S/N 017 and stepped pattern S/N 026 were formed as designed. Both parts ripped on the hot gas wall at the perimeter of the part. Two additional panels, fine pattern S/N 019 and stepped pattern S/N 023 were machined to remove the excess material. Both machined panels were successfully formed, which verified that the excess material is not required for forming.

4.5.5.5 Forming Different Panel Designs

Forming experiments continued to evaluate the effects of panel design on the formed panel. The three panel designs in ZrCu and CRES 304L were formed in the modified (excess material removed) form using the one-step forming process with the modified 3-D die. Panels were formed with and without polymer, and with and without tabs. Many Panels were leak tested and water flowed both before and after forming. The results of the flow tests and forming is presented in section 4.5.7.4. Several panels were sectioned to evaluate internal deformations and platelet bond quality.

4.5.5.6 Die Modification III

Inspection of the grid pattern on the First Series Panels revealed a shift in the location of the throat of the channel pattern from the flat to the formed shape by 0.050 to 0.100 inch. Tooling pins were added to the female die half at the throat plane. The pins engaged with slots on the panel, helping to maintain throat alignment.

4.5.6 Second Series Forming Experiments

Panels of a modified original design were fabricated with different thicknesses to evaluate t/R ratios. An iteration of the first design was also made, in order to evaluate the effect of throat alignment pins.

Six modified original design fine pattern panels were fabricated in two different thicknesses. Three 0.142 inch thick panels and three 0.372 inch thick panels were made with the configuration shown in Figures 4.16 and 4.17. The channel aspect ratio for the thick panel was 15.5. A new female forming die half was made to accommodate the 0.372 inch panel. The

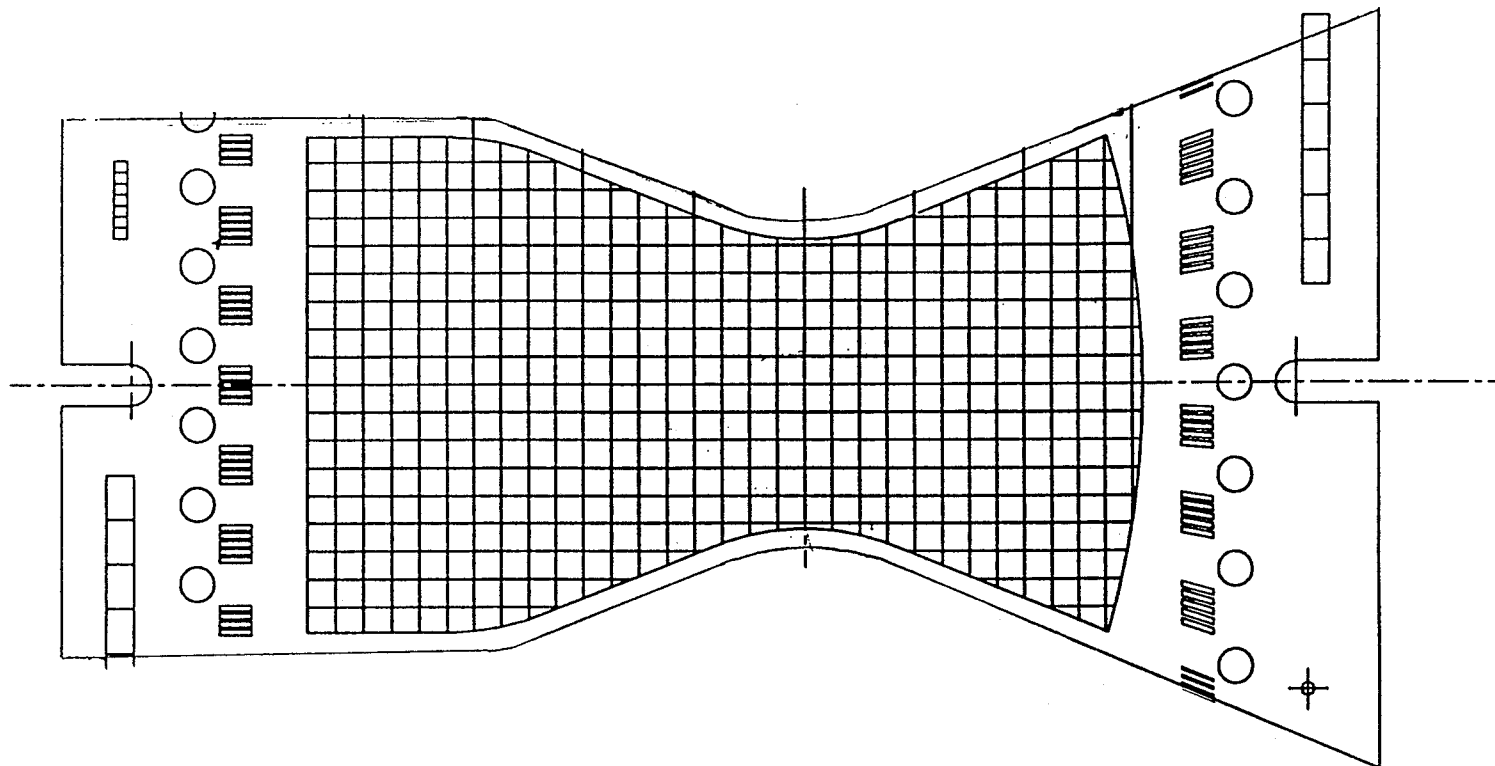


Figure 4.15. Material Outside of 90° Chamber Section Was Removed to Study the Effect on Chamber Deformation

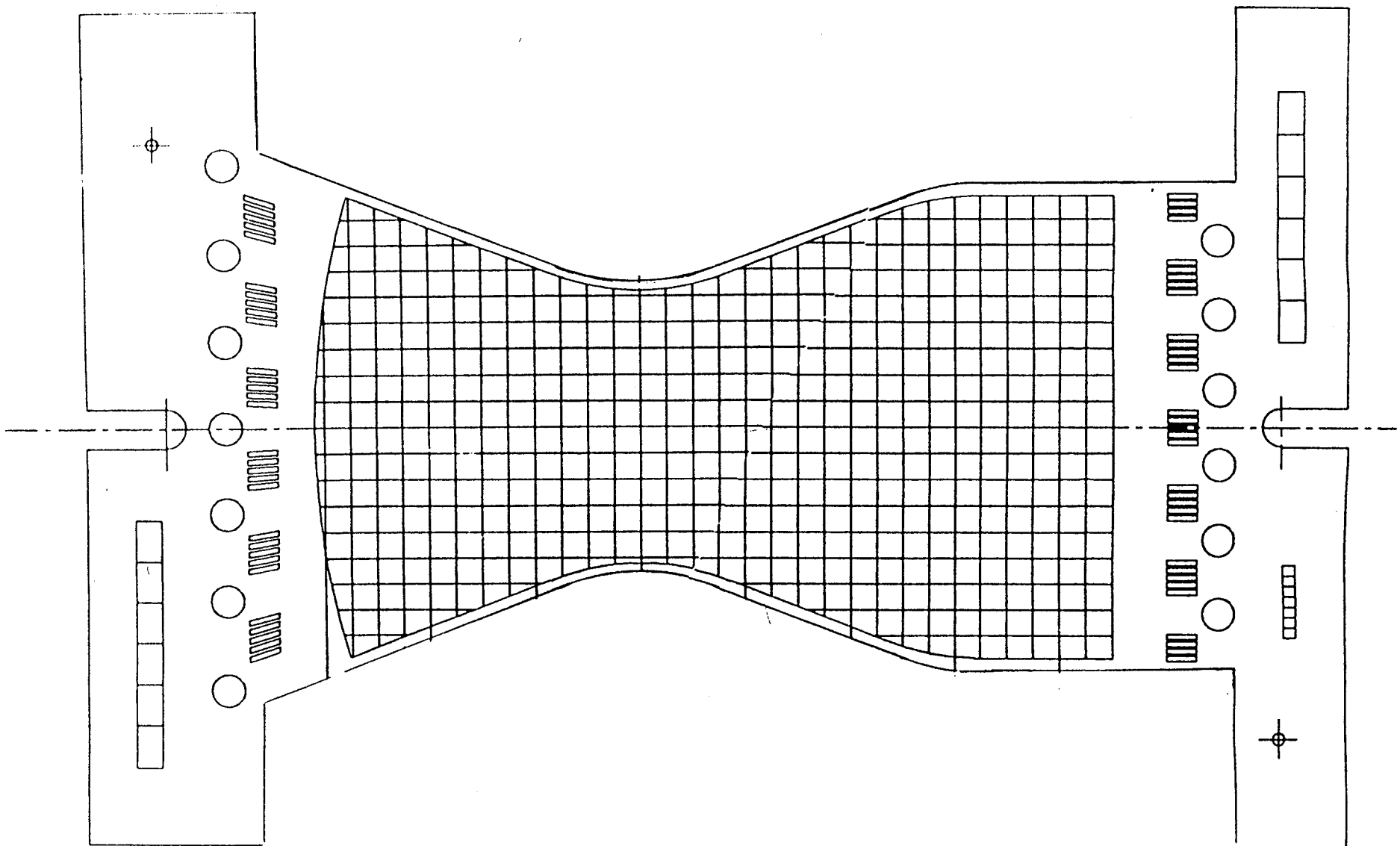
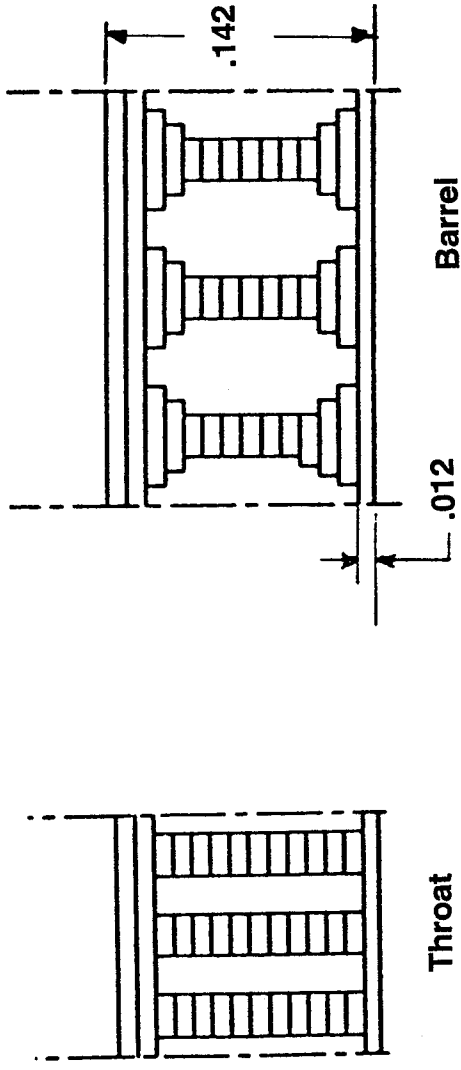


Figure 4.16. Fine Pattern Artwork Was Modified for T/R Study

Thin Panels



Thick Panels

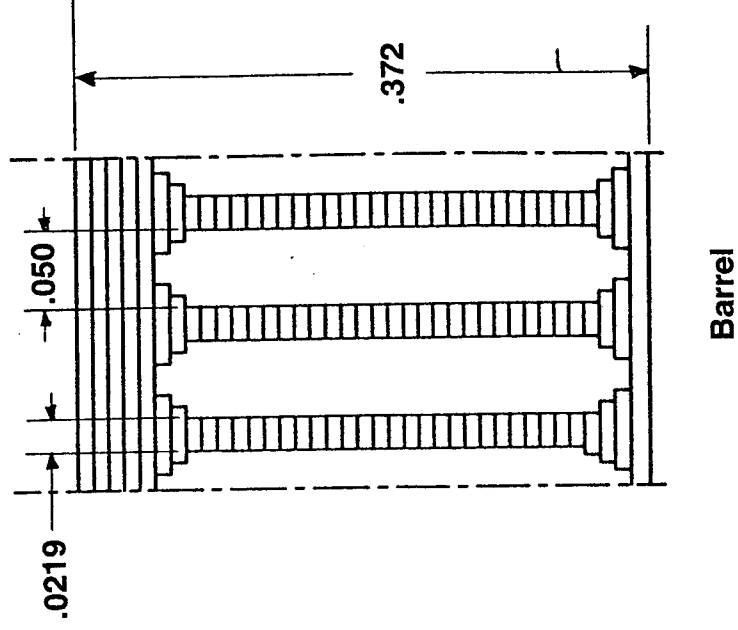
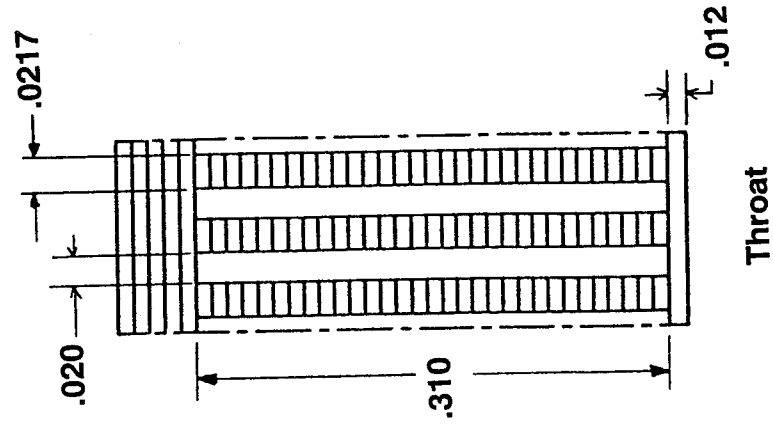


Figure 4.17 Second Series Panel Designs T/R Ratio Series

0.142 inch panels were mated to a 0.125 inch thick stainless steel shim and formed in the modified 3-D die with 0.250 opening.

A new panel design was made which was an iteration of the first fine-pattern design. This panel was the first attempt to take the as-formed location of the outer channel and re-position the channel on the flat panel design, such that when formed, the channel lies along the 90 degree edge of the part. The contours of a formed fine-pattern panel were measured with the Coordinate Measuring Machine (CMM) measuring machine. This data was put in a CAD database by the machine.

The grid pattern on the hot gas wall surface, which locates the outer channel, was then measured with the Optical Gaging Products (OGP) CMM. The OGP optically measured the location of the intersection of the grid pattern, and the data entered manually into the CAD database. The two pieces of data were then overlaid to find the three-dimensional location of the channel, and the distance from the 90 degree edge. The location of the new channel on a flat panel was then adjusted by this distance. The remaining channels were evenly spaced between the two outer channels.

The new panel also incorporated an expendable forming frame as shown in Figure 4.18. The frame is separated from the panel by a slot, to prevent channel deformations. A slot was included in each frame at the throat. Tooling pins on the die set engaged in the slot to help maintain alignment of the panel throat to the die throat. The tooling pins were added to the die as die Modification III. Channel layout and cross-sections are shown in Figures 4.19 and 4.20.

The second series panels were formed using the one-step forming process. Results of forming the thick and thin panels, as well as the remaining panels is presented in the Formed Panel Evaluation section.

4.5.7 Formed Panel Evaluations

4.5.7.1 Introduction

Numerous evaluation methods were used to analyze the formed panels. The evaluations were used to select the forming procedures and panel designs for best results. The methods are as follows:

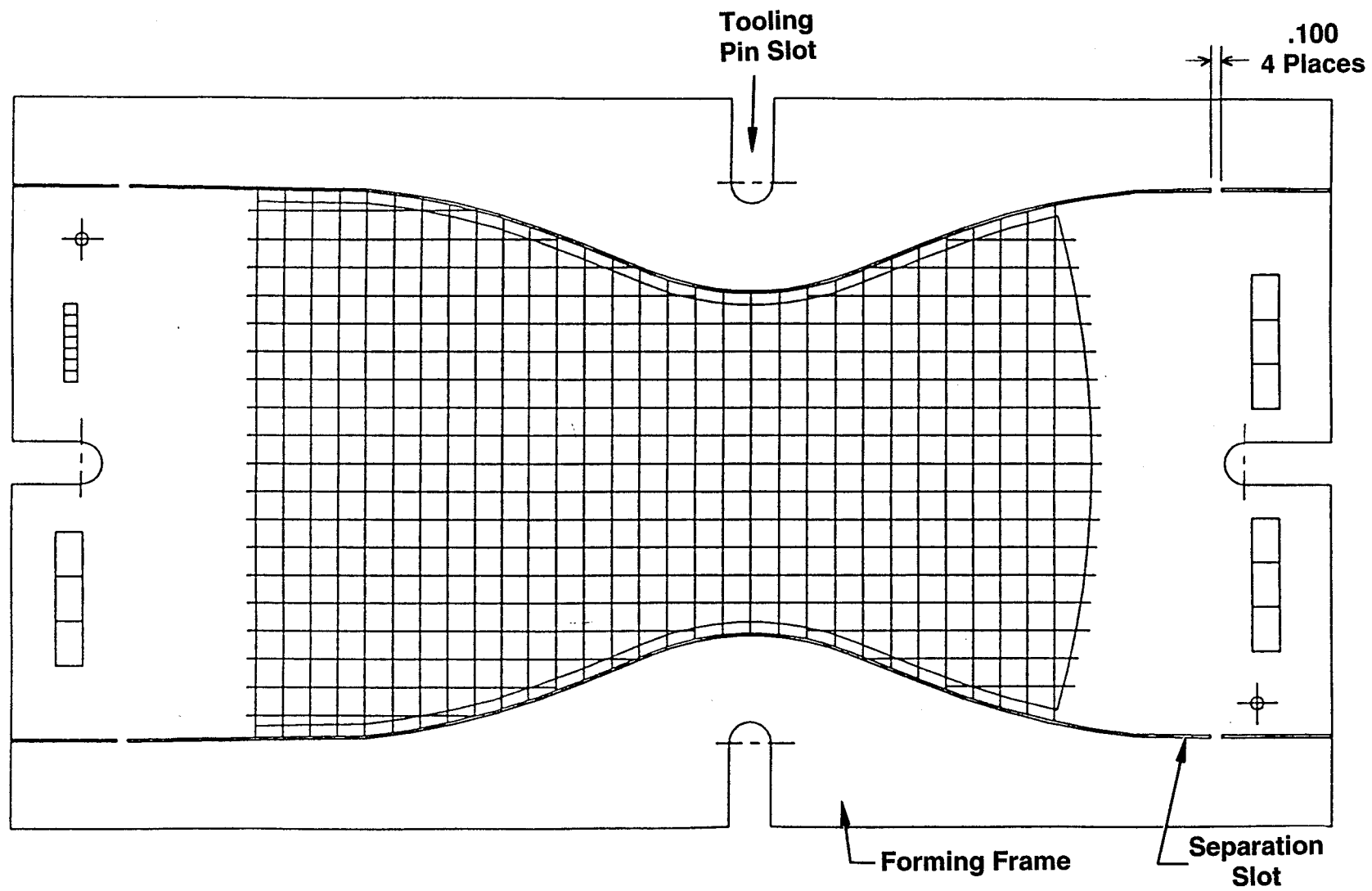
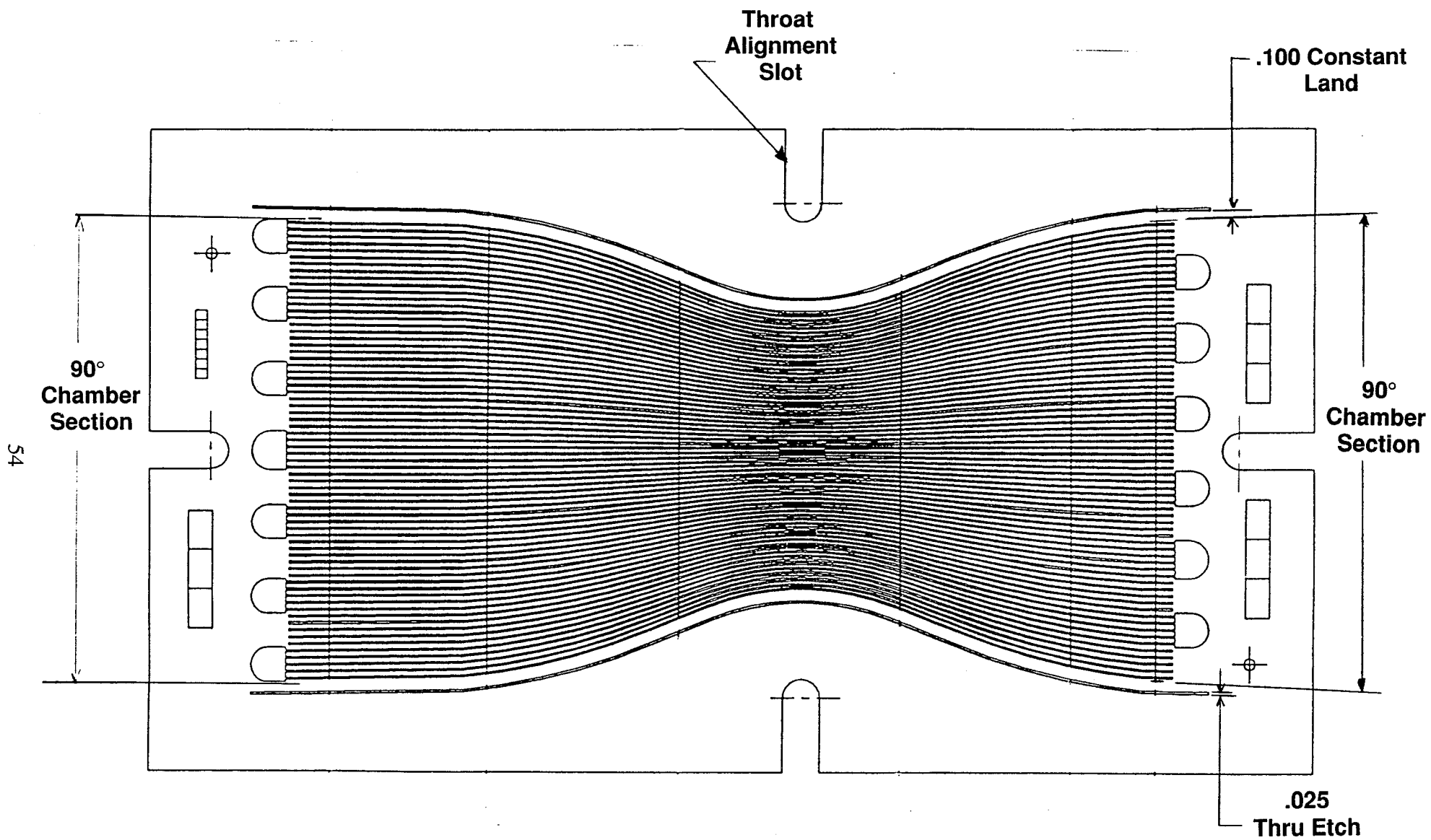


Figure 4.18. Second Iteration Panel Design



1

Figure 4.19. Second Iteration Platelet Design

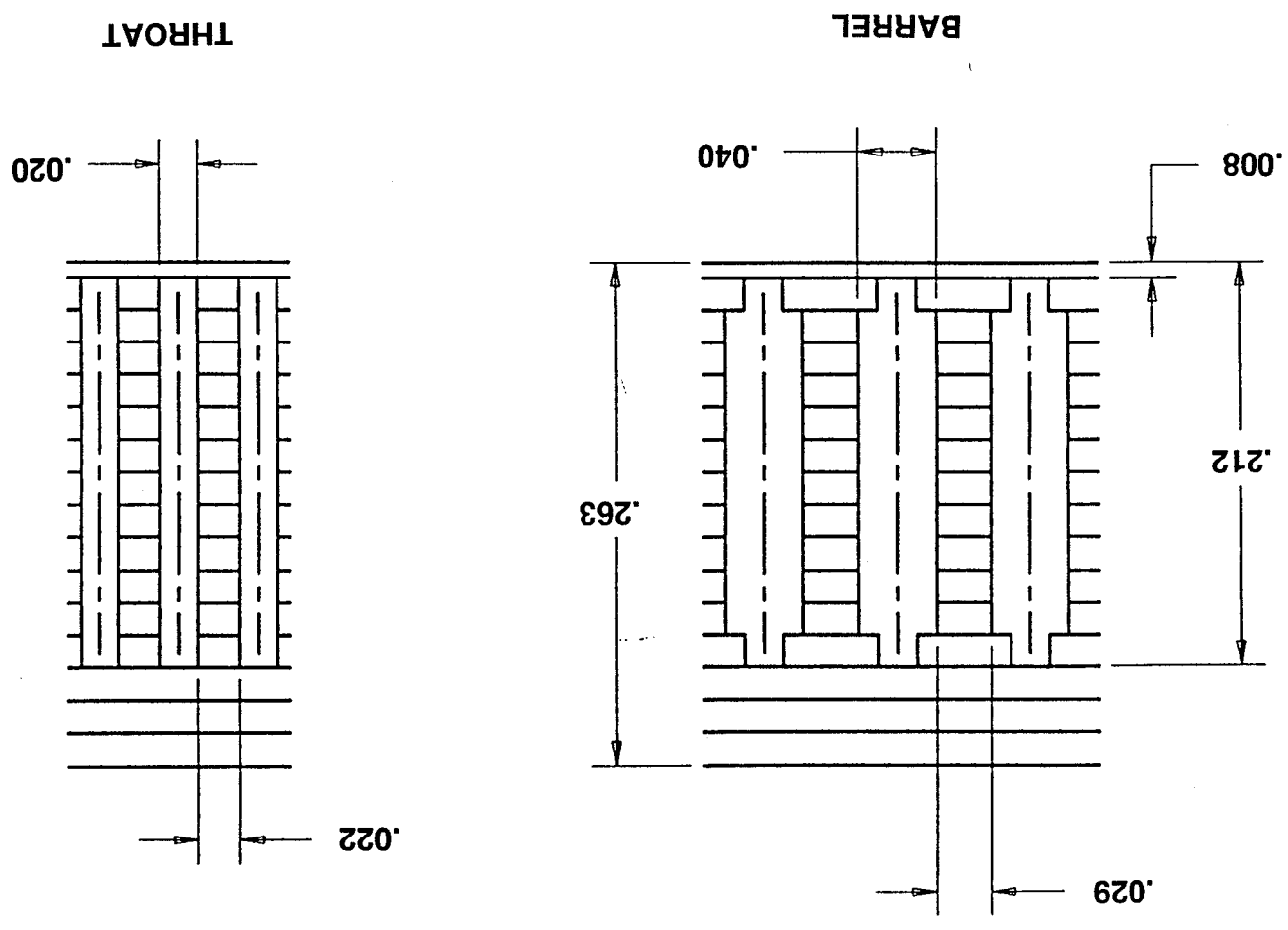


Figure 4.20 Second Iteration Channel Design

- Visual Examination
- Inter-Channel Leak Check
- Water Flow (Kw)
 - Flat Panel
 - Formed Panel
- Dimensional Inspection
 - Contour
 - Grid Pattern
- Sectioning
 - Metallographic Exam
 - Measurement
- X-Ray
- Ultrasonic
- Eddy-Current

4.5.7.2 Visual Examination

Visual examination of panels after forming revealed the relative success or problems associated with a given forming process. Cracking of close-out walls, as shown in Figure 4.10, provided the basis for die and panel modifications, and showed that single step forming superior is to the two-step method.

4.5.7.3 Leak Check

Most panels were inter-channel leak checked as flat panels. The panels were leak checked between the groups of channels, a group of three course pattern channels or five fine pattern channels. If a panel exhibited gross leakage, it would have been scrapped. No panels exhibited gross leakage.

A small amount of interchannel leakage could be tolerated in a functional panel. Three flat panels out of 43 indicated only a trace amount of leakage. The leakage was attributed to scratches on the platelets. Some of the early panels formed were also leak checked after forming. A leak after forming would indicate poor bond quality or tearing of the lands due to forming. No leaks were found in any formed panel.

4.5.7.4 Water Flow Testing

Two panels of each design were water flow tested. Water flow data of both flat and formed panels was used to compare the effect of panels formed with and without filler, as well as the channel deformation from forming. Because the channels were manifolded in groups, 5 for the fine pattern and 3 for the coarse pattern, individual channel flow variations are 'averaged' by the flows of adjacent channels. Flow results are shown in Figures 4.21 thru 4.26.

The results of flow testing show that forming does not adversely affect the flow characteristics of the platelet panels. The changes in mass flow rate are minimal from flat panel to formed panel. Changes in flow across formed panels previously filled with polymer were approximately 2% for coarse and fine pattern ZrCu panels. CRES 304L panels exhibited about 3% change in flow across the panel. Panels formed without polymer filler had mass flow variations of about 10%, which showed the benefits of using a channel filler. These flow rate variations are consistent with OME chamber data (a milled slot configuration), which also approached in the 10% range.

Cold flow results show that 3D forming of the platelet panels does not significantly affect the flow characteristics of the part. Because of the part to part repeatability between panels of the same design, any change in flow rate can be predicted and designed for. Mass flow distribution across the panel can be controlled by using the polymer filler material.

4.5.7.5 Dimensional Inspections

The formed panels were inspected with a Coord-Ax Coordinate Measuring Machine (CMM) and an Optical Gaging Products (OGP) CMM. The Coord-Ax touches the panel with a small diameter ball at pre-programmed locations, and returns the actual X, Y and Z coordinates of the locations to a CAD database. The OGP was used to measure optically the cross-grid locations of the grid pattern, giving their X and Y coordinates. The dimensional data was used to evaluate the contour, seam channel and throat locations of the formed panels.

The contour of the formed panels was measured using the Coord-Ax CMM. The inspections showed that cold forming of panels with net-shaped dies does not result in the desired contour, due to springback. The springback increases as the panel thickness increases, as shown in Figure 4.27.

The results of the contour measurements are illustrated in Figure 4.28. The data shows that the barrel radius was very close to the desired radius of 2.830 inches for all panel

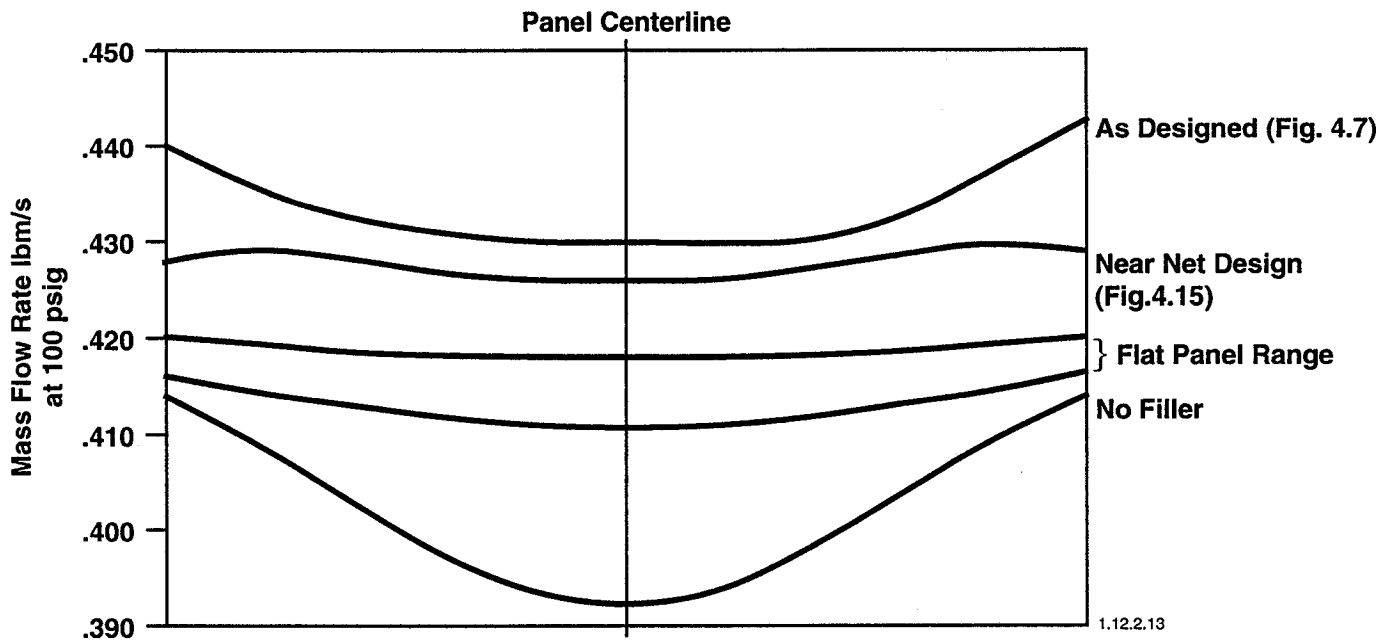


Figure 4.21 Flow Data Results ZrCu Coarse Pattern Panels

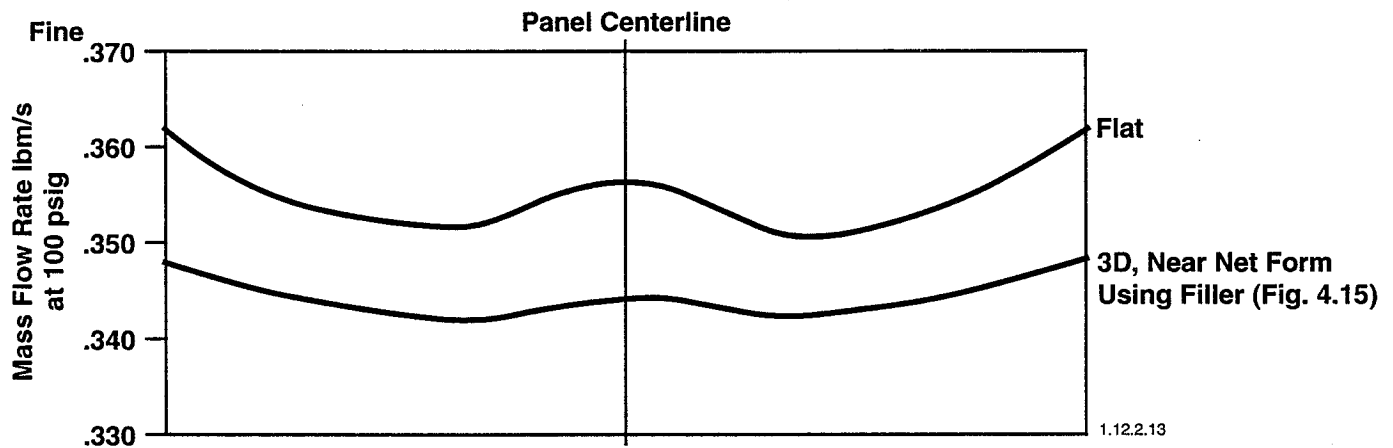


Figure 4.22 ZrCu Fine and Stepped Patterns Cold Flow Results

- Fine Pattern panels formed in near net configuration with filter material maintained mass flow distribution across panel within 2%

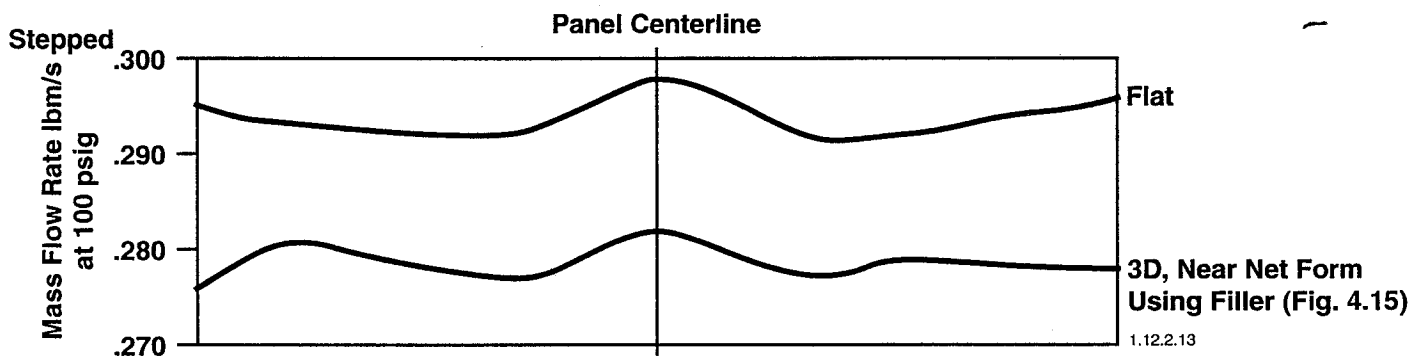


Figure 4.23 Cold Flow Results ZrCu Stepped Pattern

- Fine Pattern panels formed in near net configuration with filter material maintained mass flow distribution across panel within 2%

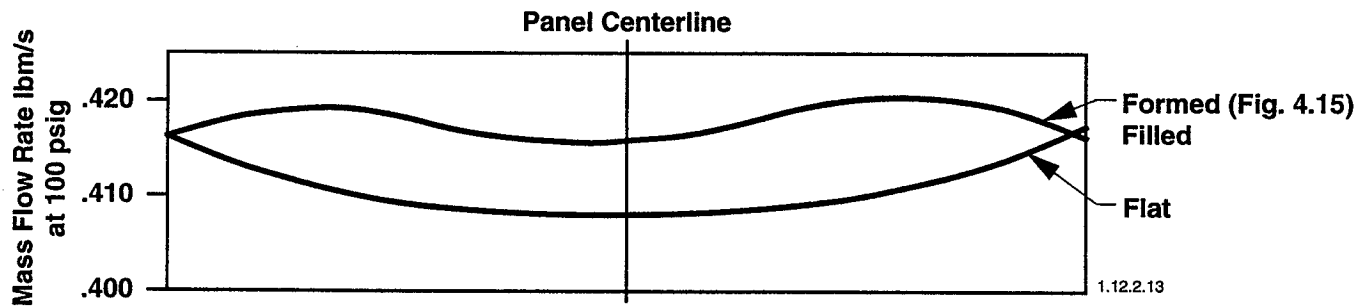


Figure 4.24 Cold Flow Results CRES-304L Coarse Pattern

- Fine Pattern panels formed in near net configuration with filter material maintained mass flow distribution across panel within 3%

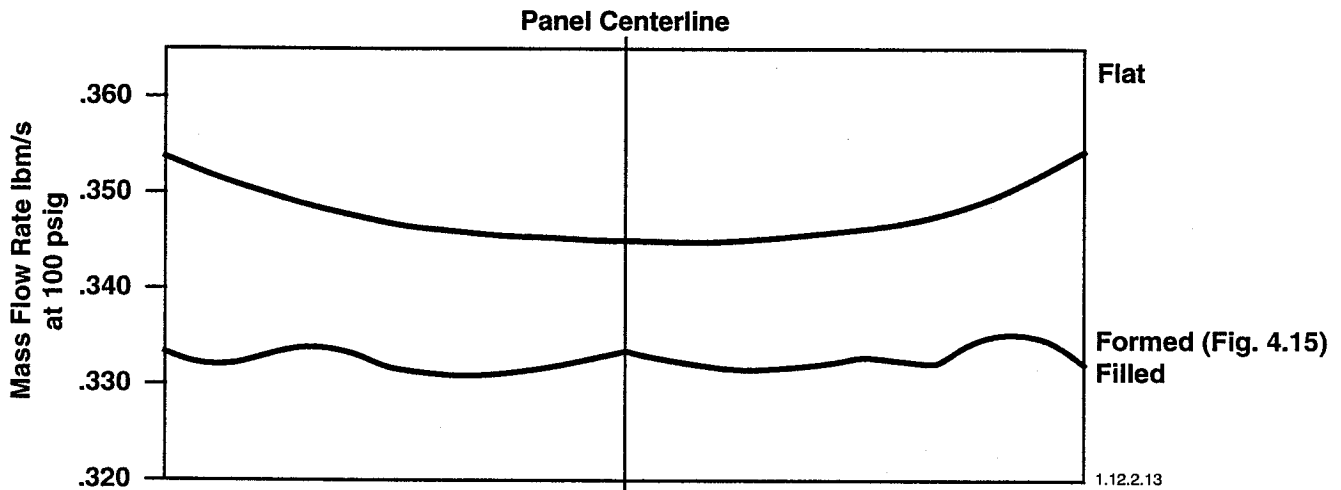


Figure 4.25 Cold Flow Results CRES-304L Fine Pattern

- Fine Pattern panels formed in near net configuration with filter material maintained mass flow distribution across panel within 3%

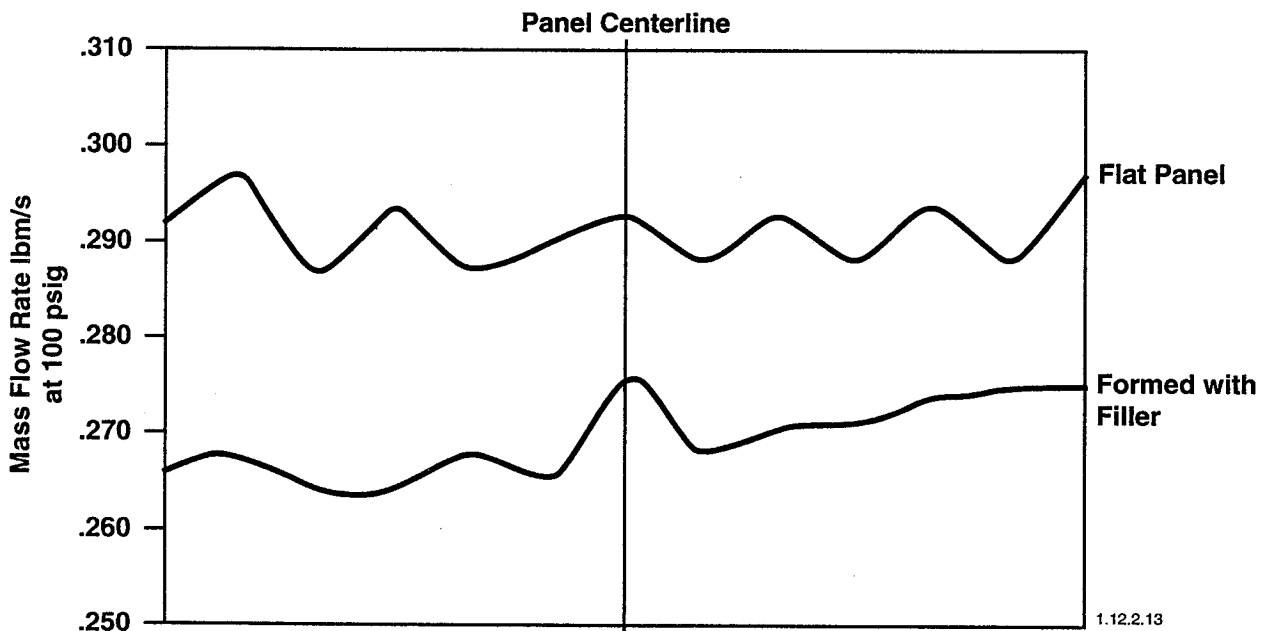


Figure 4.26 Cold Flow Results CRES-304L Stepped Pattern

- Fine Pattern panels formed in near net configuration with filter material maintained mass flow distribution across panel within 4%

Part No.	SN	Panel Thickness	R Barrel	R Throat	
Die Design	—	0.262	2.830	1.655	
1204190-19	SN019	0.255	2.830	1.715	1st Iteration Fine Pattern
1204435-9	SN003	0.142*	2.833	1.724	Thin Panel/Fine Pattern
120796-9	SN001	0.266	2.828	1.727	2nd Iteration Panel Design/Fine Pattern
1204435-19	SN001	0.376	2.837	1.832	Thick Panel/Fine Pattern

13.4.22

* Thin Panels Were Formed Using 0.125 Stainless Steel Shims.
Total Part Thickness While Forming Was 0.267

Figure 4.27. Spring Back in the Throat Section Increases With Panel Thickness

Serial #	Stack Height	R _{barrel}	R _{throat}	
006	.242	2.876	1.666	Coarse pattern ZrCu Not machined prior to form
011	.242	2.860	1.662	
014	.242	2.866	1.662	
005	.242	2.835	1.676	Secondary form with original 1 step die
005	.242	2.839	1.702	Coarse ZrCu, Near Net
009	.242	2.827	1.688	
027	.250	2.825	1.704	Coarse SS, Near Net, 1st Hit
027	.250	2.834	1.696	Coarse SS, Near Net, 2nd Hit
039	.254	2.826	1.704	Coarse SS, Near Net, Tabs Removed
018	.254	2.818	1.699	Fine ZrCu, Near Net
019	.255	2.830	1.715	
031	.250	2.836	1.728	Fine SS, Near Net
032	.251	2.821	1.730	
021	.254	2.834	1.676	ZrCu Fine, No Filler, Near Net
023	.256	2.834	1.728	ZrCu Stepped, Near Net
024	.255	2.827	1.717	
035	.250	2.844	1.744	SS Stepped, Near Net
Nominal Design		2.830	1.655	

VARIATIONS IN CONTOUR DATA IS DUE TO DIFFERENT PART THICKNESSES

Figure 4.28. Results of Contour Measurements 1st and 2nd Panel Design

thicknesses. All panels showed spring-back in the throat. Comparison of all panels indicates that the amount of spring-back in the throat is a function of panel thickness. Thicker panels show more spring-back than thinner panels. The 0.142, 0.255 and 0.266 inch thick panels all have similar contours. Since the thin panels were formed using 0.125 inch stainless steel shims, the total thickness of the part while forming was 0.267. Thick panels show a marked increase in the amount of spring-back in the throat.

The contour of the forming dies was also measured using the Coord-Ax CMM. The data indicates the alignment between the male and female dies is within about 0.002 in. The gap, however, varies from 0.253 to 0.256 inch in the converging section to 0.262 inch in the throat, barrel and aft sections. This gap was shown to be acceptable. The die gap is illustrated in Figure 4.29.

Seam channel and throat locations were determined with the OGP. This OGP data, when coupled with the contour inspection data using the CAD, located the edge of the seam channel in three-dimensional space. The distance could then be measured from the actual edge of the channel to the desired location (90 degree sector.) This distance was then used to adjust the flat platelet design layout to relocate the seam channel on the flat panels. The data coupling method was used for panel designs two and three.

Subsequent improvements to the OGP software programs allowed all three coordinates of a grid cross-pattern to be measured optically. This eliminated the need for the Coord-Ax measurement step and improved the accuracy of the CAD database. Formed panels of the third design were measured in this method.

To join four quarter panels properly the axial interface between the four panels must be in perfect alignment along the entire length of the contour. Panel interfaces must be flat and parallel to each other to accommodate a laser beam seal weld on both the inside and outside diameter on each seam.

A comparison of the actual panel edge locations for the first and second designs is shown in Figure 4.30. Although the second design had the panel edge closer to the desired 90 degree plane, there was sufficient deviation to prevent joining of two panels.

4.5.7.6 Sectioning

Various panels were sectioned after forming to allow metallographic examination and dimensional inspection of the internal geometry.

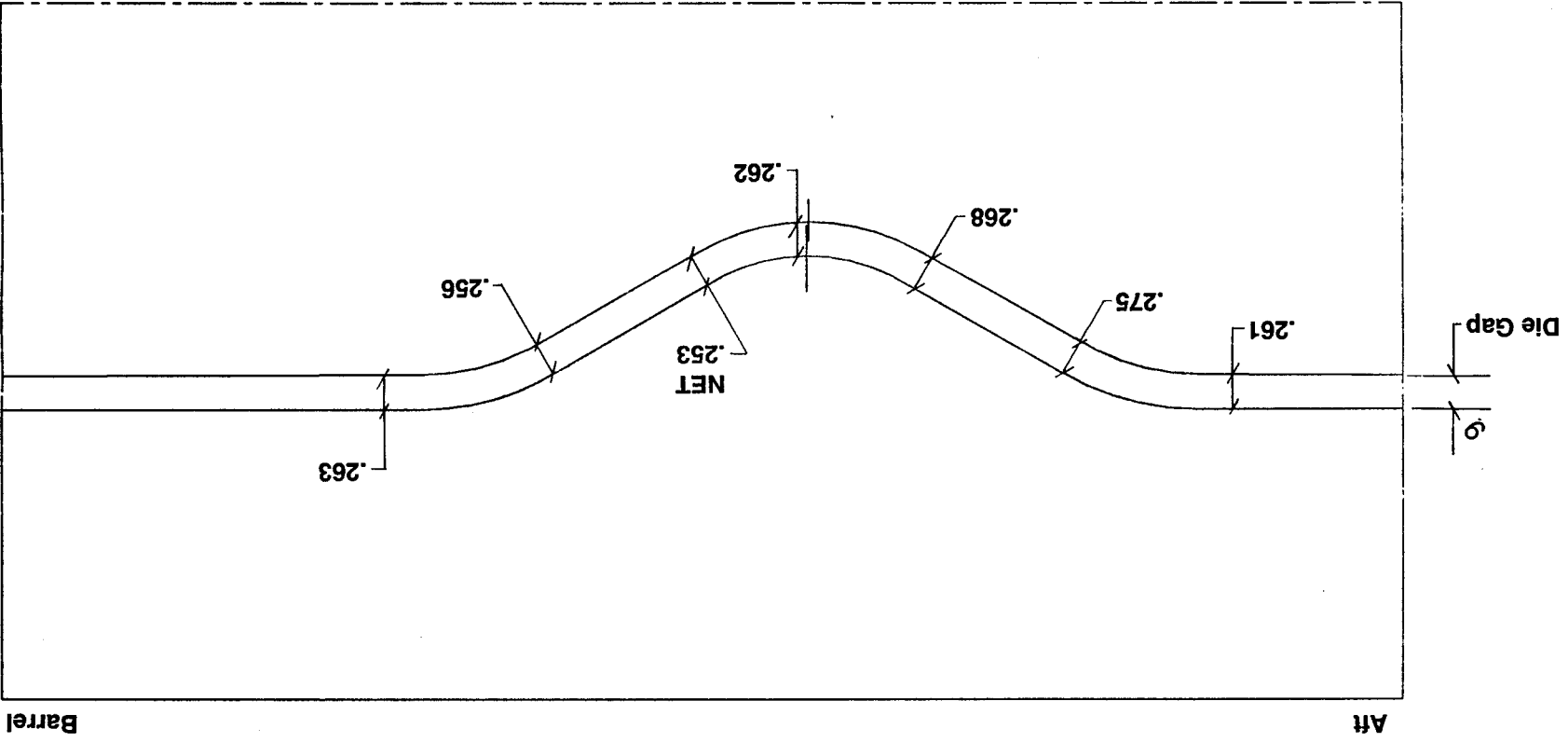
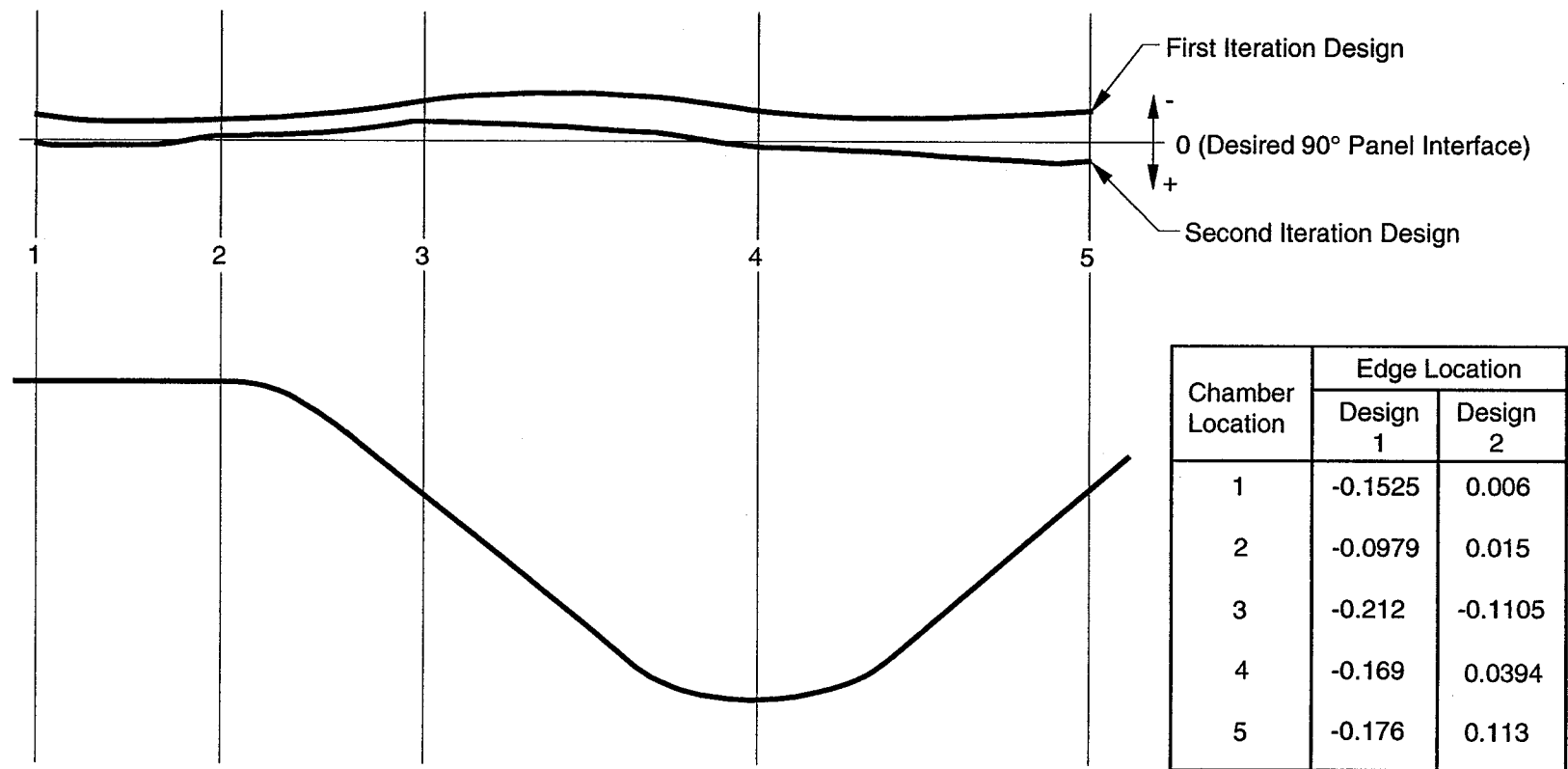


Figure 4.29. Die Gap Varies Along the Chamber Axis



13.4.23A

Figure 4.30. Second Iteration Design Showed Improved Edge Location After Forming

Metallographic examination revealed quality bonds on all sections examined. No disbonds or delaminations were evident in any of the cross-sections. Photomicrographs of typical bonds are shown in Section 5, Platelet Stack Joining.

Measurements were made of the channel orientation, channel geometry and hot gas wall thickness. Skewing of the channels near the outer edges of the panels was observed. The channels tended to tip, or lean toward the panel center at the O.D. of the panel, as illustrated in Figure 4.31. Filler material reduced the amount of channel tip as shown in Figure 4.32.

The channel and land dimensions changed slightly after forming. In ZrCu fine, stepped pattern panels the hot gas wall thickness at the throat increased about 0.001 to 0.002 inch, and the channel decreased in width by 0.001 to 0.003 inch. Measurements made of various panel designs are presented in Table 4.3.

4.5.7.7 Additional Evaluations Performed

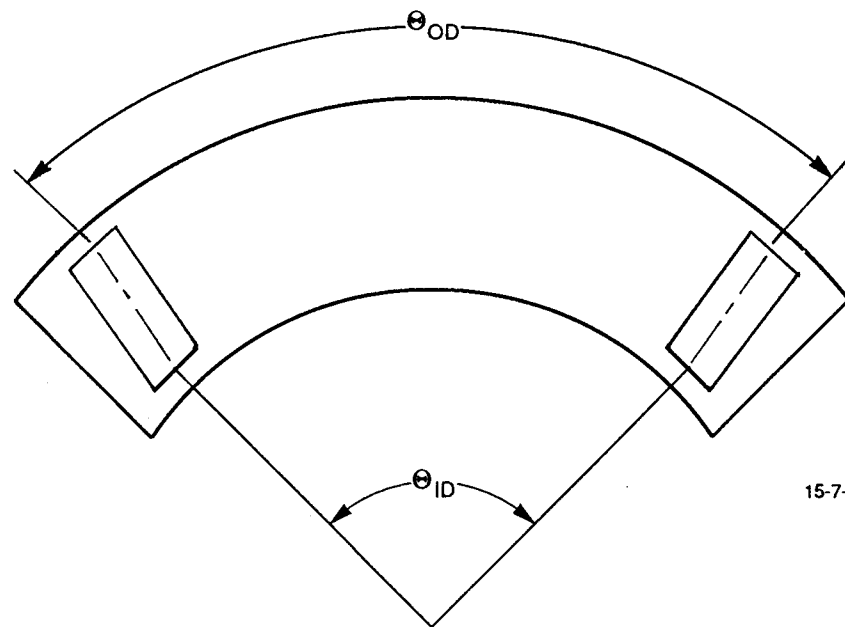
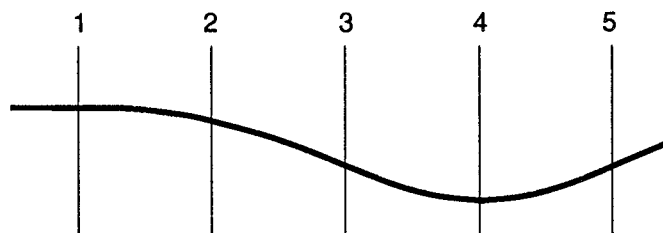
Several additional non-destructive test techniques were studied to determine their effectiveness in evaluating the internal geometry of formed panels. X-Ray, Ultrasonic, Eddy-Current and CT-Scan inspection techniques were evaluated. The techniques were to be used to determine the location of the outboard, or seam channel such that the seam land thickness after panel trimming could be determined. The CT-Scan appeared to be the most promising of these techniques, but further development would be required before using it to locate channels. However, improvements in OGP CMM technique allowed direct measurement of the grid pattern in X, Y, and Z coordinates. Thus the location of the seam channel was determined without the need for additional inspections.

4.6 TASK 1.7 3D PANEL JOINING DEMONSTRATION

4.6.1 Introduction

Task 1.7 demonstrated the joining of formed platelet panels. A new channel configuration was designed, panels fabricated and formed and two assemblies of two panels each was made. Only the panel design and forming will be discussed here. The assembly procedure will be discussed in Section 5, Panel Joining Demonstration.

Part Number	Panel Thickness	1		2		3		4		5	
		θ_{ID}	θ_{OD}	θ_{ID}	θ_{OD}	θ_{ID}	θ_{OD}	θ_{ID}	θ_{OD}	θ_{ID}	θ_{OD}
1204435-9	0.142	87.9	87.4	89.0	88.5	85.8	84.6	79.7	78.5	87.0	85.6
1204190-19	0.252	83.9	83.5	86.1	85.9	80.1	78.6	79.8	77.5	81.7	81.0
1204435-19	0.376	83.9	81.0	87.6	82.0	78.2	77.6	76.5	69.0	78.6	78.2

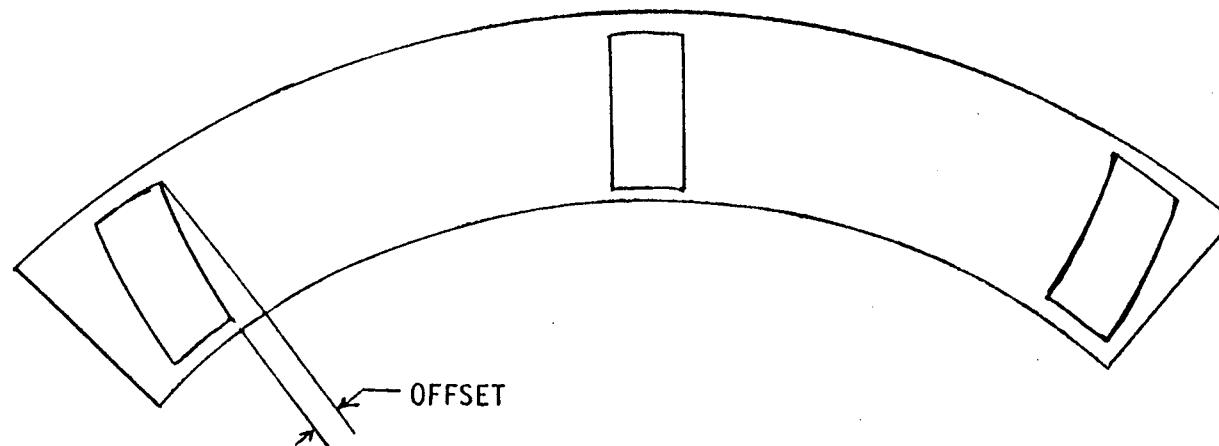


15-7-23

Figure 4.31. Skew of the Channel Along the Chamber Axis Increases With Part Thickness

MAX
CHANNEL
OFFSET

COURSE PATTERN	
FILLER	NO FILLER
.006	.015



FILLER MATERIAL REDUCES DISTORTION OF CHANNELS DURING FORMING

Figure 4.32. Section Testing Results

TABLE 4.3

SECTION TESTING RESULTS ZrCu COARSE PATTERN, Page 1 of 5

		GAS SIDE WALL THICKNESS	CHANNEL WIDTH		CHANNEL HEIGHT	CLOSEOUT THICKNESS
			I.D.	O.D.		
THROAT	Nominal Design	.030	.040	.040	.190	.020
	Formed with Filler	.032 to .033	.033 to .035	.035 to .040	.197 to .198	.021 to .023
	Formed No Filler	.330 to .0353	.028 to .030	.030 to .036	.184 to .190	.023 to .025
	Near Net Formed with Filler	.029 to .030	.035 to .038	.040 to .044	.190 to .195	.019 to .021
BARREL	Nominal Design	.030	.080	.080	.190	.020
	Formed with Filler	.030	.079 to .083	.083 to .086	.187 to .190	.020
	Formed No Filler	.030 to .031	.080 to .083	.083 to .086	.189 to .191	.019 to .020
	Near Net formed with Filler	.031 to .032	.078 to .081	.084 to .085	.190 to .191	.018 to .020

TABLE 4.3

SECTION TESTING RESULTS CRES 304L COARSE PATTERN, Page 2 of 5

		GAS SIDE WALL THICKNESS	CHANNEL WIDTH		CHANNEL HEIGHT	CLOSEOUT THICKNESS
			I.D.	O.D.		
THROAT	Nominal Design	.030	.040	.040	.190	.030
	Formed with Filler	.029 to .032	.035 to .036	.039 to .043	.186 to .194	.030 to .032
BARREL	Nominal Design	.030	.080	.080	.190	.030
	Formed with Filler	.031 to .032	.079 to .082	.082 to .085	.187 to .190	.028 to .030

TABLE 4.3

SECTION TESTING RESULTS ZrCu STEPPED PATTERN, Page 3 of 5

		GAS SIDE WALL THICKNESS	CHANNEL WIDTH		CHANNEL HEIGHT	CLOSEOUT THICKNESS
			I.D.	O.D.		
THROAT	Nominal Design	.012	.020	.020	.144	.100
	3D Formed Filler	.013 to .014	.0138 to .0155	.0176 to .0199	.140 to .144	.096 to .102
BARREL	Nominal Design	.012	.050	.050	.184	.058
	3D Formed Filler	.012 to .013	.0475 to .0486	.0463 to .0497	.0186 to .0188	.055 to .057

TABLE 4.3

SECTION TESTING RESULTS CRES 304L FINE PATTERN, Page 4 of 5

		GAS SIDE WALL THICKNESS	CHANNEL WIDTH		CHANNEL HEIGHT	CLOSEOUT THICKNESS
			I.D.	O.D.		
THROAT	Nominal Design	.010	.020	.020	.190	.050
	3D Formed Filler	.009 to .011	.0176 to .021	.0199 to .0121	.184 to .192	.051 to .052
BARREL	Nominal Design	.010	.050	.050	.190	.050
	3D Formed Filler	.011 to .012	.0497 to .0508	.0508 to .0519	.189 to .190	.0474 to .0496

TABLE 4.3

SECTION TESTING RESULTS ZrCu FINE PATTERN, Page 5 of 5

		GAS SIDE WALL THICKNESS	CHANNEL WIDTH		CHANNEL HEIGHT	CLOSEOUT THICKNESS
			I.D.	O.D.		
THROAT	Nominal Design	.012	.020	.020	.190	.050
	Formed with Filler	.012 to .013	.017 to .018	.019 to .020	.190 to .193	.051 to .053
BARREL	Nominal Design	.012	.050	.050	.190	.050
	Formed with Filler	.012 to .014	.046 to .049	.047 to .050	.190 to .192	.049 to .050

4.6.2 Platelet Design

Eight panels, part number 1206530, were fabricated for this task. The channel design was an iteration of the second panel design from Task 1.3, part number 1204796. A computerized method for predicting the location for the 90° located panel edges, known as the Transformation Equation, was developed and used for the design of these panels, and is described below. The panel design was similar to the Forming Experiment panel designs, with the exception of the slots for the forming throat pins. The slots were closed, as shown in Figure 4.33, to prevent deformation (widening) of the slot during forming. Previous slot deformation had led to misalignment of the panel in the forming dies, resulting in throat shift.

4.6.3 The Transformation Equation

The forming of a platelet panel to a three dimensional chamber shape from a flat panel distorts the location of the channels. When designing the flat panel, the channels must be placed such that after forming, they end up in the proper location to allow trimming of the panels to a 90 degree segment. The desired panel design should have, after trimming, a .020 constant land width between the last channel and the edge of the part.

The channels in the first panel design were located assuming that the surface of the hot gas wall does not deform during panel forming. After measuring the location of the edge of the first panel after forming, the second channel design was modified to account for the stretch and deformation of the panel during forming. In this second design, the location of a channel station was changed by the distance from the desired to the actual location on the formed panel. Although the location of the outer channel was closer to the desired location, the channel position was still not correct. Figure 4.34 illustrates the edge locations of both panel designs.

A method was developed to improve the prediction techniques by accounting for the stretch, or deformation of the panel due to forming. A set of transformation equations was developed to predict the channel locations for new iterations. These equations related the location of features on a formed panel to the desired feature location, and then predicted the feature location on a new flat panel design compared to the old design.

The improved method of predicting channel location requires an initial panel design from which to iterate. The panel edge data and deformed areas are obtained from OGP measurements of the intersection of lightly-etched grids placed on the hot gas wall. A functional

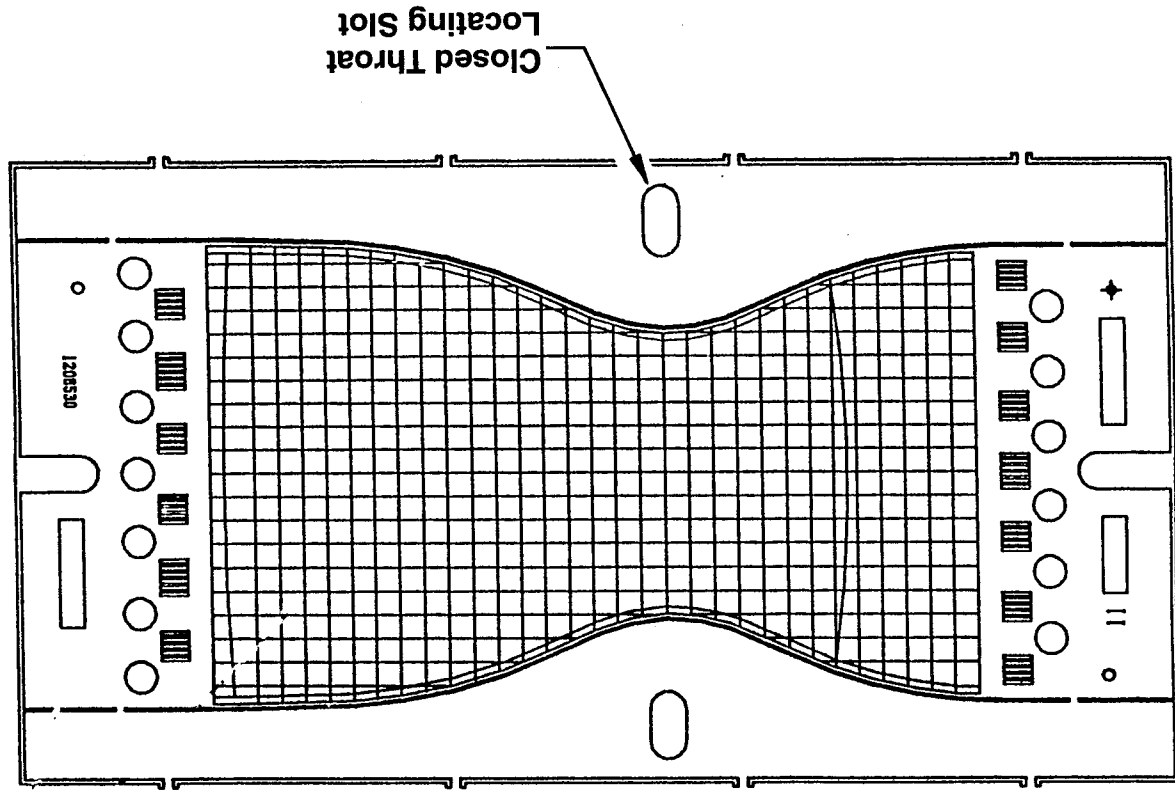


Figure 4.33. Panel Jointing Demonstration Platelet Design

EDGE LOCATION FROM NOMINAL

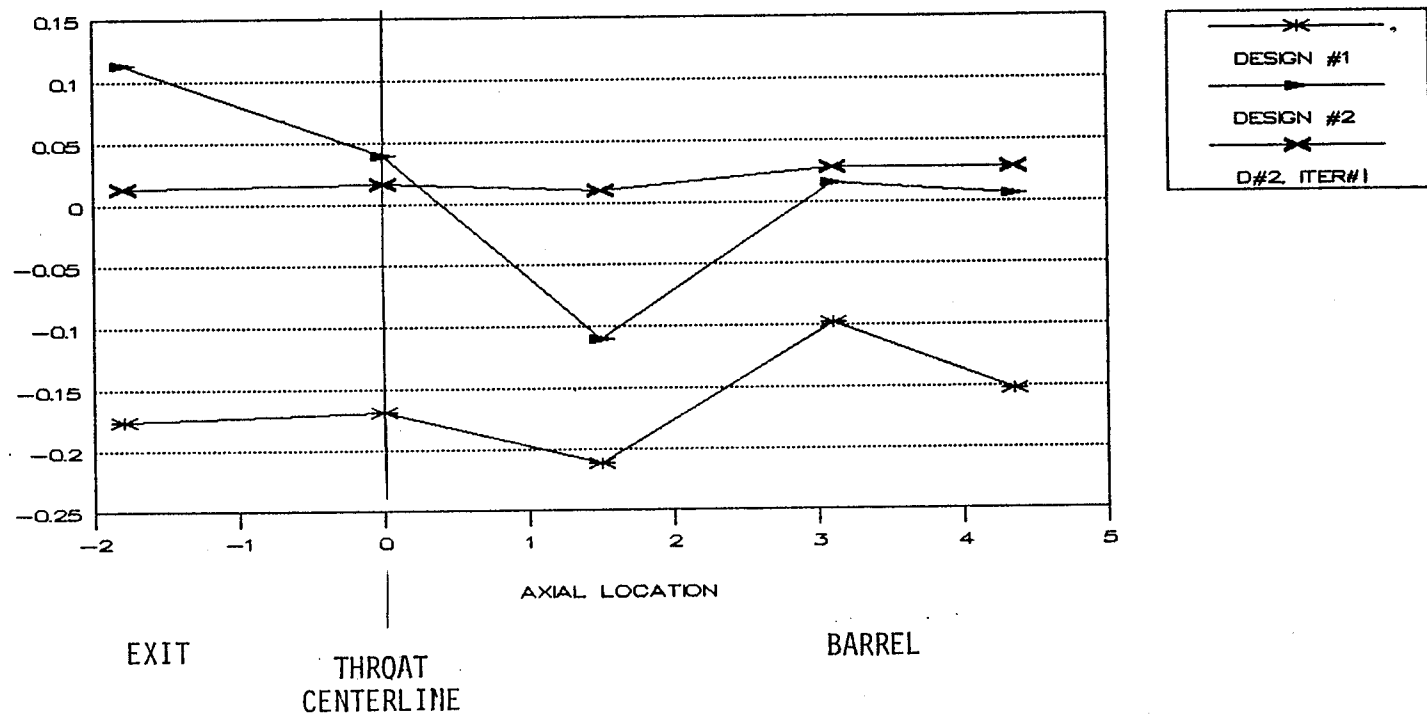


Figure 4.34. Seam Channel Land Location Results

part can be made after the proper location of the channels is known by not etching the grid pattern on the hot gas wall.

4.6.4 Forming Results

Eight panels with the improved channel design were cold formed. Measurements of the distance from the outer channel edge to the desired 90 degree edge location is shown in Figure 4.35. The channel was close enough to the desired location to allow trimming and joining of two panels while maintaining the intended 0.020 inch minimum half land. The trimming plane of the panel was slightly outboard of the 90 degree location, however, which would prevent assembly of four panels of this design.

4.7 TASK 1.9 CONTOUR FORMING EXPERIMENTS

4.7.1 Introduction

Contour measurements of panels formed during Task 1.3 indicated springback significant enough to require a modification to the forming method. Two methods of eliminating the springback were considered; over-forming and hot-sizing.

The first method, overforming the panel to a bend radius sharper than the desired radius, would require successive die contour iterations to achieve the correct contour. Although the overforming approach may be appropriate for large-quantity production runs, it was deemed too costly for the Formed Platelet Liner program due to the number of die modifications anticipated.

An alternate approach to eliminating springback, hot-sizing, was pursued. The hot-sizing method places a formed panel into a die set with the desired contour, and stress relieves the panel in a restrained condition to remove the residual stresses from forming. Three hot-sizing experiments were conducted to optimize the hot-sizing parameters.

4.7.2 Discussion

Eight new panels were fabricated for this task. The panel design used was a modified first design fine pattern, part number 1204435. Five new platelet patterns were made which decreased the channel height in the throat area. A decreased throat channel height is reflective of a functional panel, and when used in the hot-sizing experiments, would yield more

77

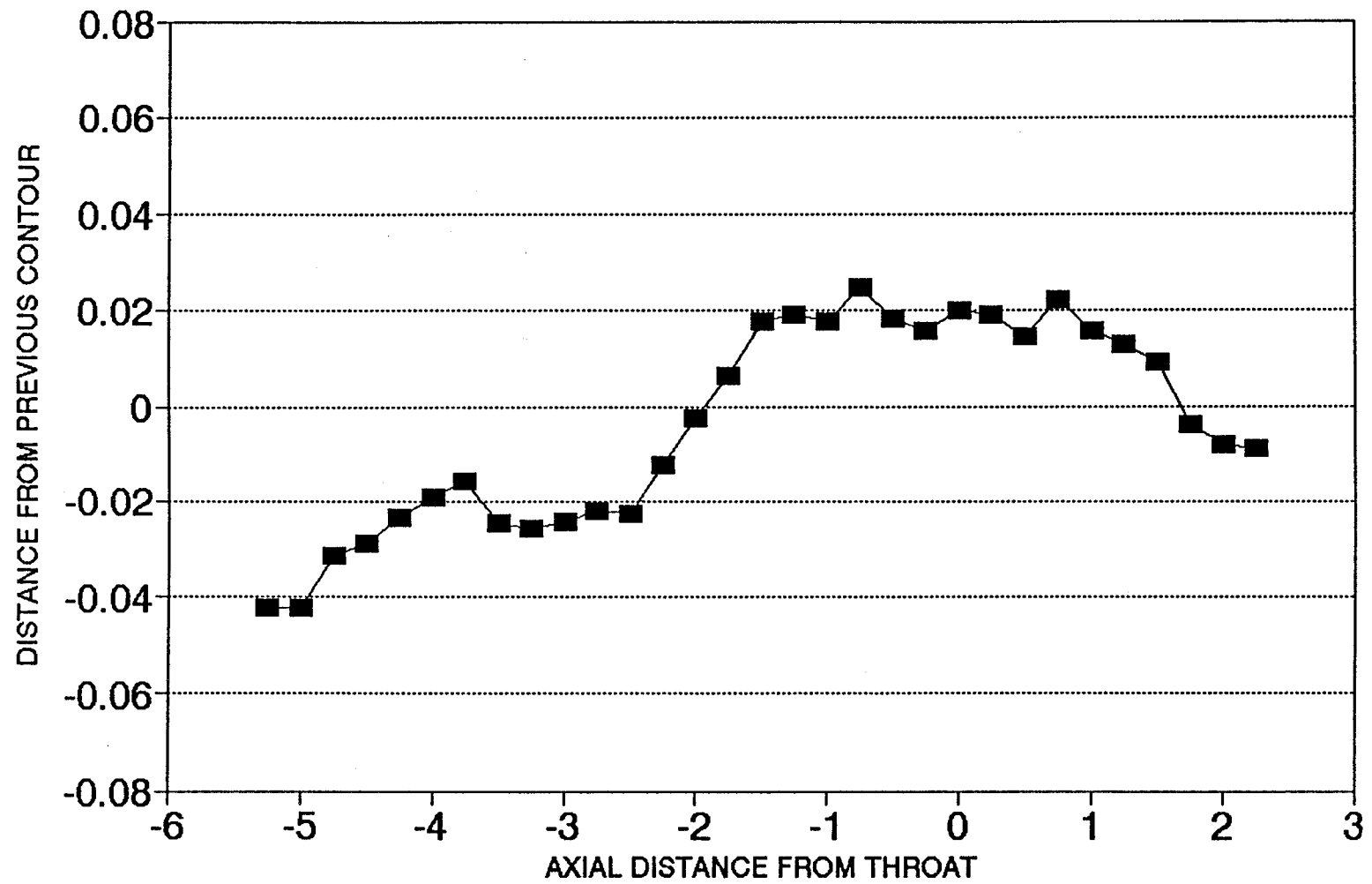


Figure 4.35. Formed Platelet Edge Deviation 3D Joining Demo Panels

pertinent data. The eight panels were cold-formed using the one-step process with the modified die set.

Another set of panels was designed and fabricated during the same time, the Panel Joining Demonstration panels. These panels also had a channel design with a reduced throat height. In addition, the outer channel location in these panels had been relocated to allow joining of two 90 degree panel segments after forming. Because the Panel Joining Demonstration panels were completed before the hot-sizing experiments began, and as these panels were to be used as a basis for iteration for the Phase B panels, they were used for hot-sizing.

A hot size die was fabricated with the desired final contour, and is shown in Figure 4.36. The die contours were measured with the COORD-AX CMM, and the die gap calculated. The die gap was found to be 0.002 inch smaller than the panel thickness in the barrel region. However, the panels were also thinner in edges of the throat region by 0.007 inch.

4.7.3 Hot Sizing Experiments

Three hot sizing experiments were conducted. The parameters for the first experiment allowed the panel to be annealed in the restrained condition. A 0.002 inch shim was placed between the die halves at the periphery, the shim prevented excessive crushing, or creep, of the panel. After the experiment was run it was found that a gap remained between the shim and the die.

Inspection of the first panel after the hot sizing operation showed that in areas where full contact was made the shape of the fixture was exceedingly well duplicated. In areas where full contact was not made the contour was improved but not to the final desired contour. The two subsequent experiments attempted to compensate for the thick areas of the panel, such that in the thin (throat) areas the desired contour could be obtained.

The results of the second experiment showed an improvement over the first, although full contact to the I.D. die was not yet made. The same panel was then run through another hot sizing at increased time and pressure. This set of parameters allows the panel to very nearly replicate the desired inside contour, as shown in Figures 4.37 and 4.38. The panel formed with the third set of hot-sizing parameters is within 0.003 inch of the nominal contour.

ORIGINAL PAGE
BLACK AND WHITE PHOTOGRAPH

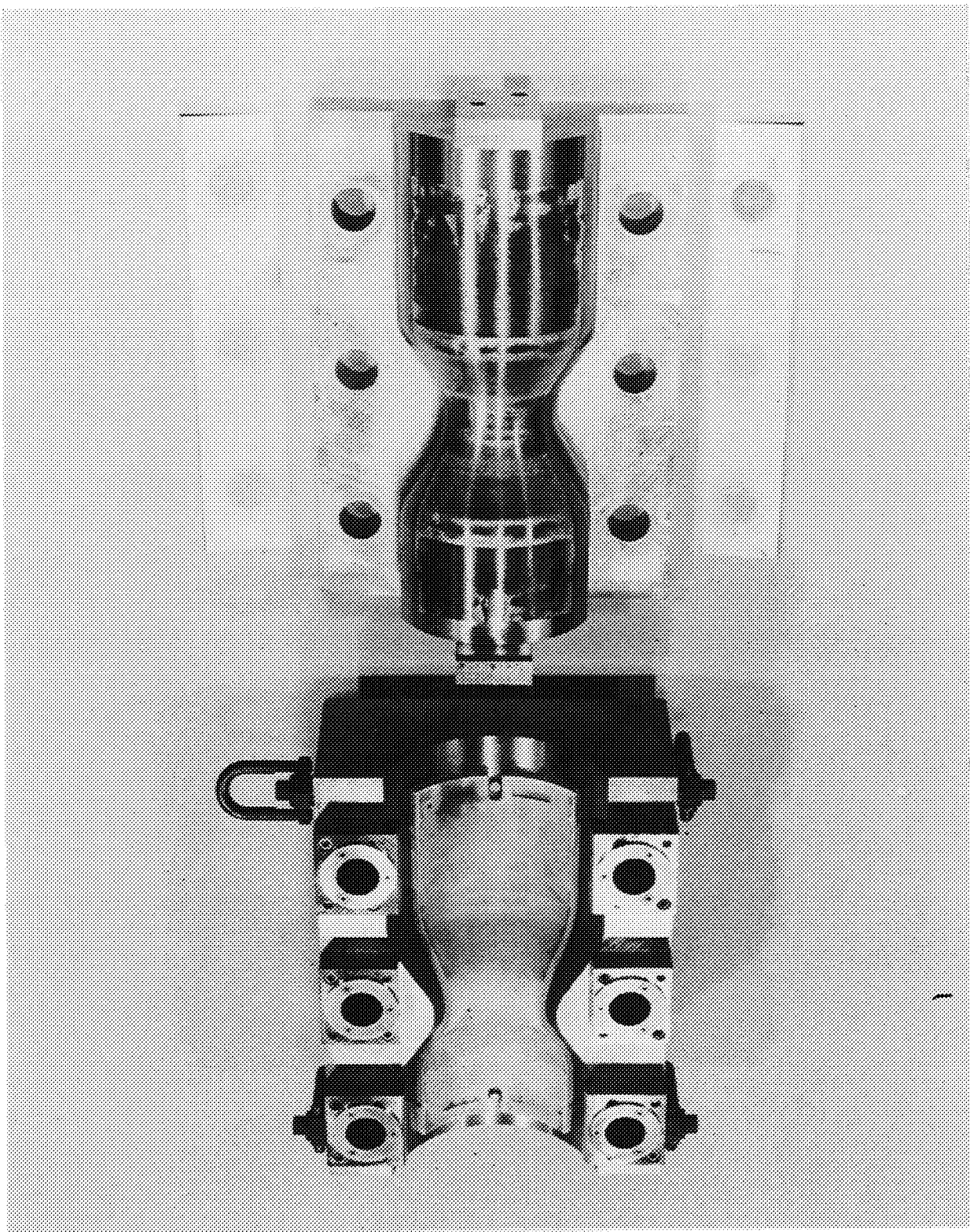


Figure 4.36. Restrain Anneal Fixture

Restrained Anneal Results

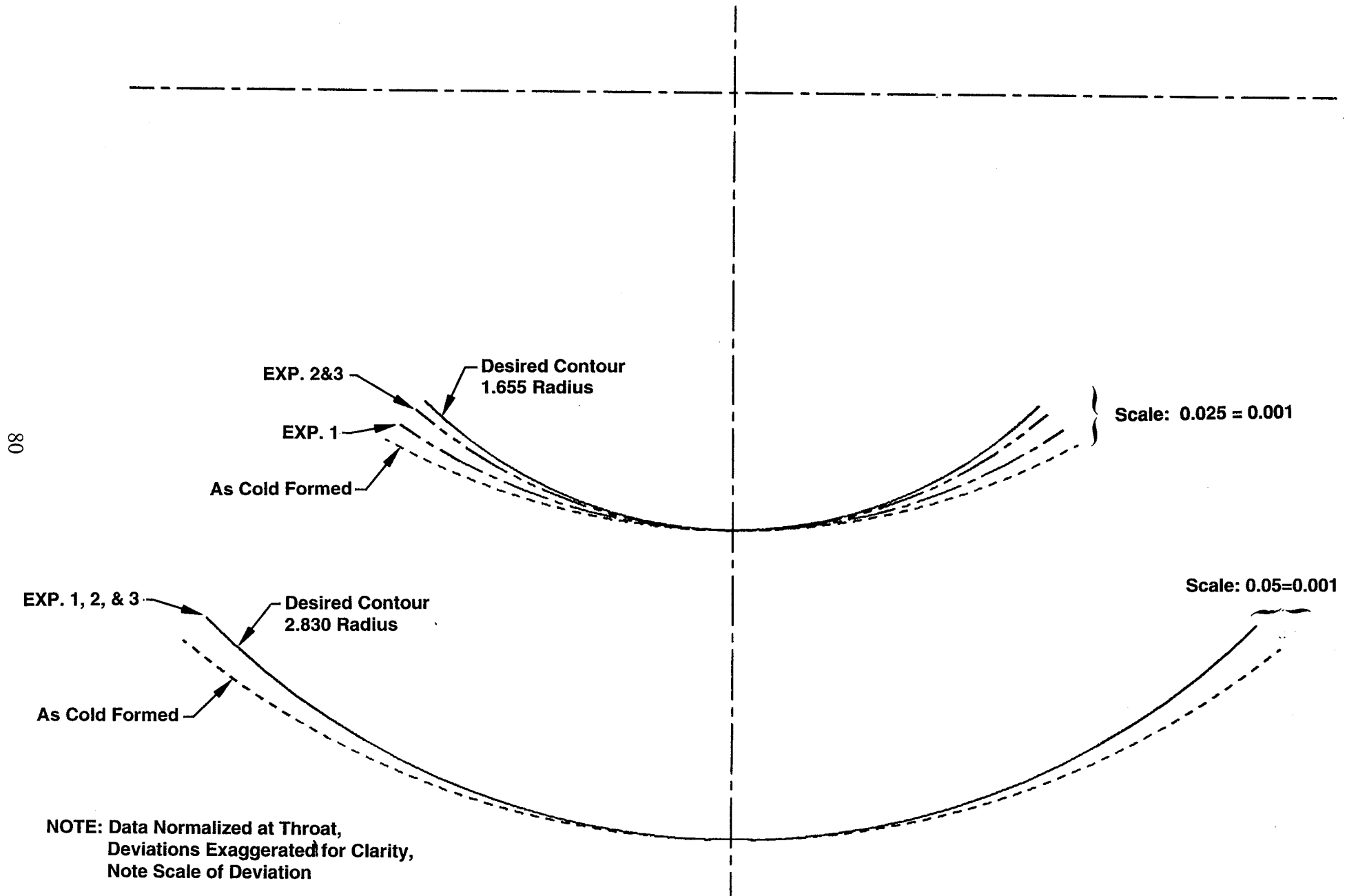


Figure 4.37. Radial Contour Comparison

Restrained Anneal Results

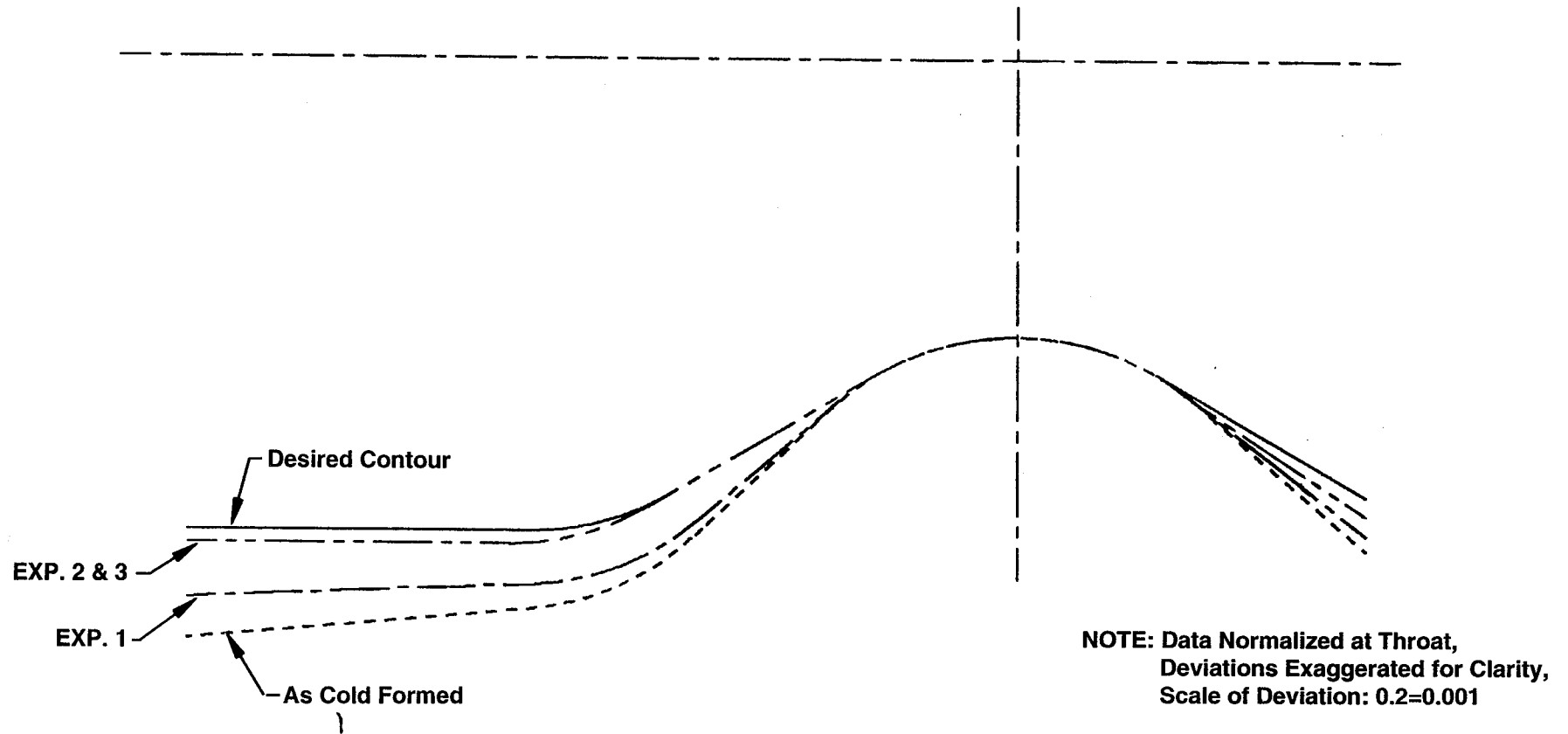


Figure 4.38. Axial Contour Comparison

4.8 FORMING EXPERIMENT CONCLUSIONS

The Phase A forming experiments demonstrated that flat platelet panels with internal coolant channels can be formed to a three dimensional shape suitable for use in a combustion chamber. Although only panels which were symmetric about the throat were formed, the forming information learned can be applied to other geometries. The basic forming process includes the following steps:

- 1) Fabricate a flat platelet panel with a near-net shape. The channel locations can be initially calculated based on actual geometry. Iterations to the channel locations are made with the Transformation Equation, which can account for the panel deformation due to forming. Include slots in the panel design for alignment of the panel to the forming dies.
- 2) Fill the panel with the Aerojet polymer to prevent buckling of the lands during forming.
- 3) Cold-form the panels in an hydraulic press in a single-step process, aligning the panel to the die axis and throat center with pins which engage with slots in the panels.
- 4) Hot-size the panels to remove spring back.

Additional conclusions can be drawn from the forming experiments:

- 1) The forming operation is a repeatable process which provides consistent parts.
- 2) The formed panel channel flow characteristics are predictable and acceptable.
- 3) Visual inspection of critical internal geometry dimensions of all cross-sectioned formed panels (i.e. hot gas wall thickness, channel width) are not adversely affected by the forming process, and are acceptable for fabricating functional parts.
- 4) Panels with a smaller thickness to bend radius ratio are easier to form.
- 5) Hot gas wall thicknesses of 0.008 to 0.033 inch can be successfully formed.
- 6) Panels with channel aspect ratios of 15.5:1 can be successfully formed.

- 7) The Transformation Equation is a viable tool in predicting channel locations.
- 8) Hot-sizing of formed panels removes spring-back from cold-forming, and results in panels with the desired contour.
- 9) The platelet bond integrity is unaffected by the forming operation. Visual inspection of all cross-sectioned formed panels confirmed good platelet to platelet bonding.

5.0 PLATELET STACK JOINING

5.1 INTRODUCTION

A regeneratively cooled combustion chamber liner made from formed platelet segments may require that the segments making up the liner be joined together. The joint may be required for functional chamber operation or to accommodate certain combustion chamber assembly techniques. Methods to affect such a joint were investigated in this task.

There are two primary locations where a joint between adjoining segments can be made; in the land or in the channel. Both of these joint locations were attempted. Joining methods investigated were laser and EB welding and diffusion bonding. Braze assembly was not pursued but is considered to be a potentially viable process.

Development and demonstration of the joining processes and techniques was made using flat samples, 2D samples and, on the selected process, 3D samples. Contract Task 1.4 covered the flat and 2D work; Task 1.7 covered 3D work. Concurrent with the development of the joining process was the development of inspection processes to allow non-destructive evaluation (NDE) of the joint.

5.2 OBJECTIVE

The objective of this study was to develop and demonstrate a process, or processes, for the joining of the longitudinal seams that exist between adjacent formed platelet liner panels. A further objective was to identify inspection or verification techniques that can be used to assess whether or not a joint had been affected and to assess the quality of the joint.

5.3 APPROACH

The approach taken was first to identify the issues associated with making a joint between liner segments. A list of these issues appears in Table 5.1, below. The next portion of the task was to decide what type of samples and what basic processes would be used for the process development and process demonstration. Figure 5.1 is a graphical depiction of the logic of the program plan. Due to the need to obtain joining data concurrent with the forming experiments it was decided to first do feasibility assessments with platelet stock alone and then use simplified flat bonded platelet specimens for further process assessment and development. These investigations utilizing platelet stacks for further development were limited to ZrCu as the material of interest.

TABLE 5.1

IDENTIFIED JOINING ISSUES

- Joint Location
- Joint Configuration
- Channel Aspect Ratio
- Gas Side Wall Thickness
- Land Width
- Material Weldability
- Contoured Weld
- Machining of Contoured Part
- Preparation of Joint
- Tooling
- Verification of Joint
- Sealing of Joint, if Required

At the completion of the feasibility and flat sample studies a down-select of the most promising process was made and then demonstrated on 2D specimens having a contour identical to the Phase A panel forming specimens. This task also provided additional process development and refinement. Successful completion of the 2D samples was intended to be followed by demonstration of the process on 3D panels taken from the Phase A forming experiments.

Techniques used to evaluate the samples included visual examination, dissection and subsequent metallography, and scanning electron microscopy. For some samples, in process leak check procedures were also developed. Radiographic inspection was also employed to detect the presence of a bonded joint in those samples examining diffusion bond joining.

5.4 DISCUSSION

5.4.1 Joining Issues

The joining issues are identified in Table 5.1 and are those that were addressed by the joining studies of Tasks 1.4 and 1.7. Each of the identified issues were addressed as follows:

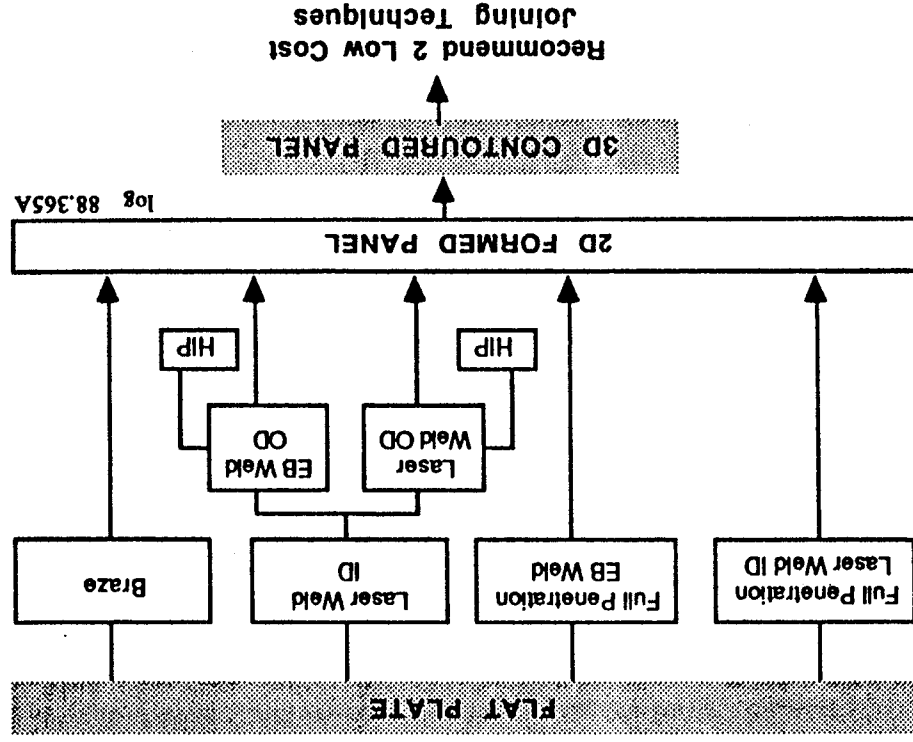
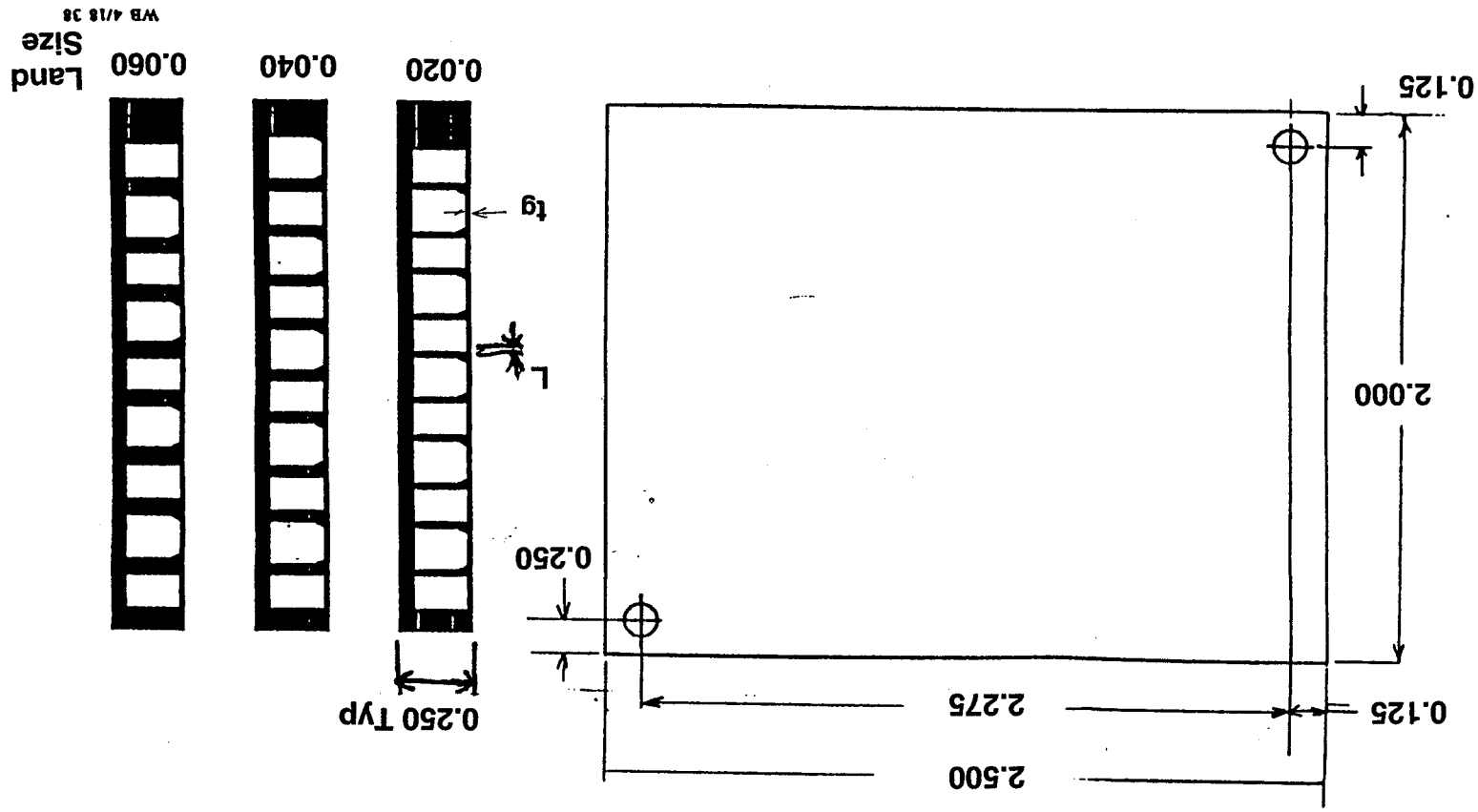


Figure 5.1. Task 1.4 Phase A Test Logic for Joining

- Joint location: Evaluate whether to place the joint in the land or in the channel; both were examined in this study.
- Joint configuration: Evaluate the actual shape of the joint, i.e. straight, stepped or contoured. In this study only straight joints that would simulate a radial joint in a true assembly were considered .
- Channel aspect ratio: Evaluate the impact of channel aspect ratio on panel joining. Panels with high aspect channels may be more difficult to join, as seam land machining and handling, and (weld) joint depth become more difficult. In this study simplified flat samples that had lands sufficiently tall to simulate high aspect ratio channels were used. A sketch of these samples appears as Figure 5.2. For the 3D joining demo of Task 1.7, the aspect ratio was 10.2.
- Gas side wall thickness: The effects of hot gas wall thickness on panel joining were studied. A thinner gas side wall would present more of a problem than a thick wall, especially in joints made in the channel. Joint preparation limitations and thermal mass considerations were addressed. Hot gas walls as thin as 0.008 inches thick were studied.
- Land width: Thin lands can pose problems similar to that of high aspect ratio channels. Panel joining can be further complicated by the decreased thermal mass of thin lands that could affect the ability to make certain types of weld joints. On the flat samples half-land widths as small as .010 were examined. Figure 5.2 shows the three land widths of the flat samples examined. The 3D demo had .020 lands.
- Material weldability: The material of the formed panels must be easily welded for processes employing welding as either an in-process seal or as the primary joining method. Two materials were originally considered: 300 series CRES and ZrCu. Early screening tests narrowed this down 304L CRES and ZrCu, two readily weldable alloys. Further narrowing of the program eliminated the CRES samples and all remaining work was performed on ZrCu.
- Contoured weld: As the actual hardware employs a converging/diverging nozzle contour, the ability to make a contoured weld was of prime importance. This is further complicated by the fact that the gas side wall welds must be made from the inside of the part. This concern was addressed by the fabrication

Figure 5.2. Panel Joining Samples – Flat Samples



of both 2D and 3D samples and by tooling that allowed welding from the ID of a part.

- **Machining of contoured part:** This issue deals with the initial preparation of the joint. The means for accurately machining the joint to provide the desired location, the land width, and the surface required for the subsequent joining operation were evaluated. Methods investigated included wire Electrical Discharge Machining (EDM), milling, and grinding.
- **Preparation of joint:** For each type of joint considered there are different requirements for the surfaces. For example, for a diffusion bonded joint the cleanliness and the presence of a bond aid can be critical; for welding edge rounding is not desirable. The study looked at processes of multiple pass EDMing to minimize recast, lapping, chemical etching, electro-polishing, and electro-plating and combinations of these processes.
- **Tooling:** For certain processes special tooling is required. Machining or trimming of the panel edges requires fixturing, as does assembly of the panels edge-to-edge. Welding of the inside of the panels requires special tooling. These issues were addressed by this study.
- **Verification of the joint:** This issue deals with a means for detecting whether a joint has actually been effected or not and means for evaluating the quality of the joint. Methods investigated included radiographic inspection and destructive metallography.
- **Sealing of joint:** Certain joining processes, most notably HIP diffusion bonding, require that a seal be effected around the entire joint periphery. To assure a seal has been made and maintained requires a means for leak detection; such means was evaluated and developed during this study.

5.4.2 Initial Joining Experiments - Task 1.4

Following initial screening of available processes and configurations, and considering the above issues, a down-select of the desirable parameters was made. Table 5.2 defines the joint configurations, the land widths and the joining processes that were investigated in the initial joining study.

TABLE 5.2
**JOINING PARAMETERS INVESTIGATED USING
SIMPLE/LINEAR SAMPLES**

2 Joint Configurations:

Joint in Land

Joint In Channel

2 Land Widths:

0.020

0.050

3 Methods of Joining

Laser Weld

EB Weld

Diffusion Bonding

- User Laser And/Or EB Weld for Sealing
- Use HIP

The platelet joining samples used in the initial study are shown in Figure 5.2. They were designed to have a simple geometry to eliminate high machining and tooling costs and to provide meaningful joining data early in the program. Table 5.3 lists the design part numbers and the configurations options of the basic design. All samples were ZrCu material, except as noted. Note that the land width mentioned in the parameter list of Table 5.2 is a composite land width made from two halves of a sample that had previously been cut in two.

TABLE 5.3**JOINING PARAMETERS INVESTIGATED USING
SIMPLE/LINEAR SAMPLES**

<u>Part No.</u>	<u>Land Width "L"</u>	<u>Gas Side Wall Thickness, tg</u>
1204189-9A	.020	.008
1204189-9B	.020	.012
1204189-9C	.020	.017
1204189-19A	.040	.008
1204189-19B	.040	.012
1204189-19C	.040	.017
1204189-29A	.060	.008
1204189-29B	.060	.012
1204189-29C	.060	.017
*1204189-39A	.020	.010
*1204189-39B	.020	.014
*1204189-49A	.040	.010
*1204189-49B	.040	.014

Figure 5.3 shows pictorially the two weld joint configurations investigated. For the channel weld evaluations it was recognized that the kinetic energy associated with an electron beam (EB) weld made it a high-risk candidate for a full penetration hot gas side weld; therefore only laser welding was considered for this weld. Thermal input considerations, coupled with mechanical limitations when welding internal to an actual liner, eliminated EB as a candidate for even the land weld option. Laser and/or EB were considered viable for backside welding for either the land weld or channel weld configurations.

Laser welding technology has many distinct advantages for this type of application, including the ability to direct the beam with prisms and mirrors into what might otherwise be inaccessible areas. One definite disadvantage with the laser welding of copper alloys is the high power required to melt the substrate resulting from its high reflectivity. This limits practical depths of weld penetration to a few thousandths of an inch, generally in the range of .003 to .010. Increasing weld depth by increasing energy input seems to have a deleterious effect on the weld surface as material vaporizes leaving a rough appearance. Further, a phenomenon occurs wherein the energy reflected back from the part heats the focusing lens, changing the focus (de-focusing) and therefore changing (reducing) the depth of penetration as a joint is traversed. Means to overcome these problems were developed and are discussed below.

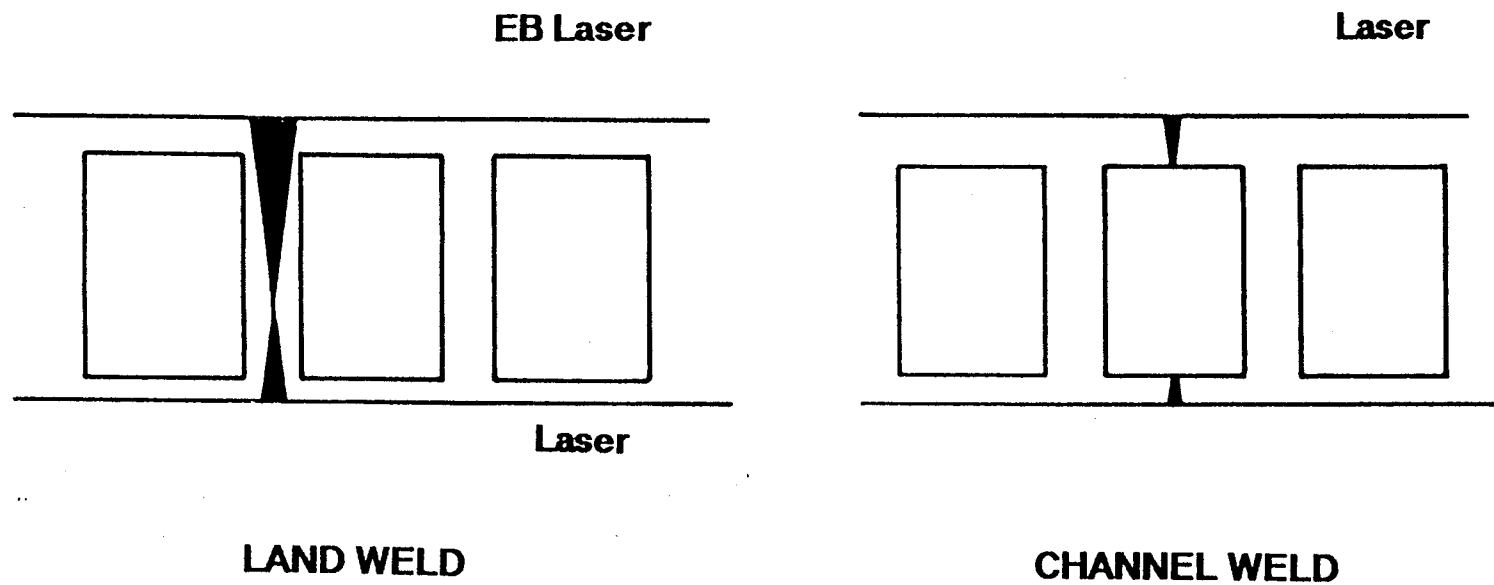


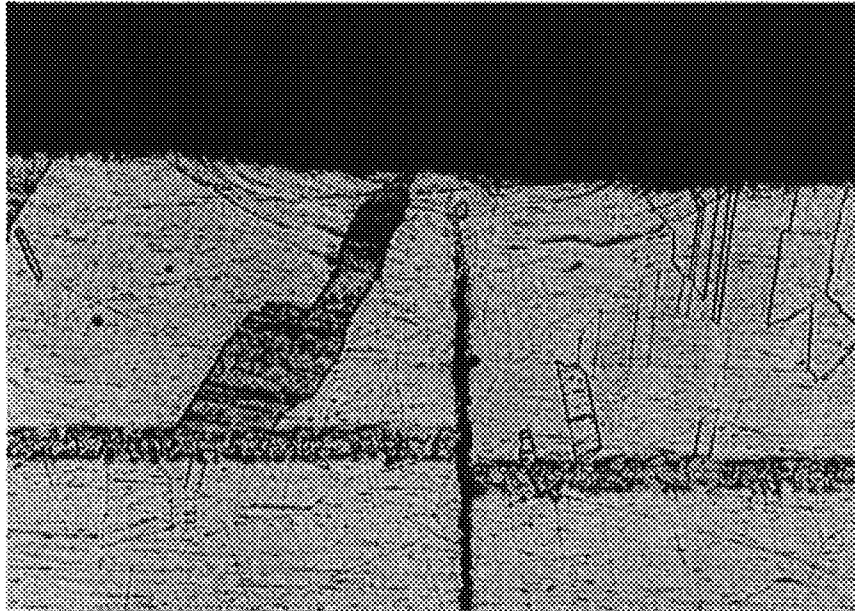
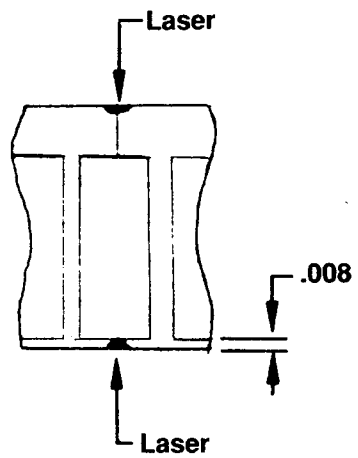
Figure 5.3. Weld Joint Configurations

An example of the results of the channel weld study is shown in Figure 5.4. In this sample laser was used for both gas side and backside welds. This sample had an 0.008 inch thick hot gas wall, near the practical limit of laser weld penetration into copper. Considering the difficulty with which such a joint is machined and handled, the criticality of the fitup of the joint, and the penetration limitations of the only viable weld option, an in-channel joint of this configuration has very limited application. It would, in fact, be viable only for very thin hot gas wall sections.

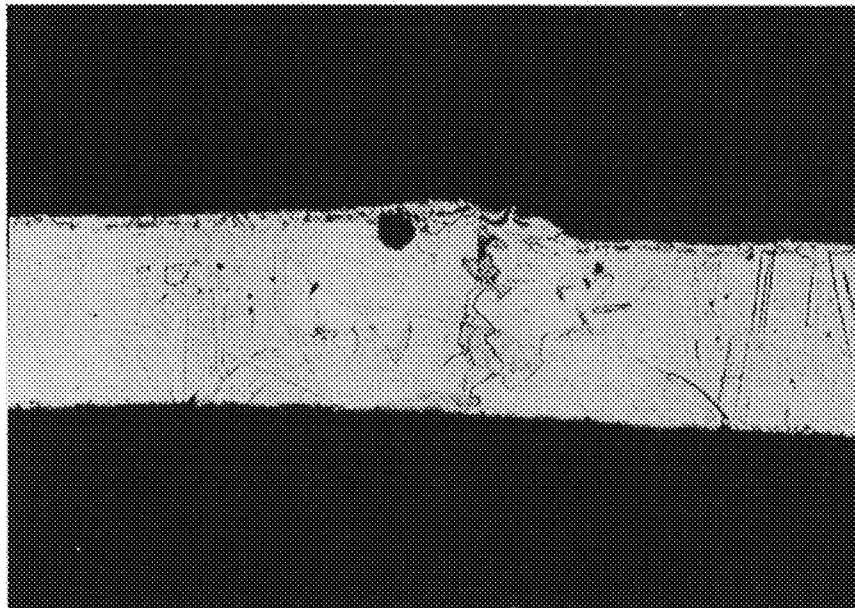
Figure 5.5 shows the results of an in-land joint sample. In this sample laser welding was employed for the hot gas wall welding and EB was used for the back side welding. The half lands of this sample were nominally .010 thick, making for a total land width of 0.020, nominally. This sample also had a 0.008 hot gas wall, and a 0.050 backside wall. These values of demonstrated parameters are approaching the practical limits for fabrication and functionality. Any increase in the numerical value of these parameters improves the producibility aspects of the assembly. As such, this method of joining appears applicable to a wide variety of combinations of land widths, hot gas wall and backside wall thicknesses. The disadvantage to this approach is that full penetration welds cannot be obtained thus leaving a non-joined area between the welds in the land.

The next series of joining specimens examined the concept of diffusion bonding the half lands together. This approach would eliminate the non-joined area associated with the above described process. The concept adopted was one of a self-tooling assembly wherein the assembly itself provided a sealed joint. The sealing would be accomplished by the welding processes developed and described above. The faying surfaces of this sealed joint would diffusion bond together when subjected to the environment of a Hot Isostatic Press, or HIP, at the prescribed pressure, temperature and duration.

Again, the flat sample design of Figure 5.2 was employed for this series of experiments. The first samples prepared were four in number and employed a 0.010 inch half land. Wire EDM was used to machine the faying surfaces and obtain the 0.010 half land thickness; these surfaces were then hand lapped. Two of the samples were plated with a bond aid and two were assembled with as-lapped surfaces. The longitudinal seams of the joints, simulating the ID and OD of a liner, were welded by laser. One end seam of each sample was also laser welded. The opposite end seams were EB welded in order to obtain a vacuum in the joint. All samples were processed in the same HIP run.

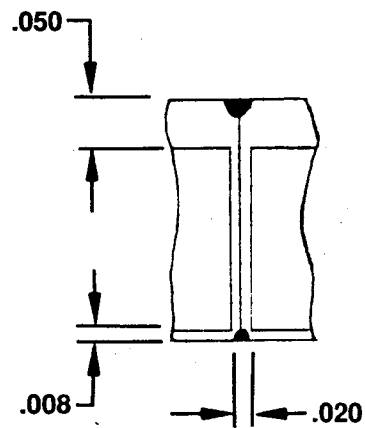


Closeout



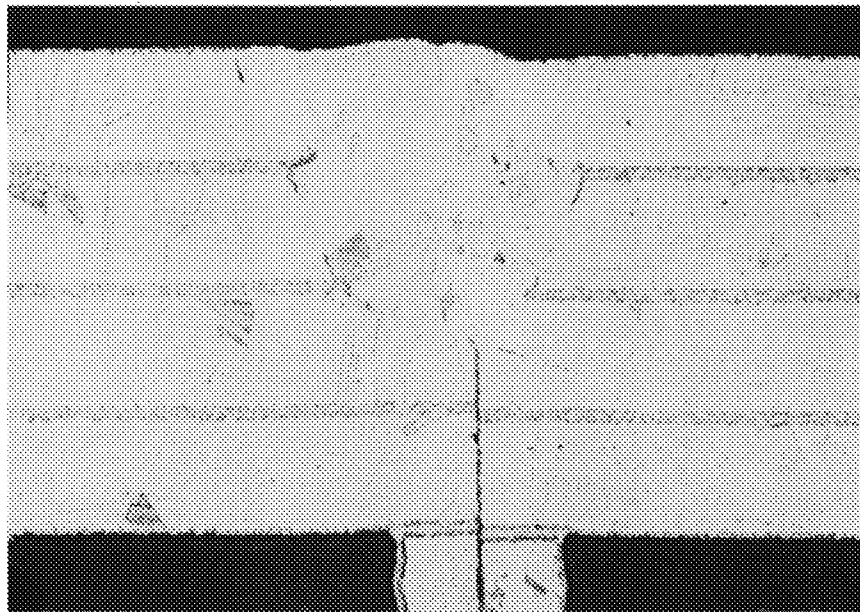
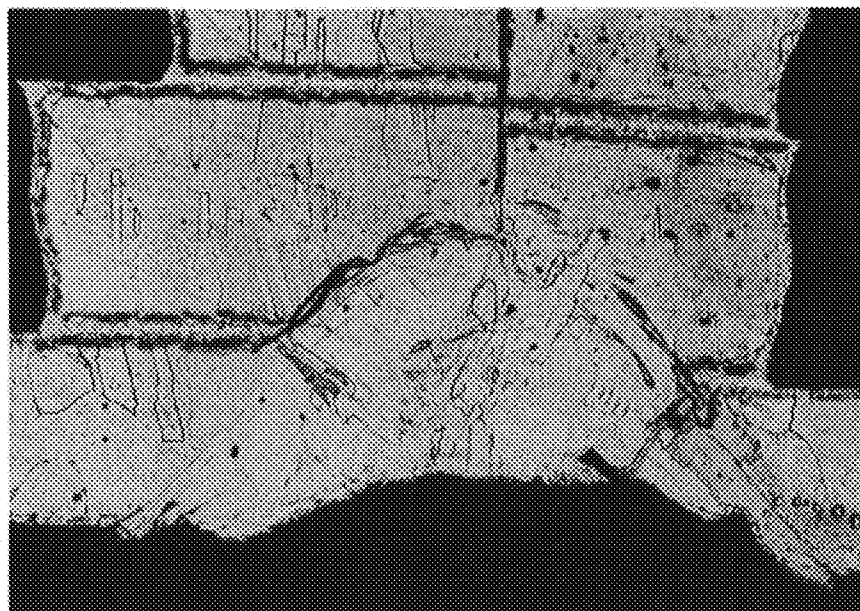
**.008 Gas
Sidewall**

Figure 5.4. Channel Weld Results



M10/D9/VG-2-2

1

**EB Weld****50X****Laser
Weld****125X****Figure 5.5. Land Weld Results**

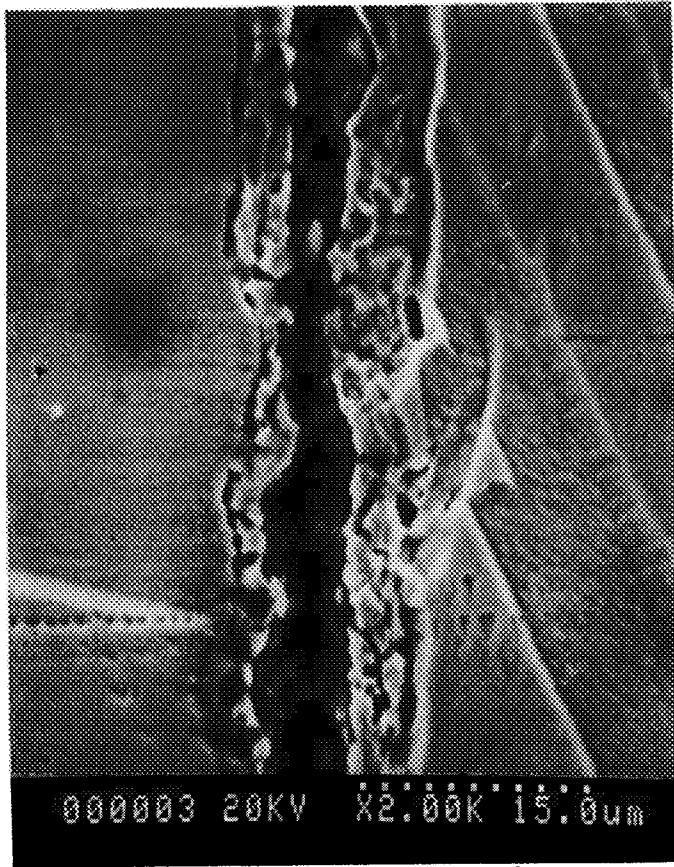
Sectioning of the four samples showed partial bonding in the aided bond joints. Bonding did not occur in the unaided samples. Photomicrographs of the sample sections are shown in Figure 5.6. In all samples there is evidence of a porous layer that exists below the bond aid. It is felt that this layer, which is residual recast from the wire EDM operation, inhibits the bonding process. Comparison of hand polished and as-cut wire EDM surfaces showed that, with the method used, approximately half of the recast layer was removed; this comparison is shown in Figure 5.7.

The above experiments illustrated the need for a complete understanding of the roles the residual EDM recast layer and joint sealing were playing in the ability to affect a diffusion bond in the samples. As such, a plan to look at different methods of removing the suspect layer and improve joint sealing was developed. Figure 5.8 and Table 5.4 were developed and used to identify and evaluate the critical parameters.

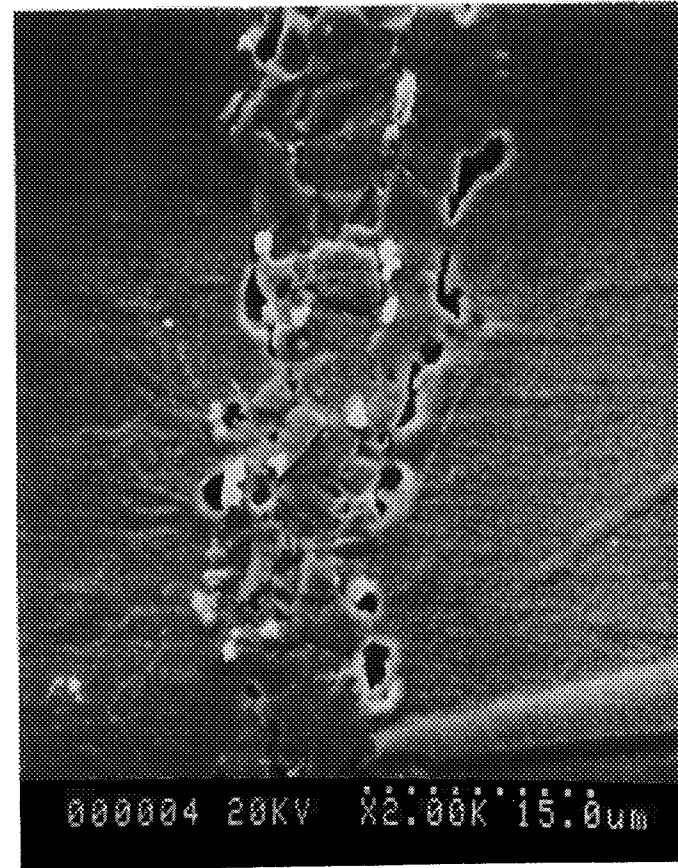
Concurrent with detailed evaluation of the critical parameters, eight additional joint samples, again using the sample design of Figure 5.2, were prepared. Four samples had their faying surfaces mechanically milled and four had their faying surfaces chemically milled. All samples had bond aid applied. Three sides of each joint were laser welded and the fourth was EB welded. All welds were inspected visually and with the aid of both an optical microscope and a Scanning Electron Microscope prior to HIP processing. This inspection revealed that a possible leak path existed in two of the joints; one joint in each of the two groups of four samples. All other welds examined showed no potential leak paths.

After HIP processing, each joint was sectioned and examined. Two of the four chemically milled prepared samples showed 100% bonding, as shown in Figure 5.9. The remaining two showed only partial bonding; one of these joints had the aforementioned suspect weld, the other had a platelet surface defect that inhibited the original platelet-to-platelet bond that was detected in the post bond examination. None of the joints in the mechanically machined prepared samples bonded.

These experiments showed that a diffusion bond could be made between mating surfaces of the edges of previously bonded platelet stacks, in a configuration consistent with that required for joining formed platelet chamber sections at a land. These, and previous, experiments also showed that further development of the pre-bond processing parameters was required to improve the reliability of the bond process. Experiments to optimize the pre-bond processing as identified in Figure 5.8 and Table 5.4 were next carried out to improve the process reliability. The basic process is as shown in Figure 5.10. Experiments were designed to optimize



**Unaided Joint
No Bonding**



**Aided Joint
Partial Bonding**

Figure 5.6. Photomicrographs of HIP Processed Samples

- Appeared Visually Acceptable
- Unsuccessful In Completely Removing Entire Recast Layer



← .001 → Recast Layer

Untreated Wire EDM Surface



← .0005 → Recast Layer

Polished Surfaces

Figure 5.7. Comparison of "As-EDM'd" and Hand Polished Surfaces

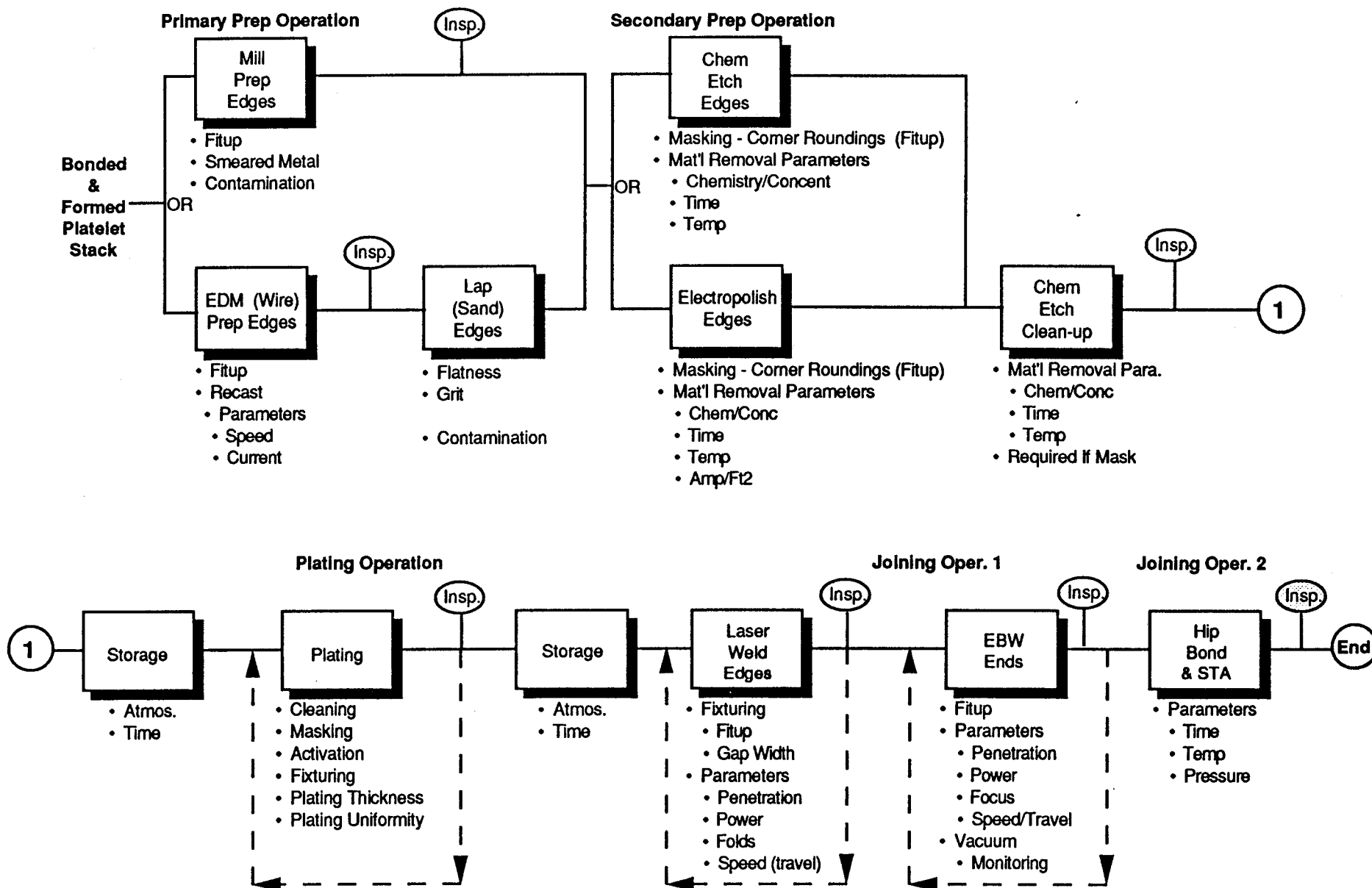


Figure 5.8. Process Flow of Diffusion Bond Joining of Formed Platelet Panels

TABLE 5.4. CRITICAL PROCESSES FOR DIFFUSION BOND JOINING, SHEET 1 OF 3

Basic Process	Specific Process	Nature Of Risk Or Concern	Criticality	Risk Reduction
Edge Prep	Mill Edge	• Fitup of Matting Edges	1	Full Size Sample - Process Control
		Excessive Gap		
		Inability to Weld (Seal)		
		Excessive Deformation Req'd for Bond		
	EDM Edge	Thinning of Walls		Remove (Etch or E.P.)
		Breakthrough - Leaks		
		Inability To Seal For Bond		
		• Smeared Metal	1	
	Lap Edge	Entrapped Contaminants		Full Size Sample -
		Inhibit Bondings		
		• Fitup of Matting Edge	1	
		Excessive Gap - See Above		
Chem Etch Edge	EDM Edge	Thinning Of Walls - See Above		Remove (Etch or E.P.)
		• Recast Layer	1	
		Inhibit Bonding		
		Thickness		
	Lap Edge	Consistency		Samples - Set's Control Parameters Minimize Recast Minimize Mat's Removal Use Si Carbide Paper Of 600 Grit or Finer Consider Eliminate By "finer" EDM cut
		• Flatness	2	
		Corner Rounding		
		• Material Removal Control	2	
	Chem Etch Edge	• Contamination Potential	2	
		• Corner Rounding	1	Minimize Mat'l Req'd To Be Removed Chem Etch Cleanup If Req'd Samples To Define Process & Req'd CTRLS
		Masking Req'd (If req. a lot of mat'l removed)		
		• Contamination Potential	2	
		• Material Removal Control	1	
		• Preferential Etch of Elements	1	

TABLE 5.4. CRITICAL PROCESSES FOR DIFFUSION BOND JOINING, SHEET 2 OF 3

Basic Process	Specific Process	Nature Of Risk Or Concern	Criticality	Risk Reduction
Edge Prep (cont'd)	Electro Polish Edge	• Corner Rounding	1	Minimize Mat'l Req'd to be removed
		Masking Req'd (if req a lot of Mat'l Rem.)	2	Chem Etch Cleanup
		• Contamination Potential	1	Samples To Define Process & Req'd CTRLS
		• Material Removal Control		
	Chem Etch Cleanup	• Req'd If Mask For Etch Or Electro Polish	-	
		• Material Removal Control	2	Use Data From Chem Etch Of Edges Expmnt. To Define Process & CTRLS
Storage	Storage	• Contamination Or Oxidation	2	Cleaning For Plate S/B adeq. Plating Expmnts. to Verify
Plating	Vapor	• None		
	Degrease			
	Caustic	• Adequate Cleaning	1	Samples to Define Process & CTRLS
	Electro-Clean	• Excessive Mat'l Removal	2	
	Rinse	• Adequate Rinsing	2	" "
	Masking	• Req'd If Want Plate Only Edges Contamination Potential	1	Investigate Eliminate Weld Sample Req'd.
	HCl Activation	• Adequacy May Not Be Adequate If Contam. (Mask)	1	" "
	Plating	• Thickness Control Excessive - Potential Cracks, etc. Not Enough - Weak Bonds	1	Samples To Define Process & CTRLS Shielding May be Req'd
		• Adhesion Inspection Difficult	1	Consider Oven Bake of Samples/Hardware

TABLE 5.4. CRITICAL PROCESSES FOR DIFFUSION BOND JOINING, SHEET 3 OF 3

Basic Process	Specific Process	Nature Of Risk Or Concern	Criticality	Risk Reduction
Storage	Storage	• Control Of Vac. Or Inert Adequate		Verify By Samples To Be Welded/Bonded, Record Actuals
Join Edges	Laser Weld	• Fitup - Fixturing	1	Full Size Sample
		Excessive Gap	1	"Flexible" Tooling
		Inability To Weld (Seal)		(See Vac Monitoring)
		• Weld Repeatability	1	Samples To Define Parameters & CTRL To These Parameters
	EBW Ends	• Rework Capability	1	" "
		Inspection to Identify Problems		
		• Fitup -	1	Samples, Incl. Full
		Excessive Gap	1	(See Vac Monitoring)
Joining Of Land	Monitoring Of Vacuum	Inability To Weld (Seal)		
		• Weld Repeatability	1	Samples To Define Parameters & CTRL
		• Rework Capability	1	" "
		Loss Of Vacuum W/O Recognition		Need Special Program To Address Issue
	HIP Bond & STA	Inability To Diff Bond		
		• Process Repeatability	2	Process CTRLS & Verification By Sample
		• Inspection Of Bond		Investigate Available NDE
		• If Concurrent w/Bond, May Degrade Properties If Rework		
		• Rework		

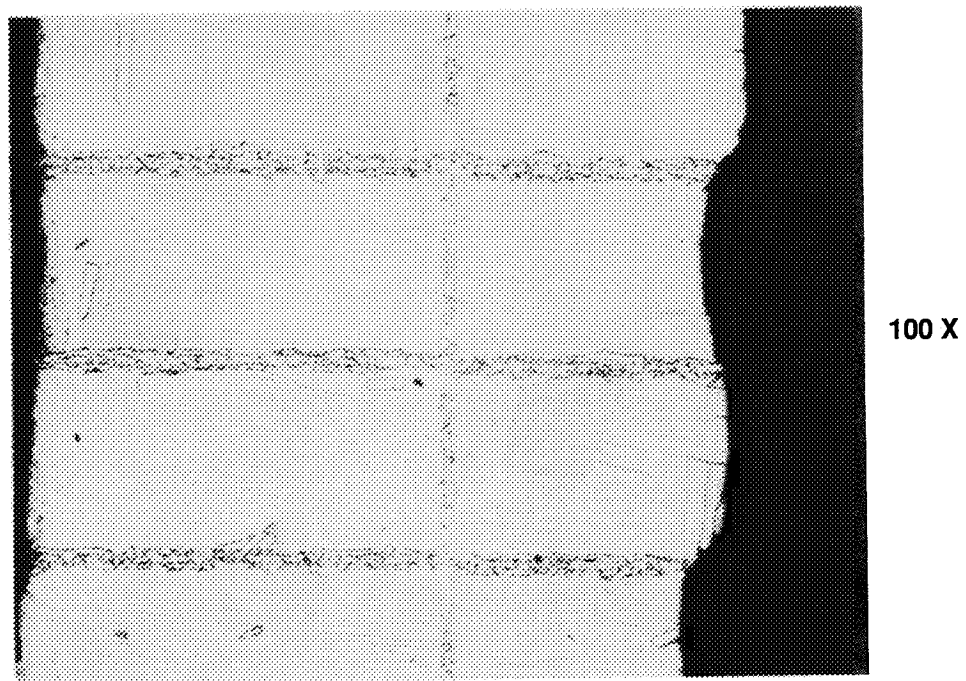
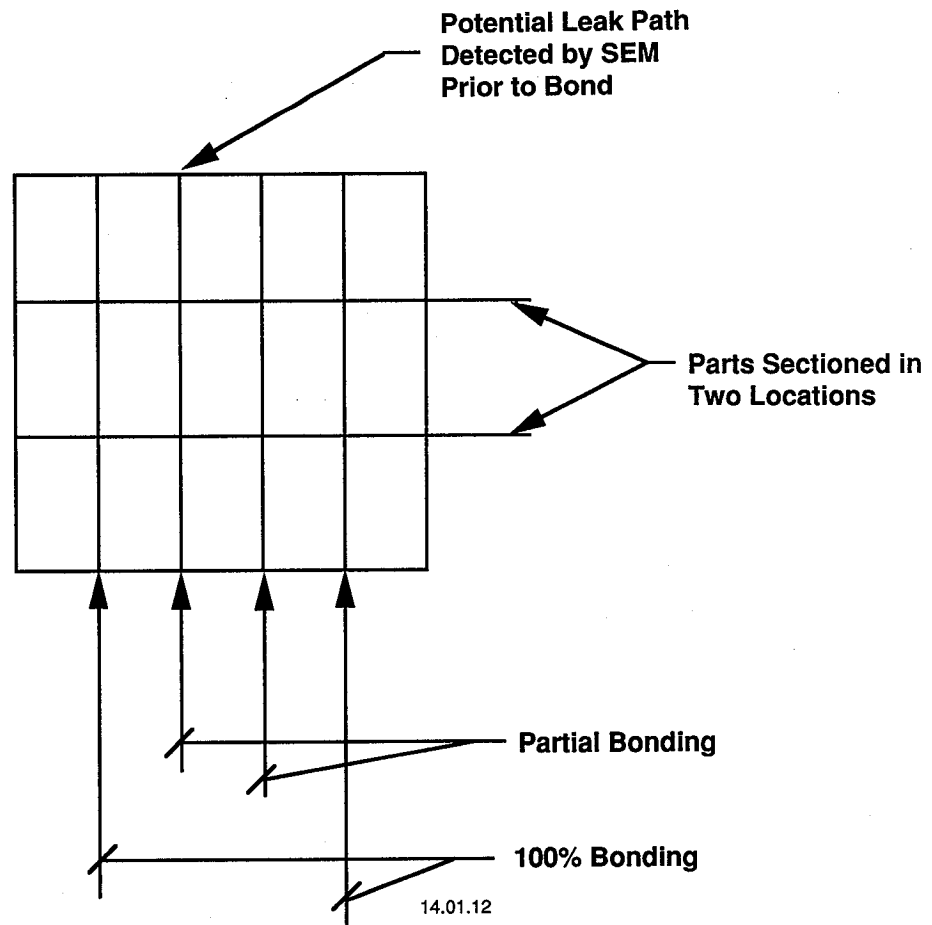


Figure 5.9. Two Interfaces in the Chemical Machined Sample Achieved 100% Bonding

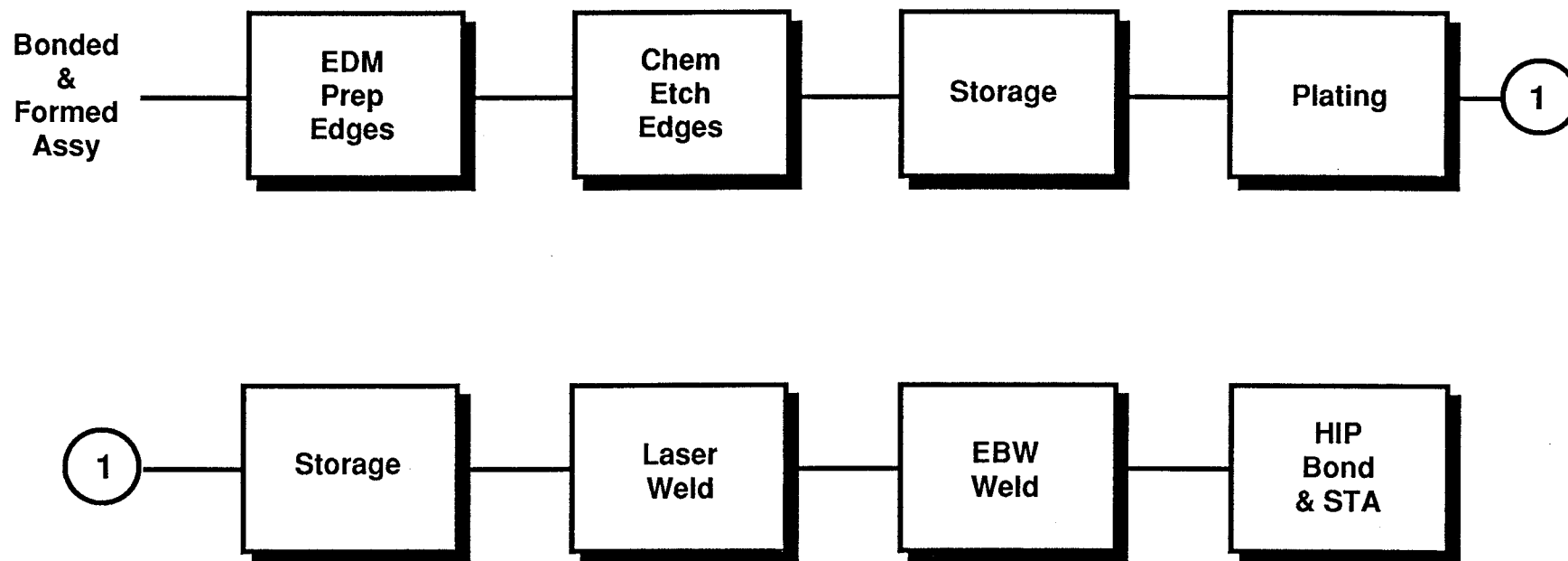


Figure 5.10. Diffusion Bond Edge Joining Process

the edge preparation and laser welding of the platelet stack interfaces prior to HIP processing. Special attention was given to minimizing the recast layer thickness during wire EDM, removing the recast layer by chemical machining, and the bond aid application process.

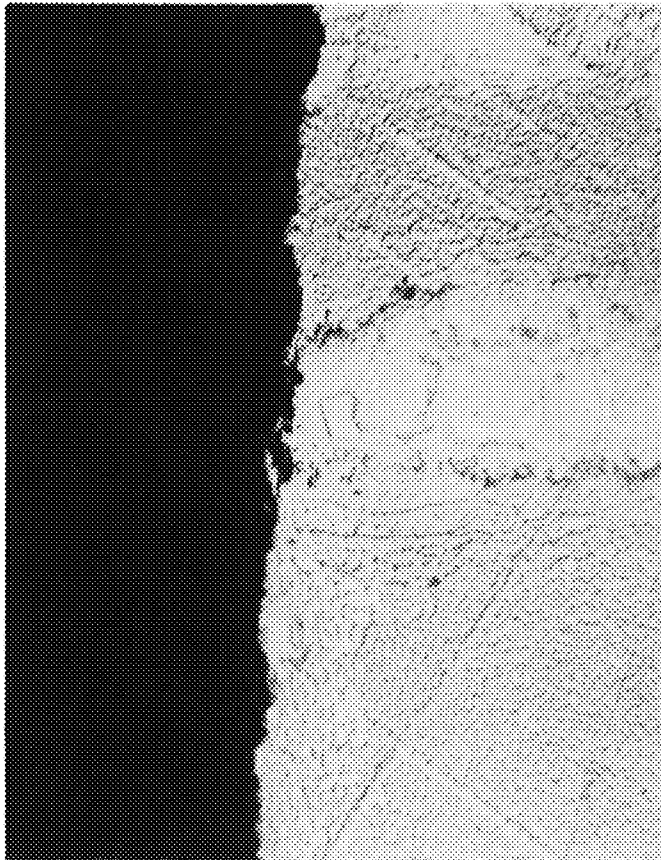
A series of copper samples were machined by wire EDM to determine parameters that would minimize the recast layer thickness. Reducing the recast layer insures that a minimum etch time will be necessary to completely remove it. Results of the EDM samples showed that the recast layer could be reduced to as little as .0001 inch. This is shown in Figure 5.11 that compares a previously prepared EDM surface to a surface prepared with the optimized parameters.

Etch experiments were run on samples of diffusion bonded ZrCu platelet stacks machined using the optimized EDM parameters. Solutions of HNO₃ and HF of varying concentrations and temperatures were used along with varying immersion times to determine the best etch parameters. Figure 5.12 shows the results of the optimum parameters; these parameters produced the least preferential etching and edge rounding while completely removing the recast layer.

After determining the interface preparation methods, bond aid application experiments were performed to optimize this process. Process parameters that were investigated included caustic cleaning, activation time, plating time and plating current density. Evaluation of the samples included adhesion testing, plating thickness, plating uniformity, and platelet stack-plating interface examination using the Scanning Electron Microscope (SEM). Eleven samples were machined per the processes developed in the previous optimization studies in preparation for plating. After plating, the samples were baked for an hour at 625 degrees F to evaluate plating adhesion. Plating thickness and uniformity testing was done using X-ray Fluorescence. Each sample was measured in 12 places to determine plating thickness and to evaluate plating uniformity.

Results of the plating experiments showed good adhesion for all samples tested. Optimum plating time and current density were determined from uniformity and thickness testing. SEM results showed that caustic cleaning was unnecessary following surface etching.

Laser welding experiments were next conducted to determine the effect of the plated bond aid on surfaces normal to the weld. Prior to this time efforts had been made to completely eliminate bond aid from this area; the reasoning being that it could inhibit the welding process. One of the problems noted in the initial laser weld experiments was that the high

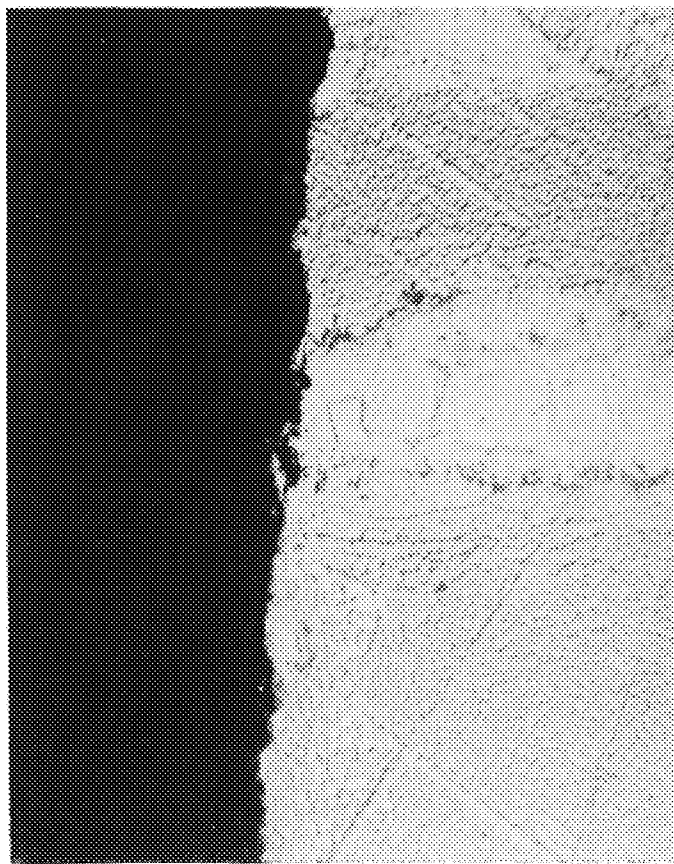


Optimized Wire EDM Technique

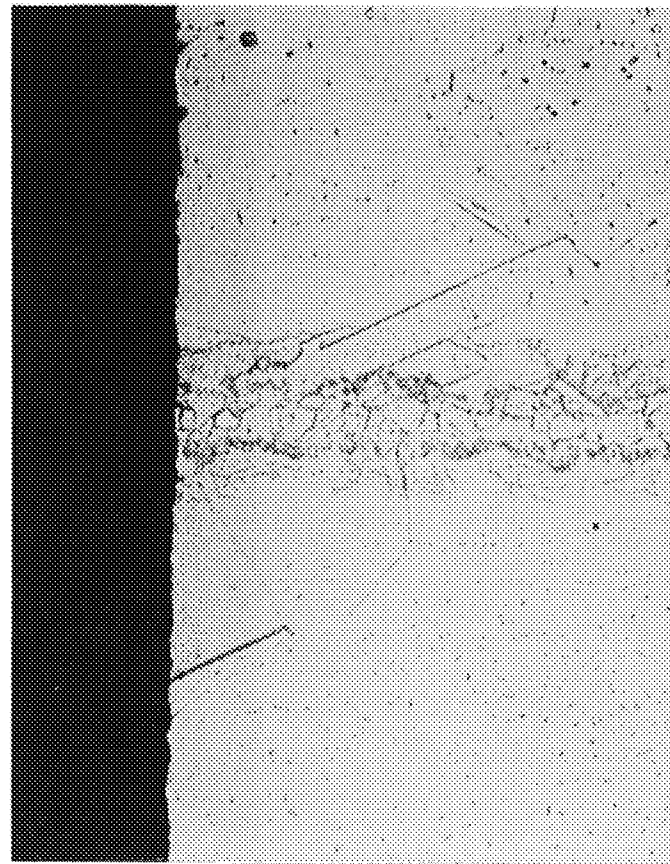


Original Wire EDM Technique

Figure 5.11. Comparison of Wire EDM Processes



As EDM'ed



After Etch

Figure 5.12. Etch Parameter Optimization Provided Complete Recast Removal

reflectivity of the copper requires very high power densities to affect a weld. This energy reflected from the workpiece causes heating of the laser optics and a resultant change in beam focus. The change in beam focus in turn causes varying weld characteristics along the length of the weld. This series of experiments was undertaken to see if the presence of the bond aid could alter the surface reflectivity and improve the weldability of the copper alloy.

Results of the experiment showed that the bond aid could indeed improve the weld. Weld penetration in the desired range (0.008-0.012 inches) was achieved with nominal power densities. Uniformity of the depth of penetration along the weld was also improved.

5.4.4 2D Joining Experiments

Following the optimization experiments described above, bond samples having a "2D" geometry were prepared. These samples were made from platelet stacks residual from the forming studies of Task 1.3; specifically from stacks that had been through the first forming operation of the two step forming process. The resultant samples have a "converging" and "diverging" contour and essentially form a longitudinal section of the area of a joint between adjacent panels in a 40K sized formed platelet liner. For simplicity, the samples were taken from the frame portion of the panels and did not contain any channels. A photograph of a sample of this configuration is shown in Figure 5.13. This sample configuration allowed evaluation of the ability to laser weld a seam while traversing along the converging and diverging contours.

Two such 2D samples were prepared with the developed processes and laser weld assembled. Previous laser weld experiments had shown the validity of welding in an attitude non-perpendicular to the surface as would be encountered in the convergent and divergent areas. This greatly simplifies the motion, and therefore the complexity, of the laser head as it does not have to articulate as it traverses the joint path. Such a motion was employed for the fabrication of these and all subsequent bond samples.

Following laser welding of the "ID" and "OD" longitudinal seams, the joint ends were welded by EBW and the samples were then HIP processed. Subsequent sectioning and examination revealed that diffusion bonding had not occurred. Photomicrographs showed that etching and plating parameters provided bondable interfaces. Laser weld depth was as desired and weld quality was excellent. The quality of the EB welds at the sample ends was questionable and considered to be the source of leaks that would have inhibited the bonding. Problems with the EB welds were particularly evident at the corners of the part where the laser and EB welds overlap. Cracks, pits, expulsions and excessive corner erosion were observed.

ORIGINAL PAGE
BLACK AND WHITE PHOTOGRAPH

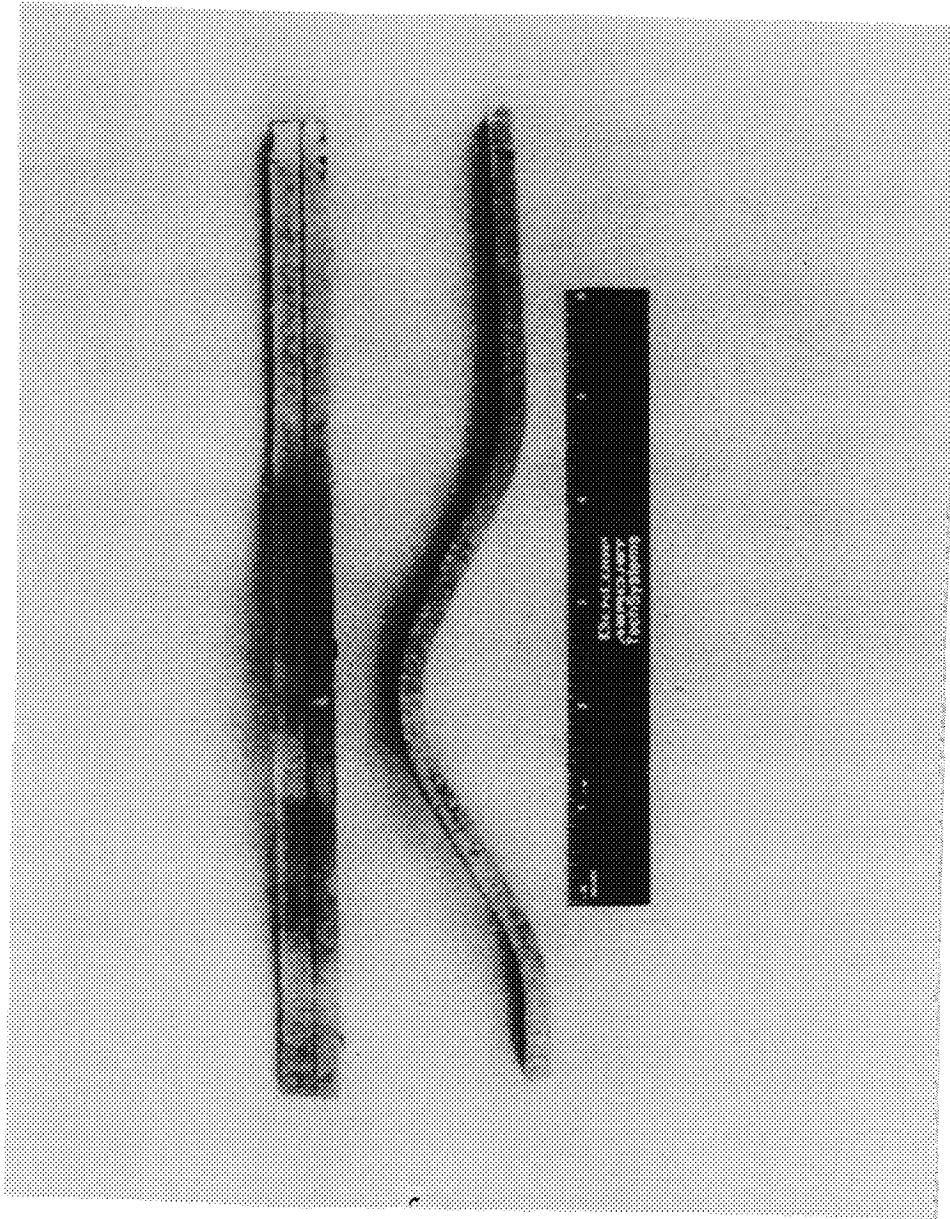


Figure 5.13. Initial 2D Sample Configuration

Additional EB weld experiments were performed to optimize the EB welding process. Changes investigated included evaluating different types of EB weld machines and the use of start-up and run-off tabs. All previous joint samples had been welded using high voltage/low amperage type welders. The advantage of using this type of welder is that they have line-of-sight capability and the interface can be easily located. This type of machine also generally produces narrow, deep welds. No run-off or start-up tabs had been used to date. Weld samples were prepared to evaluate a low voltage/high amperage EB welder and the use of run-off and start-up tabs. The low volt/high amp EB welder generally produces a wider beam shape that was thought to potentially provide better seal welds.

EB weld optimization experiments consisted of developing weld parameters that would provide a bead of the nominal dimensions shown in Figure 5.14. Figure 5.15 shows the sample configuration. Start-up and run-off tabs were used to eliminate the transient condition at the edges of the part as the electron beam traverses the part. Visual examination revealed a small expulsion at the trailing end of the joint at the corner of one sample. This was due to a small gap between the run-off tab and the sample edge. Subsequent longitudinal sectioning (Section A-A, Fig 5.15) showed excellent cross over of the EB weld with the laser weld, even at the corner where the expulsion had occurred. The results of the experiment were considered satisfactory and the feasibility of the approach demonstrated. All subsequent samples employed start-up and run-off tabs for all welding, including laser welds.

Two additional 2D samples were prepared and welded with the improved processes described above. The welds were inspected under high magnification and no potential leak paths were identified. The samples were then HIP processed. These samples were subsequently sectioned and evaluated. One sample showed 100% bonding; the other showed no bond. Cross sections of the samples are shown in Figure 5.16. Both samples had been processed at the same time, using the same methods. No record of any anomaly exists that would explain the success of one sample and the failure of the other. Examination of the cross sections of the non-bonded sample showed that pre-bond processing was adequate to obtain a diffusion bond; this lead to the conclusion that an undetected leakpath existed, preventing the HIP pressure from applying a bonding load. These results lead to the conclusion that visual examination of welds was inadequate to fully assess their integrity and assure leak free joints.

Concurrent with the fabrication of the various bond samples, a method was being sought to non-destructively assess a bond joint. A method that proved very successful was X-ray or radiographic examination. A radiograph of the two 2D samples discussed above appears in Figure 5.17. The joint in the non-bonded sample is readily visible, while the joint in

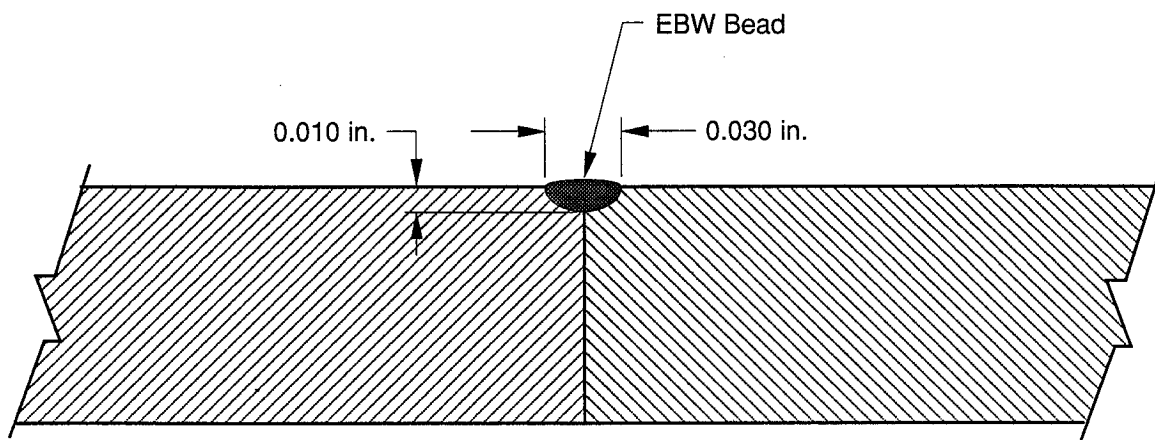


Figure 5.14. EBW Bead Dimensions

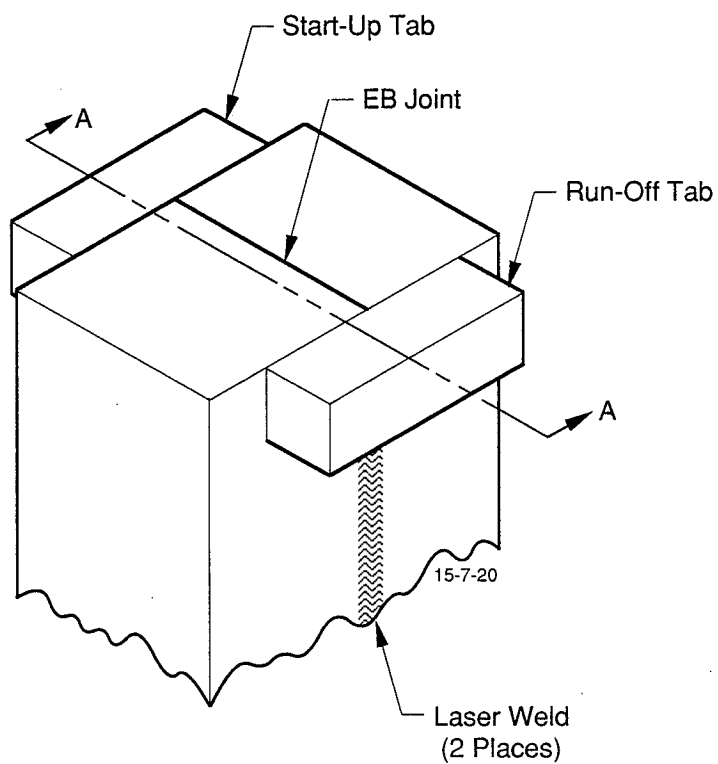
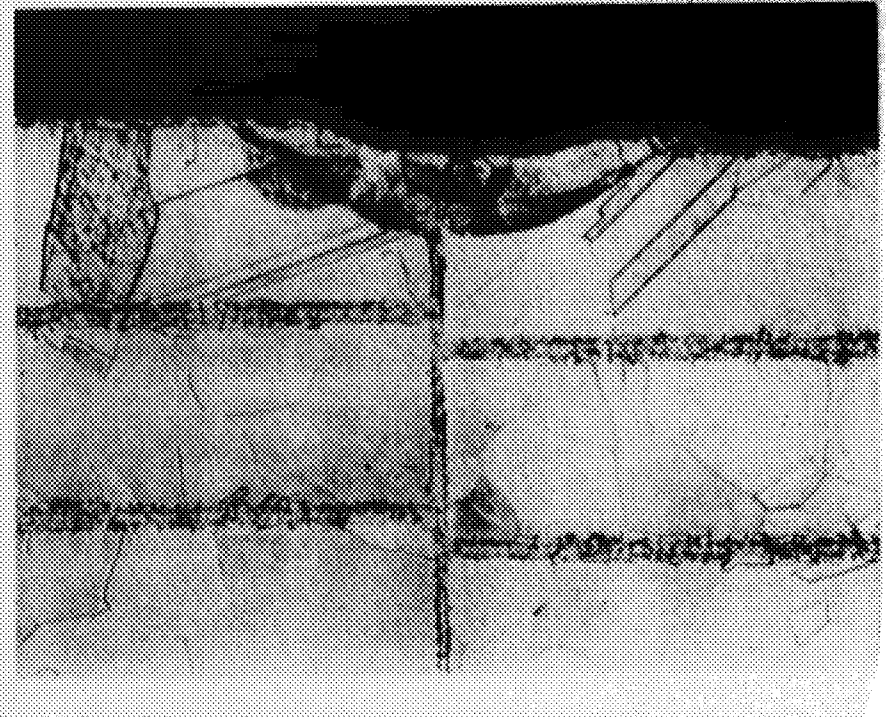
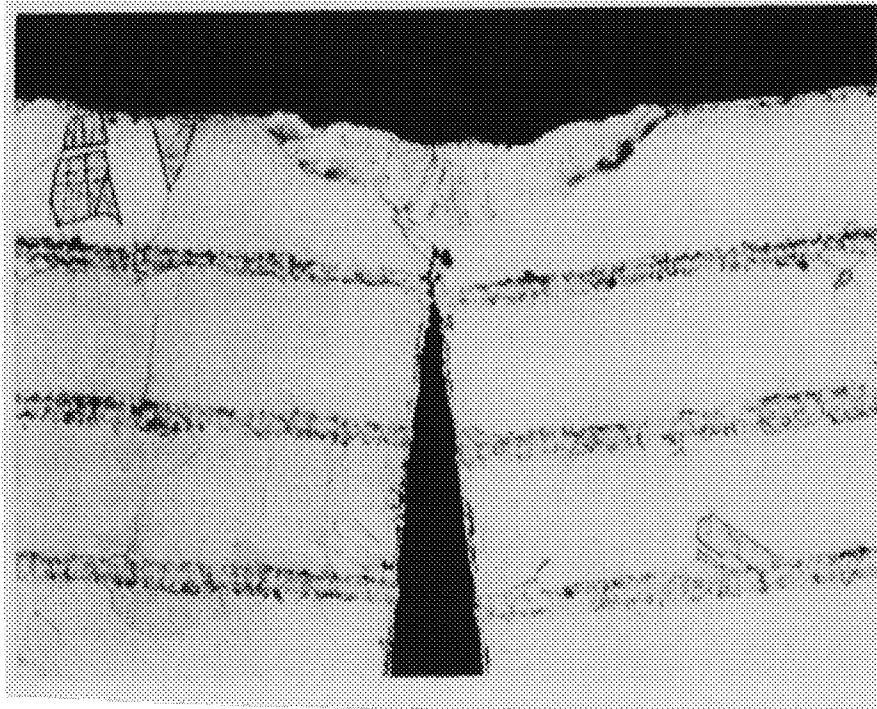


Figure 5.15. Sample Configuration



- **Sample Shows Distinct Lack Of Bonding**
(Relative Rotation Occurred During Mounting)
- **Leakage Suspect**

- **Sample Shows 100% Bonding**

Figure 5.16. Photomicrographs of 2D Bond Samples

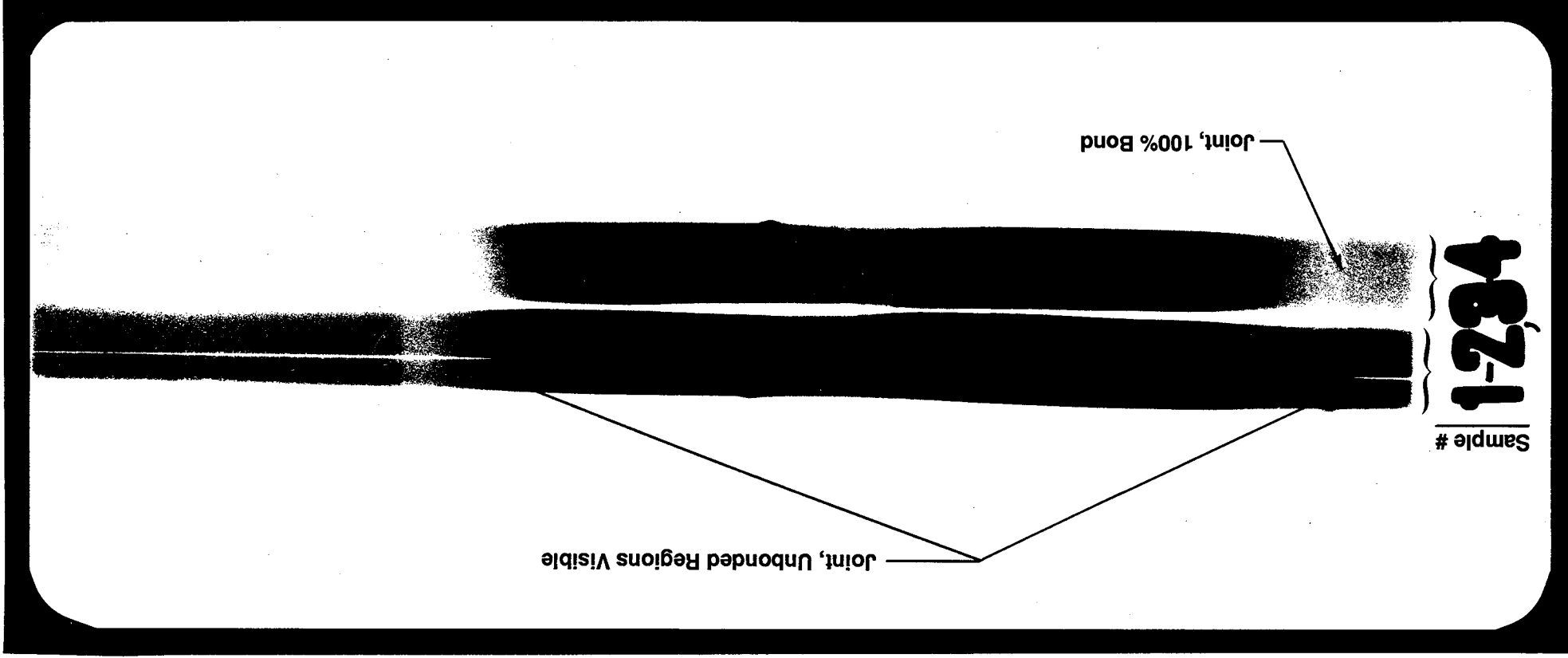


Figure 5.17. Bond Sample Radiograph

the bonded sample is not. This method continued to be employed for detecting the presence of a bond in subsequent samples.

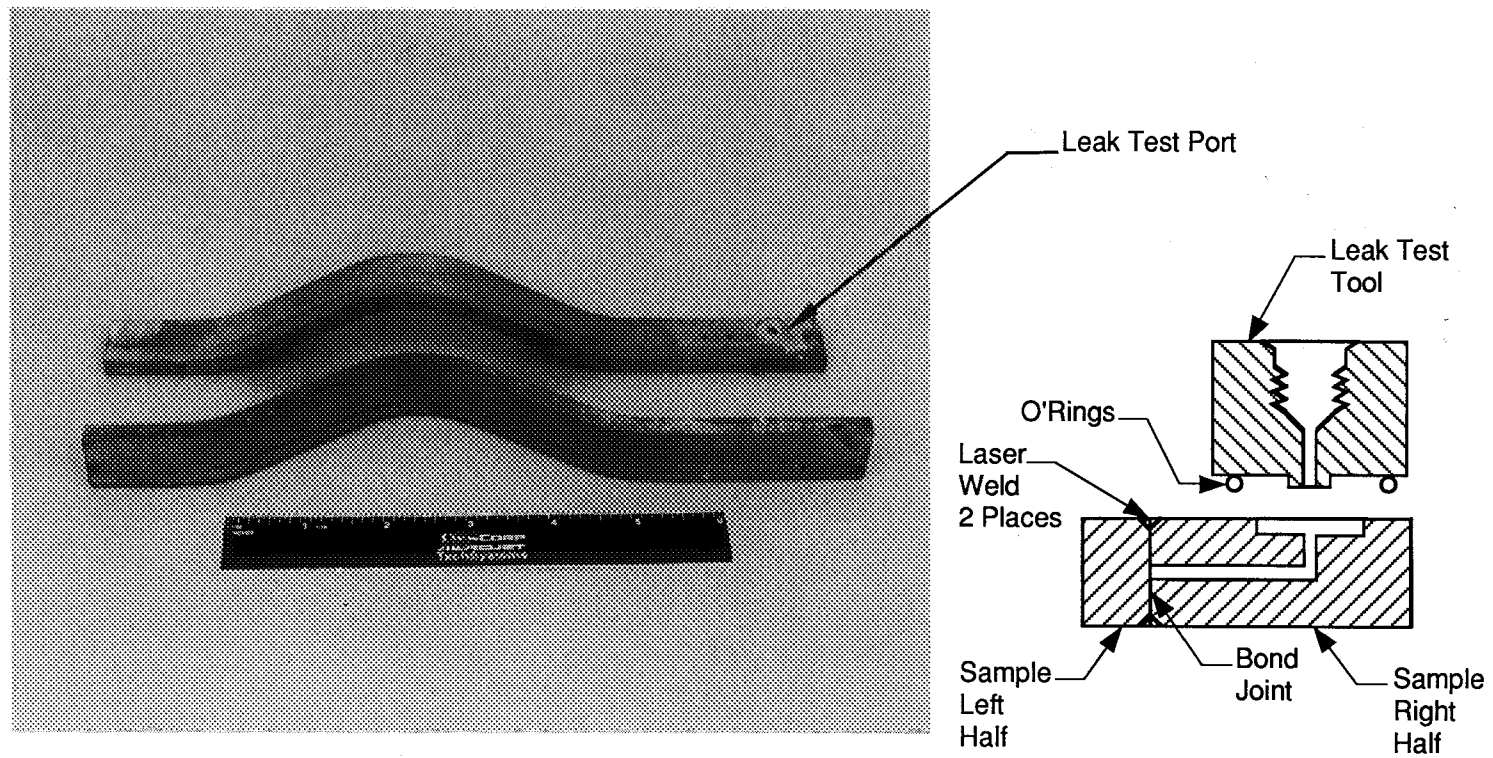
In order to improve bond reliability, with weld joint leakage being the suspect failure mechanism, a means to detect and measure leakage was required. Such a means is shown in Figure 5.18, wherein a leak check port that connects to the joint to be bonded has been incorporated in the sample. Two such samples were prepared utilizing the procedures previously developed. Following laser welding of the longitudinal joints and EB welding of the joint ends, a leak test tool was installed on the samples and connected to a mass spectrometer leak test instrument. The samples were then placed in a nylon bag flooded with helium. Neither sample showed any indicated leakage above the background of 2.0×10^{-10} scc GHe/sec. Closeout of the leak test port was made by EB welding a small button of ZrCu into the port counterbore. This final closeout weld was then leak tested. The EB weld chamber was back filled with He prior to removing the samples. The samples were then immediately placed in a bell jar, which was evacuated through a mass spectrometer. Both samples indicated a leak rated of 10^{-6} scc GHe/sec initially, but it quickly decayed to 10^{-7} scc GHe/sec. Both samples had overlapping platelet edges which could entrap He to give the initial indication noted. Since both parts reacted identically, it was felt that both were leak free. At this point both samples were HIP processed.

Following HIP processing the two 2D samples employing the leak check ports were sectioned and metallographically examined. Figure 5.19 is a reproduction of photomicrographs taken from each of the samples. As can be seen, 100% bond was achieved in both of the samples. This experiment, and the ones preceding it, showed the importance of leak tight seal welds to successful bonding. Of equal importance is the testing of the joints to assure that they are leak tight prior to the HIP operation.

5.4.5 3D Panel Joining Demonstration - Task 1.7

This task was undertaken to demonstrate the ability to edge join 3D formed platelet liner segments together, as would be required in the fabrication of a functional liner. The developed and demonstrated diffusion bonding techniques described above were selected as the joining process to be used for this 3D demonstration. The 90 degree 40k basic panel design of Task 1.3, the forming task, was chosen as the design of panels to be joined. For simplicity sake two panels were to be joined, instead of the requisite four panels of an entire 40k assembly.

The design of panels produced and iterated in the forming experiments provided an inadequate land for edge joining. Further iteration of the basic 40k panel design was required to provide panels with acceptable lands. The design and forming of these panels is



13.6.12

Figure 5.18. 2D HIP Bond Samples With Leak Test Capability

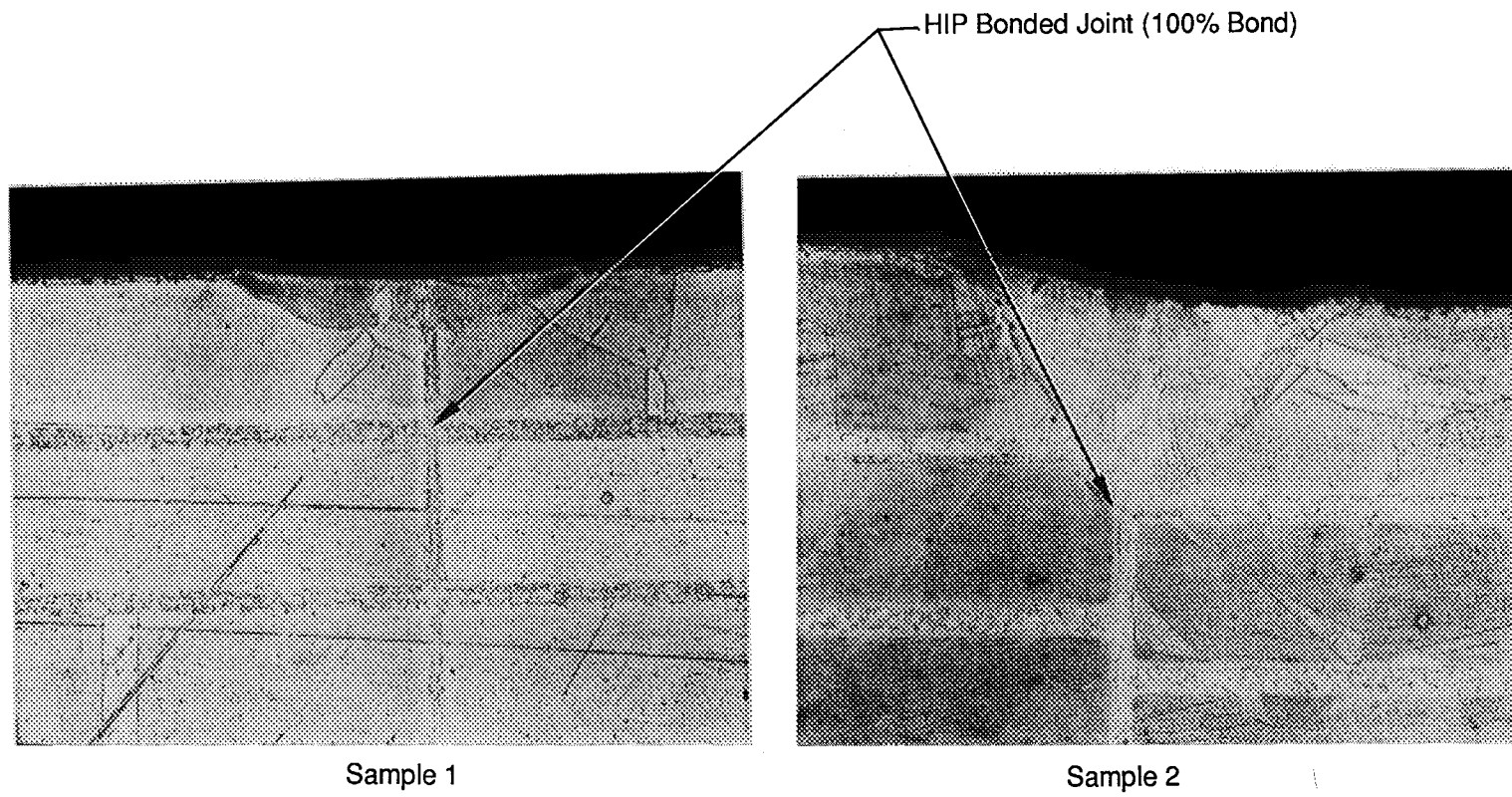


Figure 5.19. 2D HIP Bond Sample Sections

discussed in detail in the forming section of this report and will not be repeated here. The design produced an acceptable land for the joining demonstration.

Eight formed panels of the iterated design (PN 1206530) were fabricated. The panels were then setup on the edge trim/ inspection/ weld fixture and, with the aid of the OGP optical CMM, a "best-fit" average cutting plane was established. Two mating panels were then wire EDM trimmed along this established plane. The EDM process utilized the optimized parameters established in the 2D joining studies. Post EDM measurements confirmed the cuts were made as desired, with a resulting minimum "half-land" thickness of .020 in.

Following the trimming process, the panel edges were etched and the bonding aid applied. Again the previously established procedures were followed. The panels were then fixtured and the edges laser welded together. Figure 5.20 shows the laserwelding in process during the assembly of the two panels.

The laser weld joint, which provides the primary seal, was helium leak checked through it's leak check port with a mass spectrometer type leak detector. The leak check port design was identical to that of the previous 2D samples as shown in Figure 5.18. Following leak testing of the primary seal weld the leak check port was closed out by EB welding in a disk shaped closure. Visual examination of the weld showed an area of the joint that was not fully consumed and large depressions caused by a staking operation used to keep the closure from moving during welding. The non-consumed area was rewelded; the depressions remained a source of concern over potential leakage. Following the reweld operation, the EB chamber was backfilled with helium. The assembly was then removed from the EB chamber and placed in a bell jar connected to a mass spec leak detector. No indication of leakage greater than background (5.0×10^{-8} ccs) was noted. The assembly then underwent the prescribed HIP bond process. Photographs of the assembly are shown in Figure 5.21.

Upon return to APD the part joint was radiograph inspected and the joint was visible, indicating bonding did not occur. As a result of the previous work, leakage was the suspected cause of the failure to bond. To assess potential leakage, a hole was drilled through the leak check closure into the leak check port circuitry; a tube was brazed into this hole. This allowed leak testing of not only the primary seal weld (laserweld) but also the closeout port EB weld as well.

The leak check revealed a leak in the port closeout weld. The leak coincided with a small circumferential crack in the center of the EB weld. The crack was not visible after the original welding of the joint. Two leaks and coincident cracks were also detected on the ID

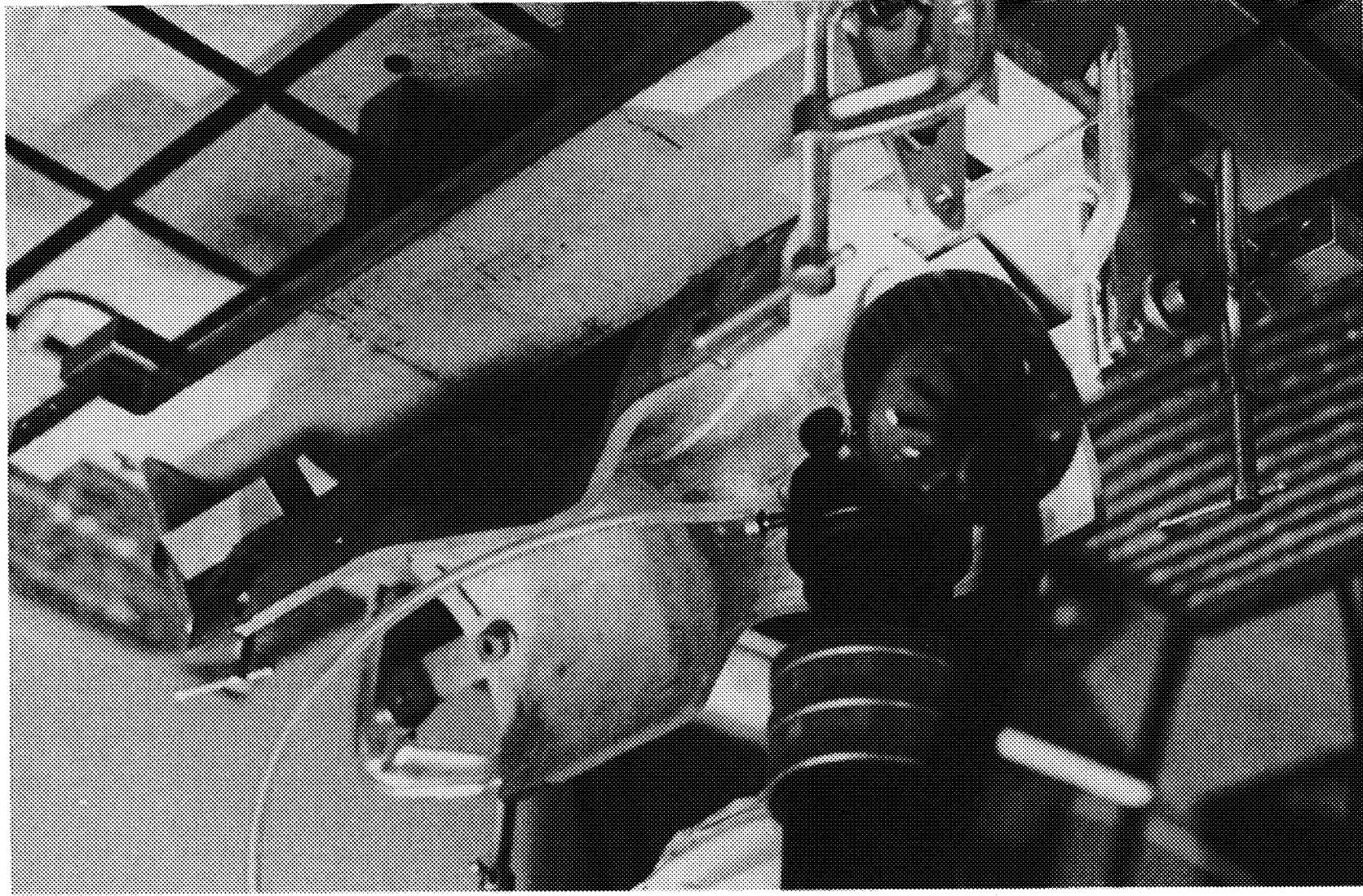
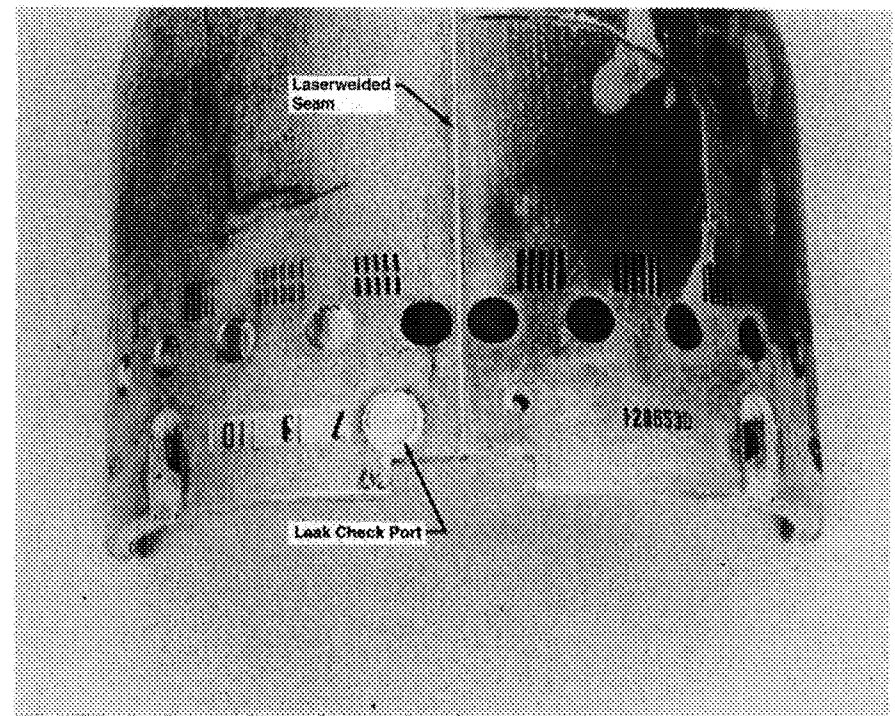
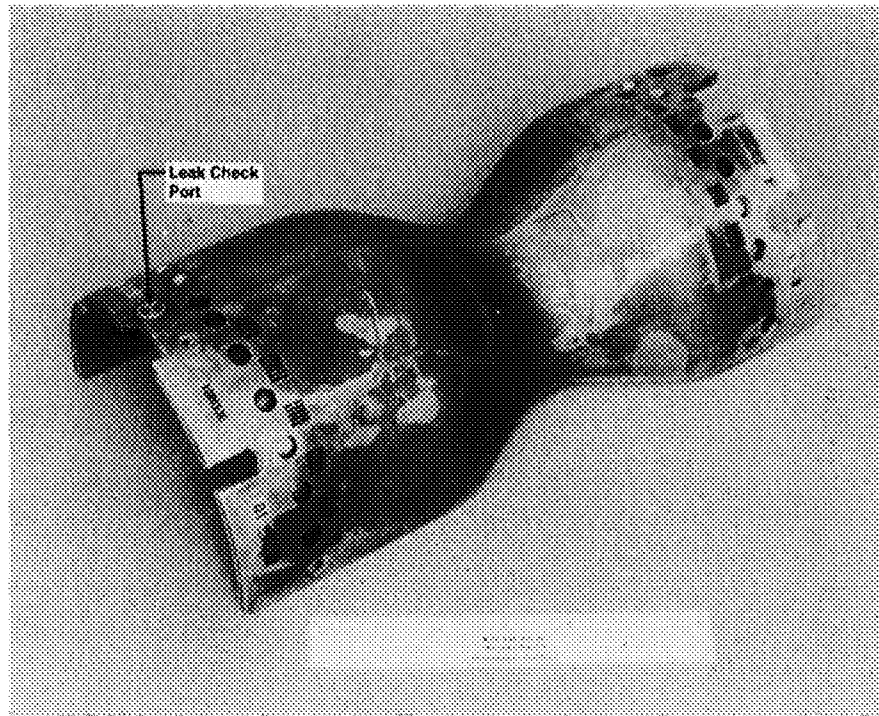


Figure 5.20. Laserwelding of 3D Demo Panels

As-Welded 3D Assembly



Assembly O.D.

Figure 5.21. Joining Study-3D Sample

laserweld downstream of the throat region. These cracks were not visible immediately after the leak check tube braze operation, the last time the welds were inspected. The part saw considerable handling, including an edge milling operation and numerous show-and-tell exposures during this period. It was conjectured that the cracks on the ID laserweld were a result of handling damage and were not present during the HIP operation.

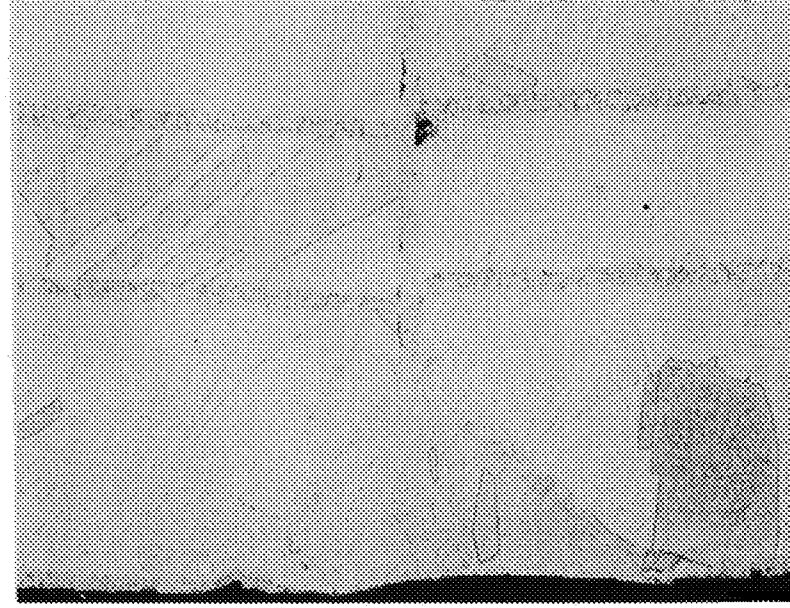
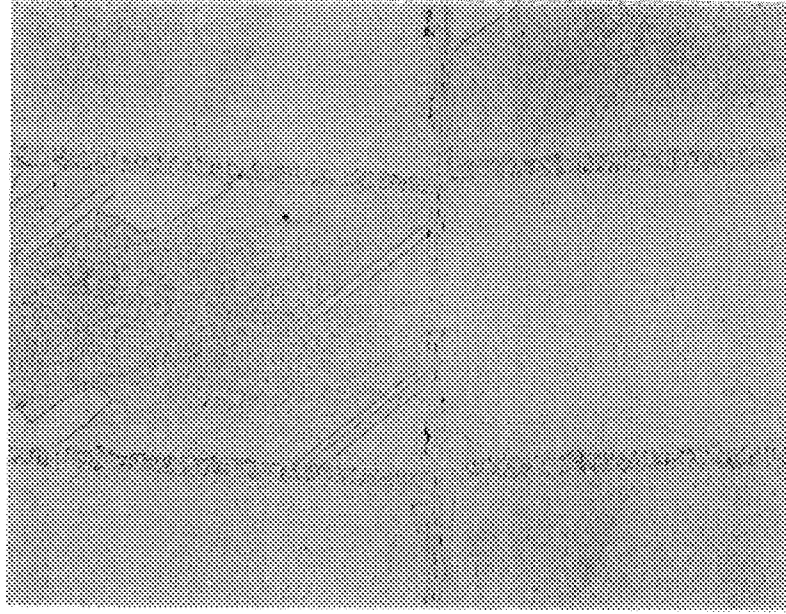
The crack noted in the EB closeout was conjectured to have occurred during the HIP operation. It was believed that the closeout button was not fully seated, allowing the EB weld to be stressed during the HIP. This coupled with potential residual stress in the weld itself led to the formation of the crack. When the crack formed, allowing the HIP gas to enter the joint, the pressure differential causing the stress was eliminated and the crack propagated no further. When the HIP gas entered the joint the forces required for diffusion bonding of the joint interface were also eliminated, thus the joint did not bond.

This assembly, which became known as 3D Demo SN01 assembly, was subsequently reworked by laser weld repairing the noted cracks and EB weld closeout of the leak check tube. The assembly was taken through a repeat of the HIP operation.

Visual inspection of the SN01 assembly showed a positive indication of the success of the HIP bond operation in the collapse of the walls of the leak test tube and of the walls of the leak test port. X-ray examination revealed the joint line to no longer be visible. Metallographic specimens were removed from the forward end and from the throat area of the joint. Copies of photomicrographs of these specimens appear as Figures 5.22 and 5.23. Review of these specimens indicate an estimated 90 to 95% bond. This is considered exceptional when considering that the part saw four thermal cycles beyond 1700°F; these being the first HIP process, which included the solution treat operation, and the three braze cycles required to successfully braze the leak test tube in place.

Figure 5.23, the section through the throat of SN01 assembly, shows an offset in the joint between the two panels making the assembly. The panel edge on the right of the photo is the nominal (planned) 0.020 inch thickness; the panel edge on the left is 0.018 inch thick, thus causing the offset noted. This is consistent with the expected joint prep machining tolerance. There is another offset of note in the vertical, or radial, direction. This measures to be .003 inch and again is consistent with expected assembly tolerance.

Concurrent with the evaluation and rework of 3D Demo SN01, a second assembly, designated SN02, was fabricated. Processing of this assembly was identical to SN01 with some notable exceptions. A change made in the edge prep process made for improved bond



- 100X Magnification
- 90 - 95% Estimated Bond

Figure 5.22. Photomicrographs of 3D Demo SN01 Joint, Forward End

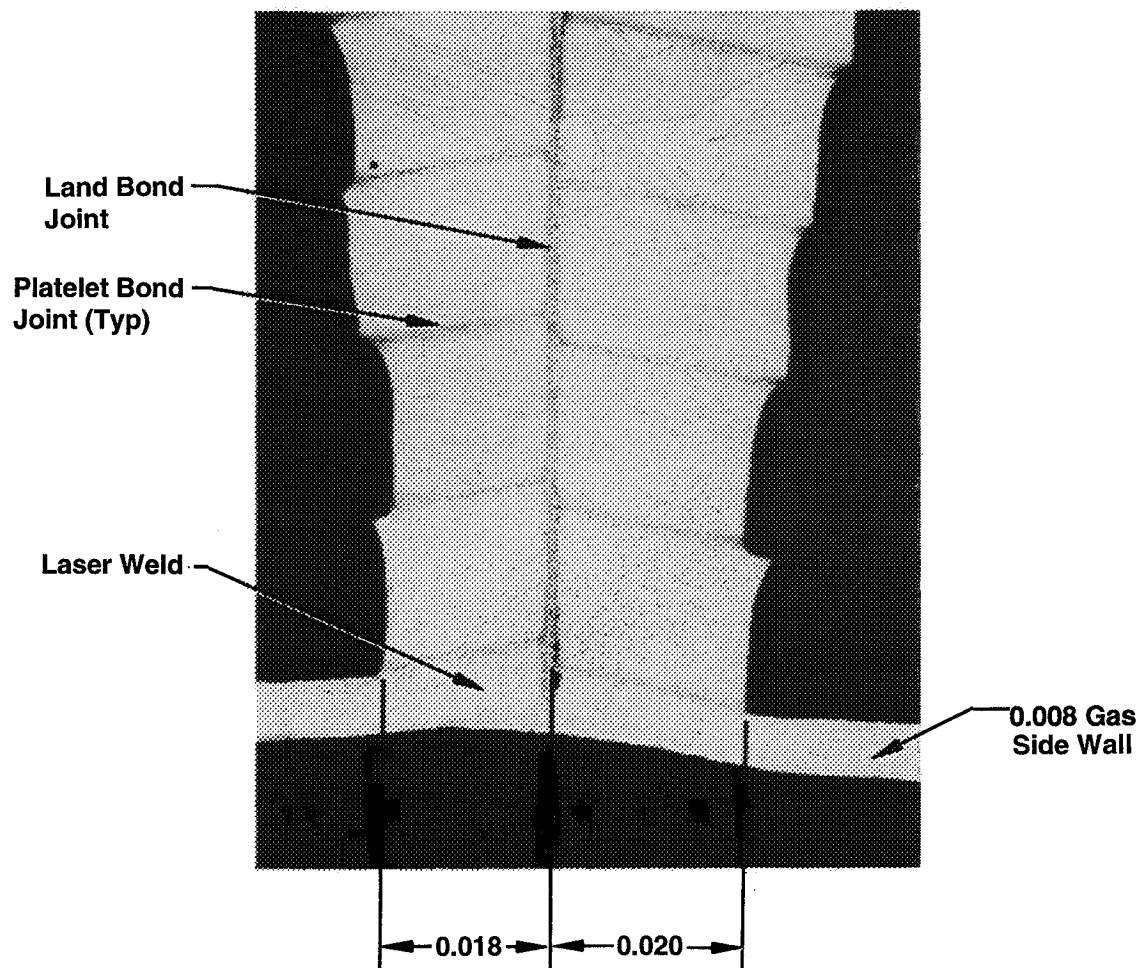


Figure 5.23. 3D Demo SN01 Assy – Throat Land Cross Section

aid application. The change dealt with combining the edge etch operation with the bond aid electroplating operations. This change was incorporated in the Fabrication baseline.

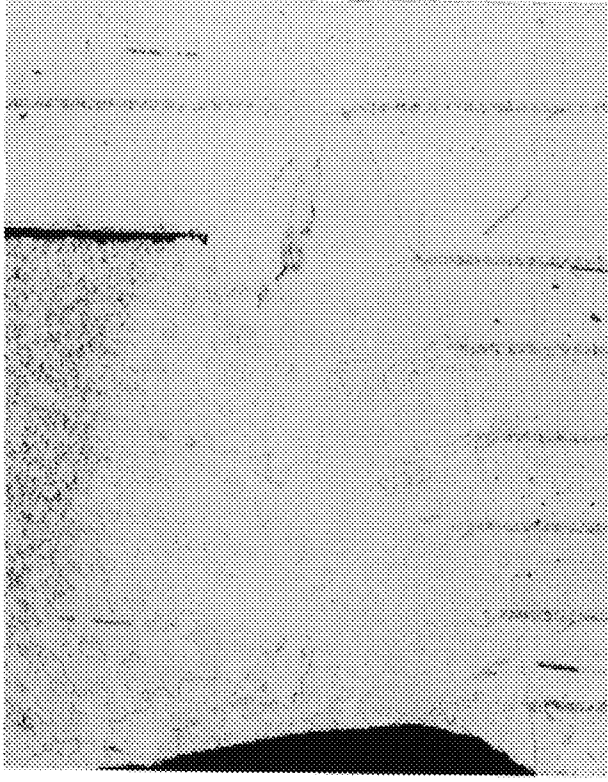
As a result of the problems encountered with the SN01 leak check port closeout button, a change in configuration was incorporated. The button contained a counterbore to better accommodate the residual stress of the weld and to provide compliance during the HIP operation. Additionally, greater care was taken in the deburring operation to assure that the button could fully seat in the port. The effective EB weld depth was also increased in an effort to increase the strength of the joint. Even with these efforts some "rocking" of the button was still evident after installation and prior to welding.

The assembly was processed through the HIP operation and subsequently examined. Visual inspection of the walls of the leak check port did not show collapse. This led to concern over the success of the HIP bond operation. Inspection, under magnification, revealed two small cracks in the EB weld of the leak check port closure. No cracks were visible in the laser seal welds of the joint itself. As all the welds were 100% inspected prior to the HIP operation, it is again conjectured that the cracks in the closure weld occurred during the HIP process. The changes made to the joint configuration between assemblies SN01 and SN02 were not effective in solving this recurring problem.

A metallographic specimen made from the pre-weld sample of the closeout weld of SN02 revealed cracks at the root of the EB weld. Figure 5.24 is a copy of photomicrographs taken from this specimen. The cracks visible indicate that the weld is less ductile than originally believed. While these cracks were of concern, as they affect the ability to successfully complete the bond operation, they are not in the functional portion of the assembly and, in themselves would not impair the function of a formed platelet liner.

A decision was made to repair SN02 assembly and reprocess it through the HIP bonding operation. As the known cracks were in the closure weld and these were believed to be the only cracks, an attempt was made to just weld over the cracked weld areas. This was not successful; the added shrinkage from the reweld caused a crack to appear in the adjacent laser weld joining the two panels of the assembly. At this time it was decided to remove the closure, re-leak check the assembly, repair the laser welds and re-install a new closure prior to HIP processing.

Review of the closure cracking problem and the alloy involved led to the recommendation to replace the ZrCu closeout button with OFHC material. It was felt that the ZrCu-to-ZrCu EB weld previously made was brittle due to the presence of the zirconium in the



- 50X Magnification
- Note Cracking at Root

Figure 5.24. Photomicrographs of Weld Sample of SN02 Closeout

alloy and its migration to the weld zone and HAZ. Replacement of one of the components contributing to the weld melt with OFHC could reduce this susceptibility to cracking.

The SN02 assembly was reworked per plan and again HIP processed. Post HIP inspection, including both visual and X-ray, revealed that again bonding did not occur. It was believed that again a leak in a weld was the cause of the problem, though this time no visible crack in any weld was apparent post HIP.

Because of the success of SN01 3D demo, and a presumed understanding of the causes of the problems with closeout welds, a decision was made to place the SN02 assembly on hold and use it for future process development work. This would be on an as-required basis.

As a result of work performed during this task, the preceding task and other related APD efforts numerous changes were incorporated in the Phase B 40K design. These dealt mainly with improved methods for leak checking, making the leak check port closeout and for assuring that the assembly was leak tight prior to the HIP operation. The basic processes required for affecting the edge diffusion bond were incorporated as they were developed during the Phase A effort.

5.5 CONCLUSION

The study resulted in the selection of diffusion bonded land joints obtained by sealing the prepared surfaces of the joint periphery with laser welding and subsequently Hot Isostatic Processing (HIP) the assembly. This provides an all-diffusion-bonded assembly that is essentially a monolithic structure. Processes developed to affect the panel to panel diffusion bond included surface preparation, ZrCu laser welding, the means for leak checking the laser seal welds, the final closeout of the leak check circuitry, and an NDE method (X-ray) suitable for detecting the presence of a diffusion bonded joint.

At the conclusion of this study it was felt that the process chosen, though demonstrated with flat, 2D and 3D samples, had not been developed to the full extent required for reliable implementation. Questions associated with maintaining leak tight seal welds throughout the HIP processing remained. Planned work on the next program phase was intended to further the understanding of the problem and its resolution.

6.0 FABRICATION PROCESS DEFINITION

6.1 INTRODUCTION

The processes developed in the forming and joining Phase A tasks provide the basis for the fabrication of a formed platelet liner. The process definition task took the information provided by the previous tasks and combined it with other necessary processes to develop a process baseline for the fabrication of an operational 40k sized formed platelet liner. The actual fabrication of this liner was performed as part of Phase B of this contract.

6.2 OBJECTIVE

The desired outcome of this task was a baseline fabrication approach that could be used for the production of a hot fireable 40K formed platelet liner.

6.3 APPROACH AND DISCUSSION

The basic formed liner processes were developed from the results and recommendations of the Phase A forming and joining studies. These were combined with standard processes for the fabrication of platelet hardware and conventional chamber liners. APD engineering, manufacturing and materials and process specialists were enlisted to develop the overall plan and to provide required process details.

A standard APD manufacturing flowchart was chosen as the vehicle for displaying the required processes for the fabrication of the 40K formed platelet liner. This flowchart appears as Figure 6.1 and 6.2. A legend explaining the nomenclature of the flowchart appears as Figure 6.3.

The flowchart displays the life of the liner from the design stage through assembly of its segments, including heat treatment to obtain optimum properties. The operations following those shown are those that are required to complete the assembly of the platelet liner into a structurally adequate and properly manifolded combustion chamber.

LINER ASSEMBLY

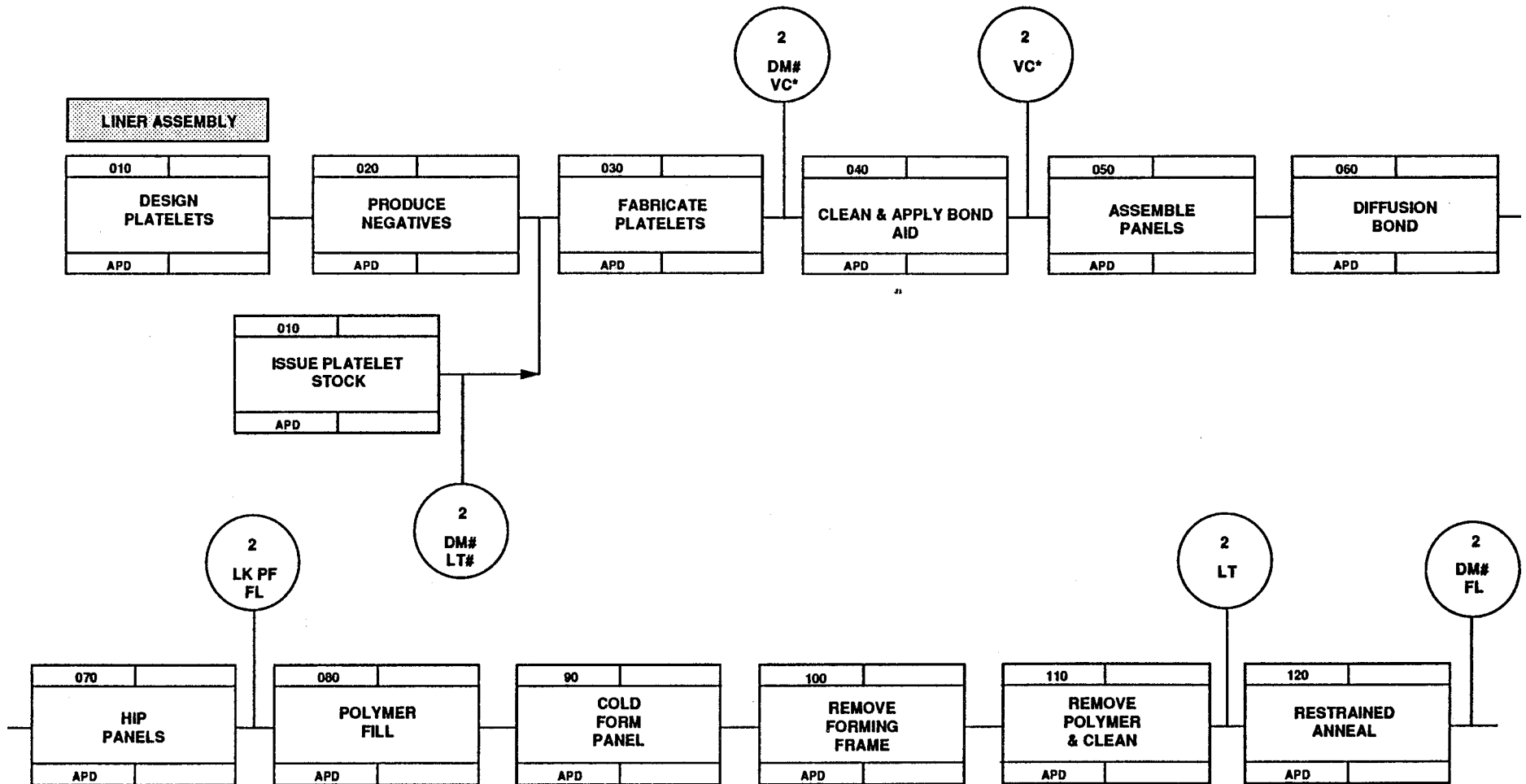


Figure 6.1. Process Definition – 40K Liner, Sheet 1 of 2

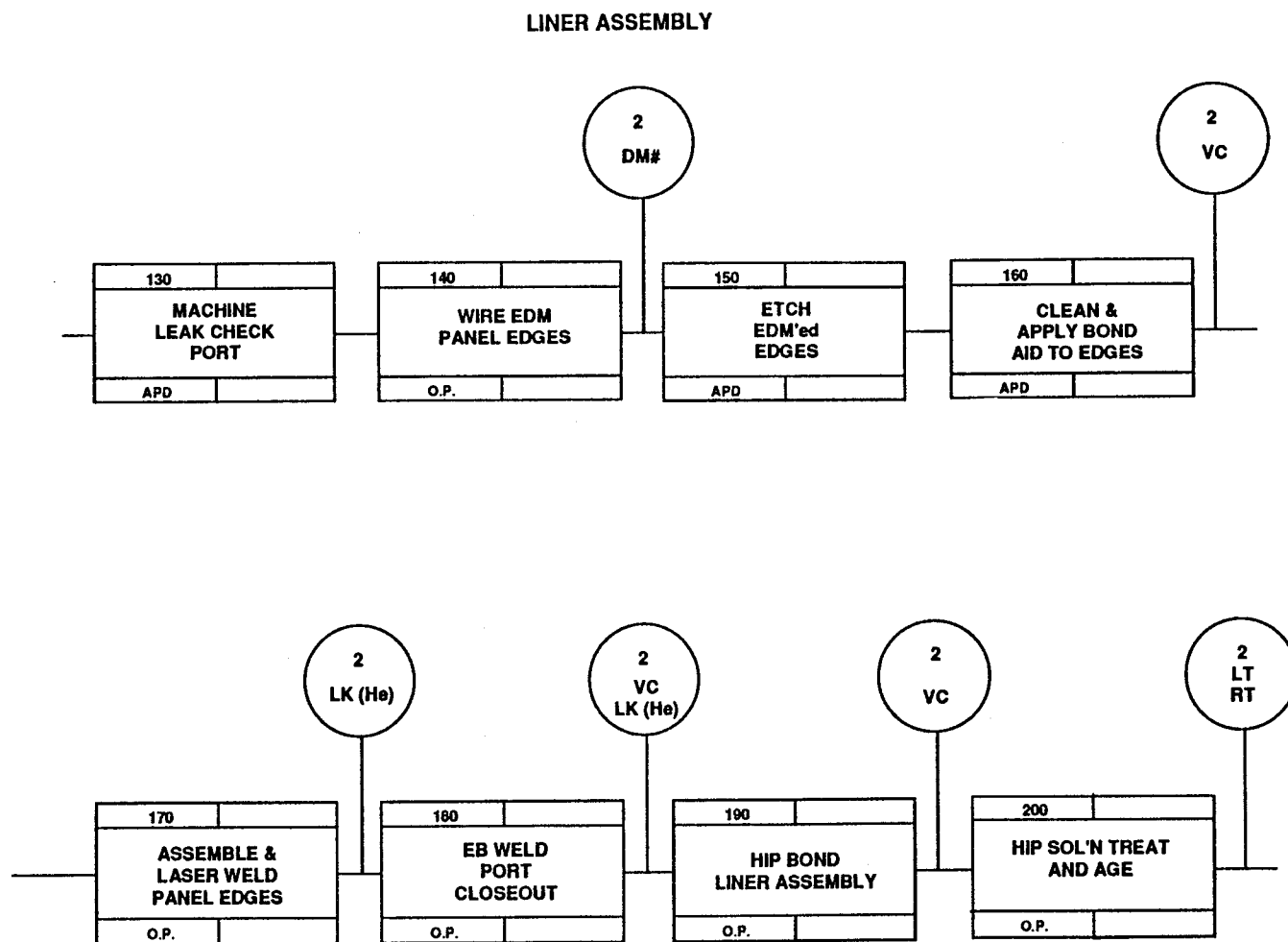


Figure 6.2. Process Definition – 40K Liner, Sheet 2 of 2

FPL 40K CHAMBER ASSEMBLY

FLOW CHART LEGENDS

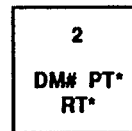
TYPE

- 1 RECEIVING
- 2 IN-PROCESS
- 3 FINAL
- 4 SOURCE

RESPONSIBILITY



EXAMPLE



MEANING:

MAKER RESPONSIBILITY
 IN-PROCESS INSPECTION
 SAMPLE DIMENSIONS
 100% PENETRANT
 INSPECTION
 100% RADIOGRAPHIC
 INSPECTION

INSPECTION/TEST

PT PENETRANT
 RT RADIOGRAPHIC
 AT ACOUSTIC EMISSION
 ET EDDY CURRENT
 UT ULTRASONIC
 MT MAGNETIC PARTICLE
 PF PROOF
 LK LEAK
 BT BURST
 VC VISUAL
 DV DATA/OPERATOR VERIFICATION
 DM DIMENSIONAL
 WS WITNESS
 EL ELECTRICAL
 CL CALIBRATION LAB
 WI WELD INSPECTION
 SH SHIPPING
 LT LABORATORY TESTING
 HT HARDNESS
 ET ENVIRONMENTAL TESTING
 GA GAGING
 FL FLOW

METHOD

* 100%
 # SAMPLE
 & WITNESS
 ~ SPC
 @ AUDIT

Figure 6.3. Flowchart Legend

7.0 SILVER AIDED BONDING

7.1 INTRODUCTION

Diffusion bonding of ZrCu platelets requires the use of a bond aid at the platelet-to-platelet interface. An aid is required due in large part to the reactive nature of the zirconium in the alloy. Zirconium oxide readily forms on the free surface of the platelet and will inhibit the diffusion bonding phenomenon. In order for effective diffusion bonding to occur, the surface oxides must be removed or chemically reduced in a cleaning operation and the oxide-free surface protected. This surface is most easily protected with a material that can be readily deposited on the surface. This material, or "bond aid" as it is known, must in itself form surface oxides that are easily reduced in the bond furnace environment or that are soluble in the bond zone. It must also be soluble to some extent with the base material. These are the basic requirements of a bond aid; additional considerations include affects on the base material. An example of these considerations are bond zone alloy constituents, concentration and phase which in turn affect the mechanical and physical properties of the bonded assembly.

One of the physical properties of concern with a cooled combustor liner is the thermal conductivity of the liner material. When a liner is constructed of diffusion bonded platelets the thermal conductivity perpendicular to the bond lines must be considered. The presence of a bond aid with a conductivity lower than that of the parent material will lower the conductivity of the bonded part. Depending upon the ZrCu diffusion bond process and bond aid parameters selected, a reduction in conductivity from that of wrought ZrCu of as much as 10% to 15% is witnessed perpendicular to the bond lines. Parallel to the bond lines there is no reduction in conductivity.

Employing an alternate bond aid could reduce or negate this thermal conductivity reduction. Silver was thought to be a viable candidate because of its solubility in copper, its high thermal conductivity and readily reduced oxides. As such, silver was selected as the bond aid for this study.

7.2 OBJECTIVE

The objective of this study was to identify and develop the processes required for diffusion bonding ZrCu platelets utilizing silver as a bonding aid. This development included pre-bond, bond and post-bond processing to allow optimization of bonded material properties. The

study was intended to provide sufficient data to allow design of combustor liners with this new bond process.

7.3 APPROACH

A program was adopted based on the design of experimentation philosophy. In this program quality optimization techniques were utilized. A Taguchi array was defined to reduce the number of test specimens required to evaluate the multiple processing alternatives of interest. The key parameters which were investigated were bonding temperature, bond aid thickness, and thermal post processing. The levels, or number of variations, examined for each of these parameters were three, two and three, respectively. The chosen selection criteria was tensile strength at room temperature and at 1000°F; with a higher value considered better.

7.4 DISCUSSION

7.4.1 Taguchi Array

A modified L18 Taguchi array was chosen for evaluating the selected process factors. A copy of this array is shown in Table 7.1. The factors and their selected levels are defined in Table 7.2.

7.4.2 Sample Preparation

Six different bond blocks, designated Blocks A through F, were fabricated for this study. The blocks were constructed from 60 pieces of 5.0 inch x 5.0 inch x 0.017 inch ZrCu platelet stock sandwiched between two 4.5 inch x 4.5 inch x 0.90 inch CRES end plates. The end plates provided grip length for tensile specimens subsequently taken from the bond blocks. All platelet stock and end plates were plated with the appropriate thickness of silver for that particular block as specified by the test matrix.

Following plating, which was performed by an outside vendor, a cleaning operation was required to remove visually apparent surface oxides. Considerable effort was required to identify and test an adequate cleaning method. The selected method utilized a commercially available tarnish remover: Noxon Quick-Dip silver cleaner, American Home Products Corp., Cranford, New Jersey.

After plating and cleaning, the six individual bond blocks were assembled and bonded per the test matrix. The blocks were then cut into 1/2 inch x 1/2 inch x 3 inch pieces. Selected pieces, identified by their block letter and location in the block as shown in Figure 7.1,

TABLE 7.1. AG AIDED BOND EXPERIMENT – TAGUCHI ARRAY

Bond Block Designation	Column Condition	L ₁₈ (2 ¹ , 3 ⁷)								(e)	
		1	2	3	4	5	6	7	8	(e)	
A	1	1	1	1	1	1	1	1	1	1	1
	2	1	1	2	2	2	2	2	2	2	2
	3	1	1	3	3	3	3	3	3	3	3
B	4	1	2	1	1	2	2	3	3	3	3
	5	1	2	2	2	3	3	3	1	1	1
	6	1	2	3	3	1	1	2	2	2	2
C	7	1	3	1	2	1	3	2	2	3	3
	8	1	3	2	3	2	1	3	1	1	1
	9	1	3	3	1	3	2	1	2	2	2
D	10	2	1	1	3	3	2	2	1	2	1
	11	2	1	2	1	1	3	3	2	2	2
	12	2	1	3	2	2	1	1	3	3	3
E	13	2	2	1	2	3	1	3	2	2	2
	14	2	2	2	3	1	2	1	3	3	3
	15	2	2	3	1	2	3	2	1	1	1
F	16	2	3	1	3	2	3	1	2	2	2
	17	2	3	2	1	3	1	2	3	3	3
	18	2	3	3	2	1	2	3	1	1	1

M7D59/FFFR-1

TABLE 7.2

FACTORS AND LEVELS FOR TAGUCHI ARRAY

<u>Factor</u>		<u>Level</u>		
1	AgThk	Thick		Thin
2	Bond Temp	Low	Med	High
3	Diff Cycle?	Yes	No	Yes (2 Levels)
4*	Diff & SOLI'N	A	B	C
5	Age Temp	Low	Med	High
6	Age Time	16,8,4 hr	8,4,1 hr	8,4,1 hr
* A Long With HIP				
B Long Without HIP				
C Short With HIP				

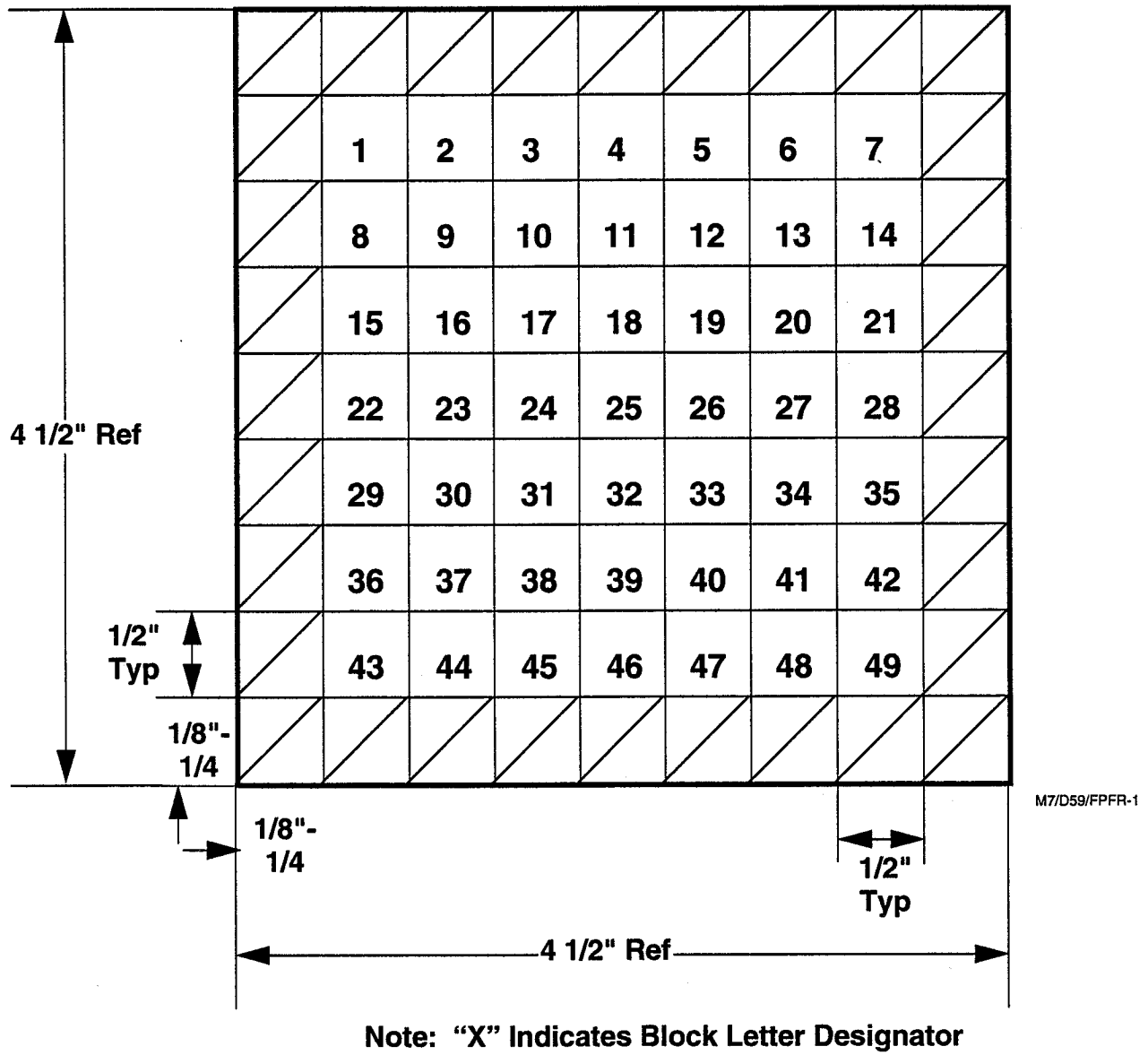


Figure 7.1. Bond Block Sample Identification

went through the post-bond processing as specified by the test matrix and summarized in Tables 7.3 and 7.4.

7.4.3 Tensile Tests

Samples from the as-processed specimens were machined into tensile bars and subjected to either room temperature or 1000 degree F tensile tests. The results of this testing are displayed in Table 7.5. Ultimate strength, 0.2% yield strength, elongation and reduction in area are tabulated for each sample tested. Several samples broke either during machining or setup and thus no data was available.

In summary, the Taguchi analysis indicates that a low bonding temperature is preferred with a thin silver bond aid thickness and post-bond thermal processing should include a long diffusion cycle and a HIP during the solution ageing. The greatest influence on tensile strength was the bond aid thickness. Some questions were raised concerning the handling of the high bonding temperature samples. Numerous samples exhibited low ductility and inconsistency in the data obtained.

Although the Taguchi analysis provides information for the understanding of influencing factors for process optimization, it does not in itself indicate whether the results are acceptable or even promising. To assess this it is necessary to compare the results to the known standard. Comparison of tensile strengths developed by the two systems show a significantly lower strength for the silver aided bonds. This effect is illustrated in Figure 7.2 which shows a comparison of silver aided v.s. typical standard aided bond ultimate tensile strengths at 1000 degrees F. The very best silver aided bond exhibited only 80% of the strength of the standard process. An even more striking comparison is the ductility provided by the two systems. The best silver aided bond tested at 1000 degrees F had a reported 1% elongation. This compares to 12% for the standard aided bond. The reason for the poor performance is evident from microstructural analysis.

7.4.4 Metallographic Analysis

Specimens were sectioned, polished and analyzed. Unstained samples were subjected to microprobe line scan analysis to characterize the distribution of copper, silver and zirconium. Fractography was conducted on a scanning electron microscope. Additional characterizations of the fracture surface oxides were accomplished using the wavelength spectroscopy capability of the microprobe. After optical microscopic examination, the specimens were etched to show the underlying structure.

TABLE 7.3. SAMPLE PROCESSING MATRIX, BONDING POST-BOND

Diffusion/Solution Cycles

ID	Ag	TEM	None	A	B	C
1	THIN	LOW		A-09, A-12, A-30, A-33		
2		LOW	A-10, A-13, A-31, A-34			
3		LOW				A-17, A-20, A-38, A-41
4		MED		B-09, B-12, B-30, B-33		
5		MED	B-10, B-13, B-31, B-34			
6		MED				B-17, B-20, B-38, B-41
7		HIGH			C-17, C-20, C-38, C-41	
8		HIGH	C-10, C-13, C-31, C-34			
9		HIGH		C-09, C-12, C-30 C-33		
10	THICK	LOW				D-09,D-12, D-30, D-33
11		LOW	D-10, D-13, D-31, D-34			
12		LOW			D-17, D-20, D-38, D-41	
13		MED			E-10, E-13, E-31, E-34	
14		MED	E-09, E-12, E-30, E-33			
15		MED		E-17, E-20, E-38, E-41		
16		HIGH				F-09,F-12, F-30, F-33
17		HIGH	F-10, F-13, F-31, F-34			
18		HIGH			F-17, F-20, F-38, F-41	

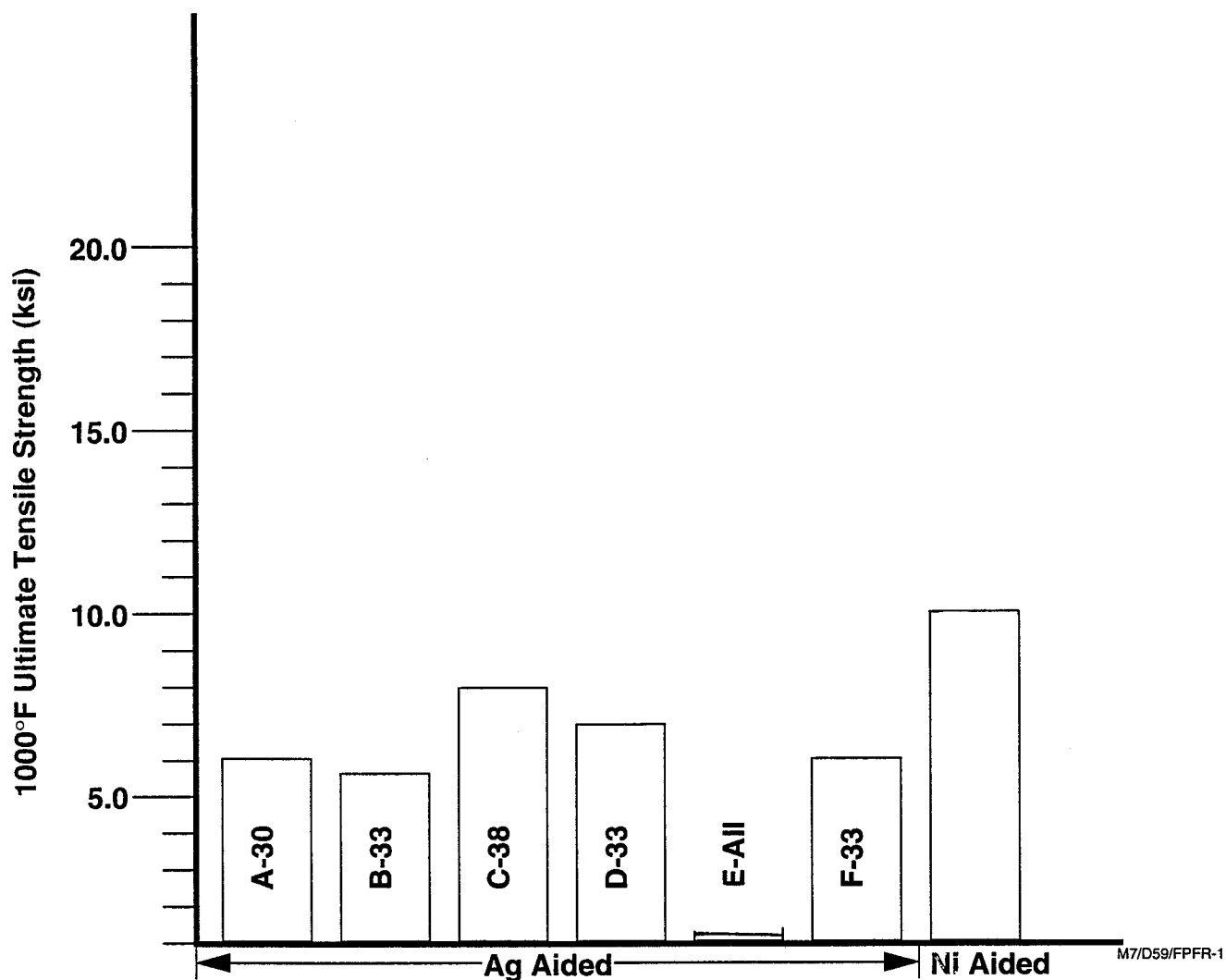
TABLE 7.4. SAMPLE PROCESSING MATRIX, POST-BOND AGE

Aging Cycles

ID	LOW / 16	LOW / 8	LOW / 4
1	A-09, A-12, A-30, A-33		
2			
3			
4			
5			
6	B-17, B-20, B-38, B-41		
7			C-17, C-20, C-38, C-41
8			
9			
10			
11			
12			
13			E-10, E-13, E-31, E-34
14			
15			
16			
17			
18		F-17, F-20, F-38, F-41	
ID	MED / 8	MED / 4	MED / 1
1			
2			
3			
4		B-09, B-12, B-30, B-33	
5			
6			
7			
8			
9			
10			
11			
12	D-17, D-20, D-38, D-41		
13			
14			
15			E-17, E-20, E-38, E-41
16			
17			
18			
ID	HIGH / 8	HIGH / 4	HIGH / 1
1			
2			
3			A-17, A-20, A-38, A-41
4			
5			
6			
7			
8			
9		C-09, C-12, C-30, C-33	
10		D-09, D-12, D-30, D-33	
11			
12			
13			
14			
15			
16	F-09, F-12, F-30, F-33		
17			
18			

TABLE 7.5. TENSILE TEST RESULTS

Sample Number	Test Temp. (°F)	FTU (ksi)	0.2 % FTY (ksi)	Elongation (percent)	Reduction in Area (%)
A09	RT	33.9	9.39	53	73.3
A12	RT	34.1	9.47	51	72.0
A17	RT	33.8	10.9	52	73.3
A20	RT	33.8	10.1	54	69.1
A30	1000	6.74	6.67	1	0
A33	1000	6.31	6.18	1	0
A38	1000	5.71	5.70	1	1
A41	1000	5.87	5.85	1	0
B09	RT	12.8	9.21	2	3.2
B12	RT	17.2	10.0	13	13.1
B17	RT	2.45	2.13	0	0
B20	RT	ND	ND	ND	ND
B30	1000	4.62	ND	<0.5	0
B33	1000	5.72	ND	1	0
B38	1000	ND	ND	ND	ND
B41	1000	BS	ND	ND	ND
C09	RT	33.9	9.87	51	71.3
C12	RT	34.1	9.51	57	70.2
C17	RT	34.5	9.19	52	70.6
C20	RT	ND	ND	ND	ND
C30	1000	ND	ND	ND	ND
C33	1000	5.96	5.93	0.5	1
C38	1000	8.0	ND	1	1
C41	1000	7.87	ND	1	1
D09	RT	23.1	9.63	7	2.3
D12	RT	25.4	10.8	9	4
D17	RT	32.1	11.2	22	19.6
D20	RT	32.7	11.0	21	19.8
D30	1000	2.73	ND	<0.5	0
D33	1000	6.54	ND	0.5	0
D38	1000	6.32	ND	0.5	0
D41	1000	6.43	ND	0.5	0
E10	RT	ND	ND	ND	ND
E13	RT	ND	ND	ND	ND
E17	RT	35.4	10.5	38	31.3
E20	RT	28.0	9.82	16	16.8
E31	1000	ND	ND	ND	ND
E34	1000	ND	ND	ND	ND
E38	1000	BS	ND	ND	ND
E41	1000	BS	ND	ND	ND
F09	RT	31.3	11.4	21	19.0
F12	RT	33.7	10.2	34	23.8
F17	RT	ND	ND	ND	ND
F20	RT	20.4	10.8	9	9.4
F30	1000	5.87	5.73	2	1.6
F33	1000	6.03	5.75	1.5	0.8
F38	1000	ND	ND	ND	ND
F41	1000	5.71	5.59	2	0.8
BS	Broke during set-up				
ND	No data				



Bar Graph Comparison of 1000°F Ultimate Tensile Strength of Best Ag Aided Bond Development Samples With Typ STD Aid Block

Figure 7.2. Comparison of Bond Aid Performance

Typical room temperature tensile tests exhibited two failure modes corresponding to ductile and brittle failure. All room temperature samples which failed in a brittle manner separated along the platelet bond interface. The ductile failures showed no tendency to fail along these planes.

Metallographic sections of typical high temperature tensile specimens after testing showed a single failure mode, that being a brittle failure. All 1000°F specimens exhibited two common features: the bond interface is characterized by a line of particles along the interface and many small cracks exist along the edges of the samples.

These particles appear to be residual intermetallics or oxides that create a connected weak boundary across the sample and are thus susceptible to failure. This condition appears to exist in all of the silver aided bond specimens produced. Note that no similar condition has been found in nickel aided bond assemblies or specimens.

7.5 CONCLUSIONS

The Taguchi analysis performed did provide an indication of the influencing factors in silver aided bonding of ZrCu. Bond aid thickness appears to have the most influence, with a thinner bond aid layer preferred. Bond temperature appears best at the lower values. Post bond treatments under HIP conditions provide an increase in elevated temperature strength.

Tensile tests and subsequent metallography indicated a lack of strength and ductility at elevated temperatures. This condition appears related to the micro-chemistry of the bond and may be an unavoidable result of the combination of constituents of the parent material and the silver bond aid.

Another disturbing condition was witnessed with this bond study. A high degree of variability and poor bonds were seen for no apparent reason. This leads one to assume that standard processing techniques that are adequate for the current bond system may be inadequate for the silver aided system. Further extensive development may be required to understand this problem.

It is felt that improvements in the bond properties could be made with further experimentation and investigation of the silver aided bond process. However, the results to date, when compared to the standard aided system, indicate that significant improvements are required before silver can be considered a viable diffusion bond aid for ZrCu.

APPENDIX A

Platelet Design and Fabrication Processes

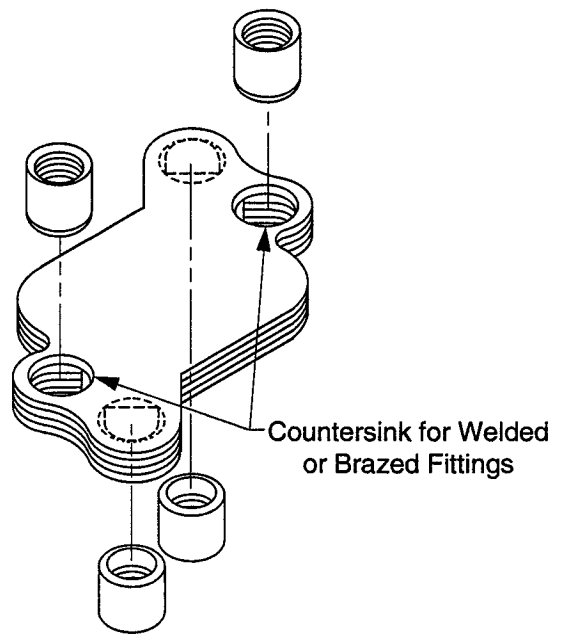
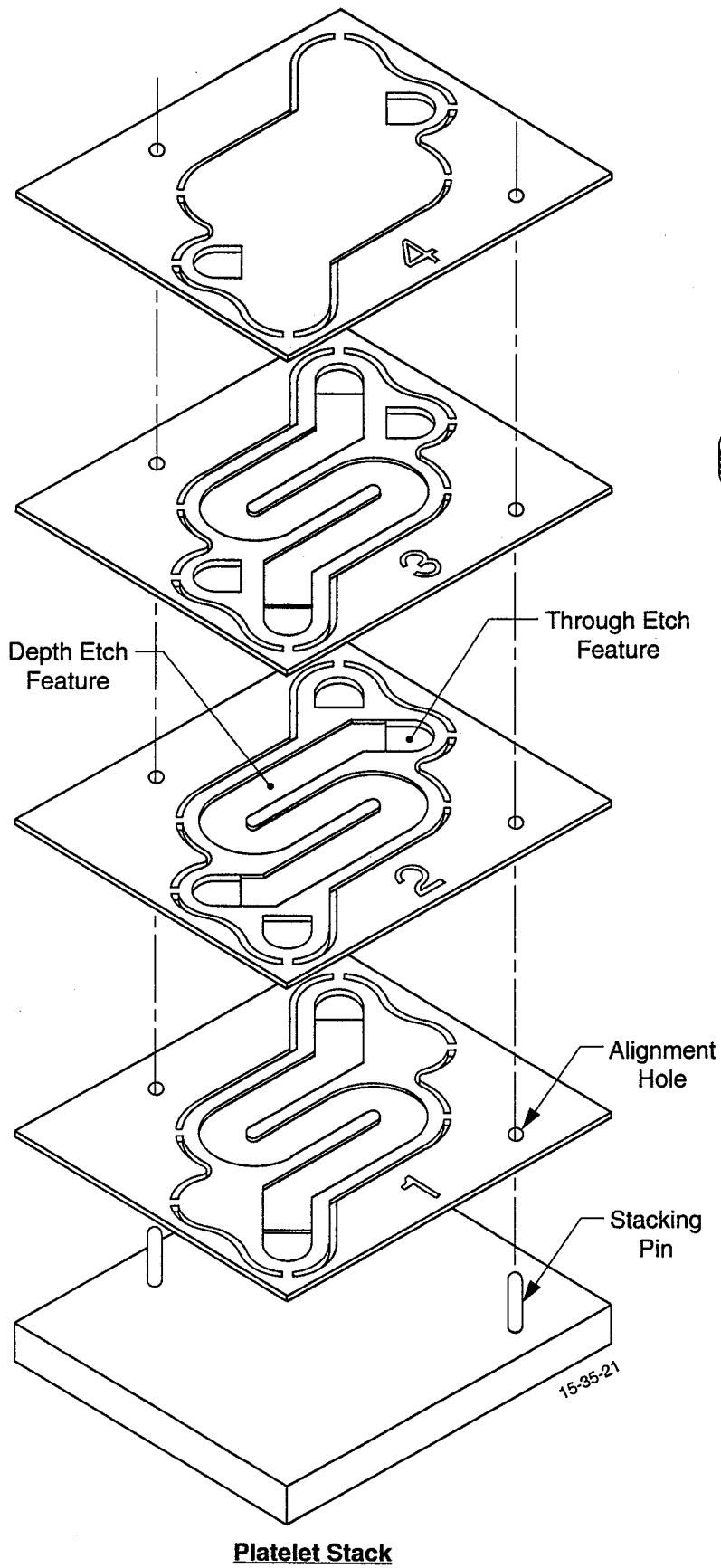
The platelet concept is a design and fabrication technique that can create compact monolithic structures containing thousands of intricate, precisely located fluid flow passages. Aerospace applications include high performance propellant injectors for large and small rocket engines, complete multiple liquid rocket thruster assemblies, cooled nosetips for reentry vehicles, transpiration cooled forebodies and radomes for hypersonic interceptors, sealed aircraft leading edges for the National Aerospace Plane, fluidic circuits for aircraft engine controls, high performance heat exchangers, and regeneratively cooled combustion chamber liners. Aerojet has fabricated hundreds of different platelet devices since the technique was developed in 1964. A summary of the thirteen different types of platelet cooling devices fabricated by Aerojet is shown in Table A-1.

TABLE A-1.

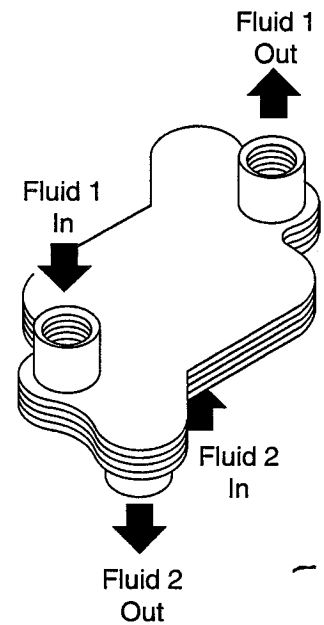
AEROJET HAS FABRICATED THIRTEEN DIFFERENT TYPES OF COOLING DEVICES USING PLATELET TECHNOLOGY

Device	Application	Date
Transpiration Cooled Chamber	Rocket Engine Cooling	1964-1990
Cooled Turbine Blade	High Temperature Turbine	1967
Transpiration Cooled Nosetips	Re-Entry Vehicle Nosetip Cooling	1968-1992
Heat Pipe Wicks	Low ΔP , High Flux Wicks	1968-1970
Heat Exchangers	Cooling or Heating O ₂ or H ₂	1976-1992
Metallic Radome	Interceptor Vehicle Cooling	1983-1992
Scramjet Strut	Cooled Structures in Hypersonic Airstream	1983-1991
Flame Arrestor	H ₂ Tank Flame Arrestor	1984-1986
Convectively Cooled Chamber	Rocket Engine Cooling	1985-1992
IR Windows	Hypersonic Interceptor Vehicle Cooling	1985-1992
Forebodies	Hypersonic Interceptor Vehicle Cooling	1986-1992
NASP Panels	Convective Vehicle Cooling	1986-1991
Leading Edges	Cooled Structures in Hypersonic Airstream	1988

Platelets are thin metal or ceramic sheets covered by a pattern of intricate through and half-depth features. Structures are formed by stacking different sheet designs in a pre-determined sequence, then diffusing bonding (in the case of metal sheets) or sintering (in the case of ceramics) the assembly. Features line up vertically between platelets to form fluid distribution and control circuits. The design concept is shown in Figure A-1. Materials used successfully in



Bonded and Trimmed Platelet Assembly



Completed Platelet Structure

Figure A1. Platelets of Different Designs are Stacked and Bonded to Create a Single, Monolithic Fluid Control Device

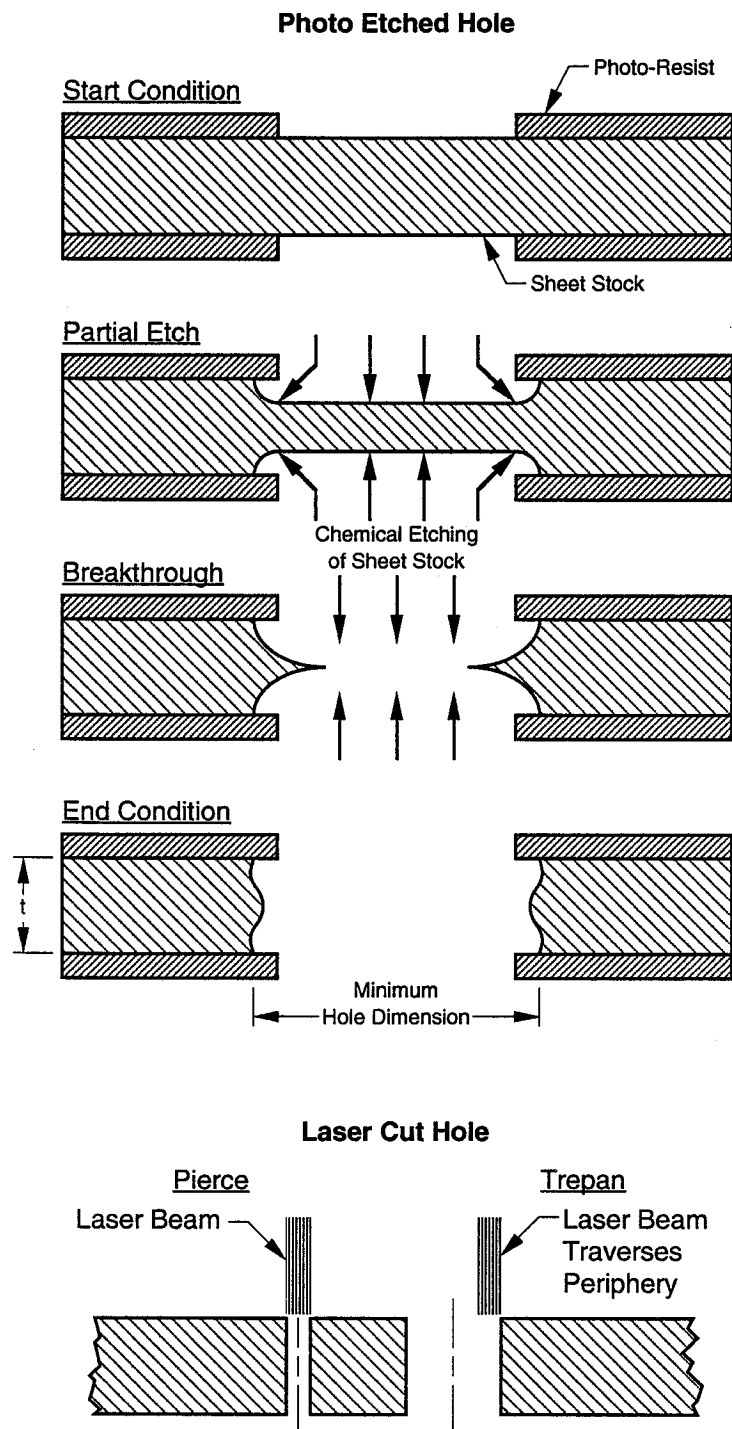
platelet devices include 304L and 347 stainless steel; Inconel 600; Nickel 200; 1100, 3003, and 5052 aluminum; commercially pure, 6Al 4V, and Beta 21S titanium; copper; zirconium-copper; Narloy Z; molybdenum; beryllium; and silicon nitride.

Platelet designs are not limited to flat, 2 dimensional applications. Metallic platelet structures can be post-processed after diffusion bonding to form more complex shapes. For example, the flat formed platelet liner chamber panels are pressed in a forming die after diffusion bonding to create final combustion chamber curvatures.

Platelets are formed in one of two ways. In the photo-chemical machining process, patterns are transferred onto a photo-resist coated sheet stock surface using photographic techniques. Sheets are then spray etched with acid to remove platelet regions previously exposed to light. Etching from one side only results in partial penetration, depth-etched features, while etching from both sides creates through-holes. In the laser cut process, a high intensity laser beam erodes material and creates through-holes. A schematic of each process is shown in Figure A-2. Both processes are currently used by Aerojet and have certain benefits. Chemical etching is fast since all features are created simultaneously. In addition, chem-etching allows depth-etched design features. Laser cutting advantages include smaller holes in thicker platelets, straight edges and angle holes.

Platelet fabrication begins in the CAD room (Figure A-3). After defining flow feature geometries by design and analysis techniques, exact platelet dimensions are defined on Aerojet's CAD system. Design files are then electronically transferred to the negative photo plotting station. An engineer translates platelet dimensions into laser scanner commands (Figure A-4). Regions of platelet exposure are light on the negative; masked platelet regions must be dark. The laser beam scans and photographically exposes only the dark regions on mylar film, which is then developed to reveal the platelet image. These dark areas become etched regions on the platelet. An example of a developed photographic master formed by the laser scanner is shown in Figure A-5.

After completing all photo masters fabrication moves to the platelet shop. Sheet stock of appropriate thickness is cleaned (Figure A-6), then coated with a light-sensitive film photoresist (Figure A-7). Photographic negatives are attached to both sides of the sheet stock, then exposed to light (Figure A-8). After removing the negatives each sheet is developed in a chemical bath, then rinsed to wash away unexposed photoresist.



1.12.2.14

Figure A-2. Platelets Are Formed by Either Photo-Etching or Laser Cutting

ORIGINAL PAGE
BLACK AND WHITE PHOTOGRAPH



Figure A-3. Platelet Detail Dimensions are Defined on Aerojet's CAD System

ORIGINAL PAGE
BLACK AND WHITE PHOTOGRAPH



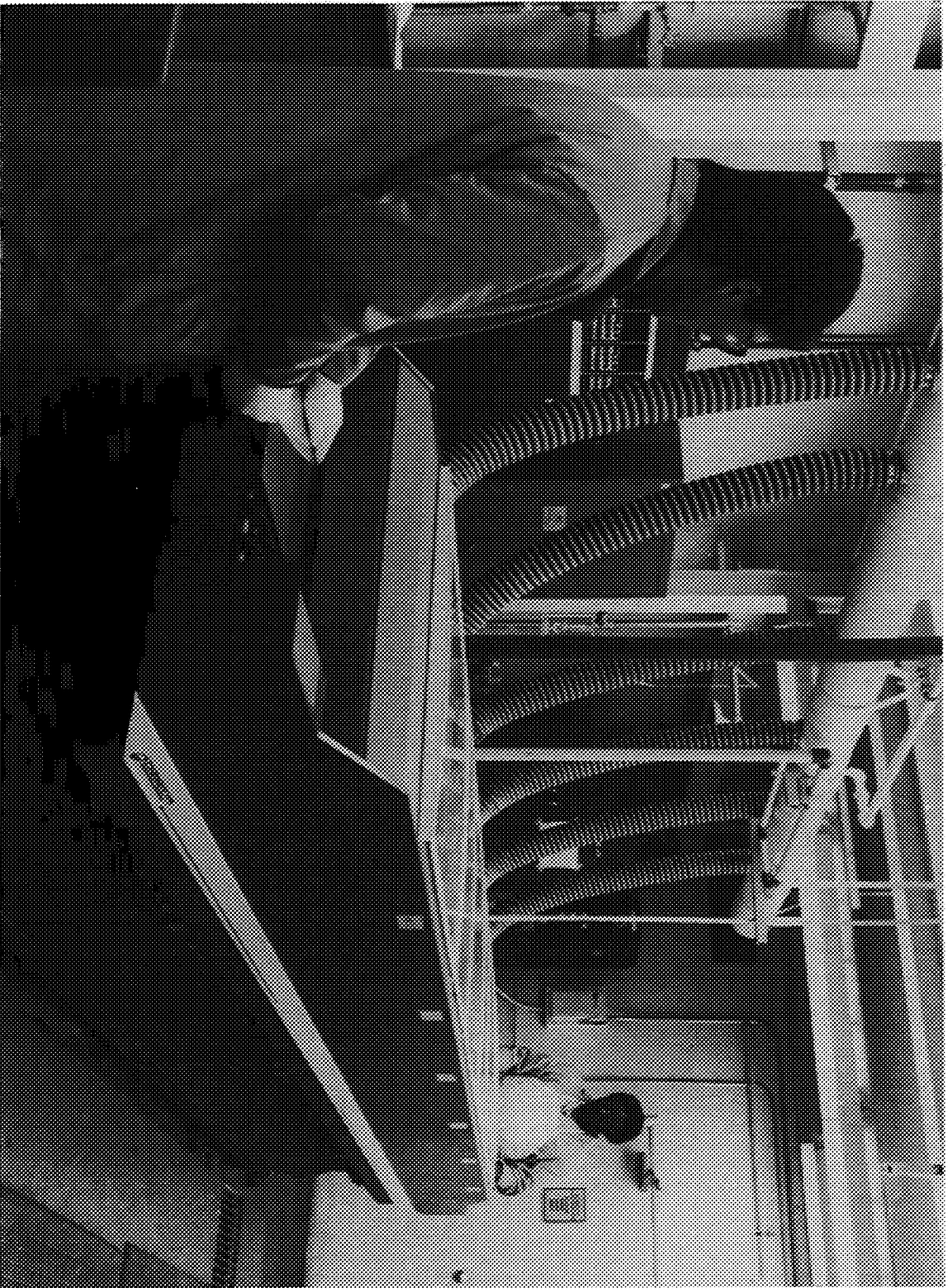
Figure A-4. CAD File Data is Translated Into Laser Scanner Commands at the Photo Plotting Station

ORIGINAL PAGE
BLACK AND WHITE PHOTOGRAPH



Figure A-5. Full Size Photographic Masters are Formed by Laser Scanner (A Large Scale Injector Photo Master is Shown)

ORIGINAL PAGE
BLACK AND WHITE PHOTOGRAPH



1 Figure A-6. Chemcut Sheet Stock Degreaser

ORIGINAL PAGE
BLACK AND WHITE PHOTOGRAPH

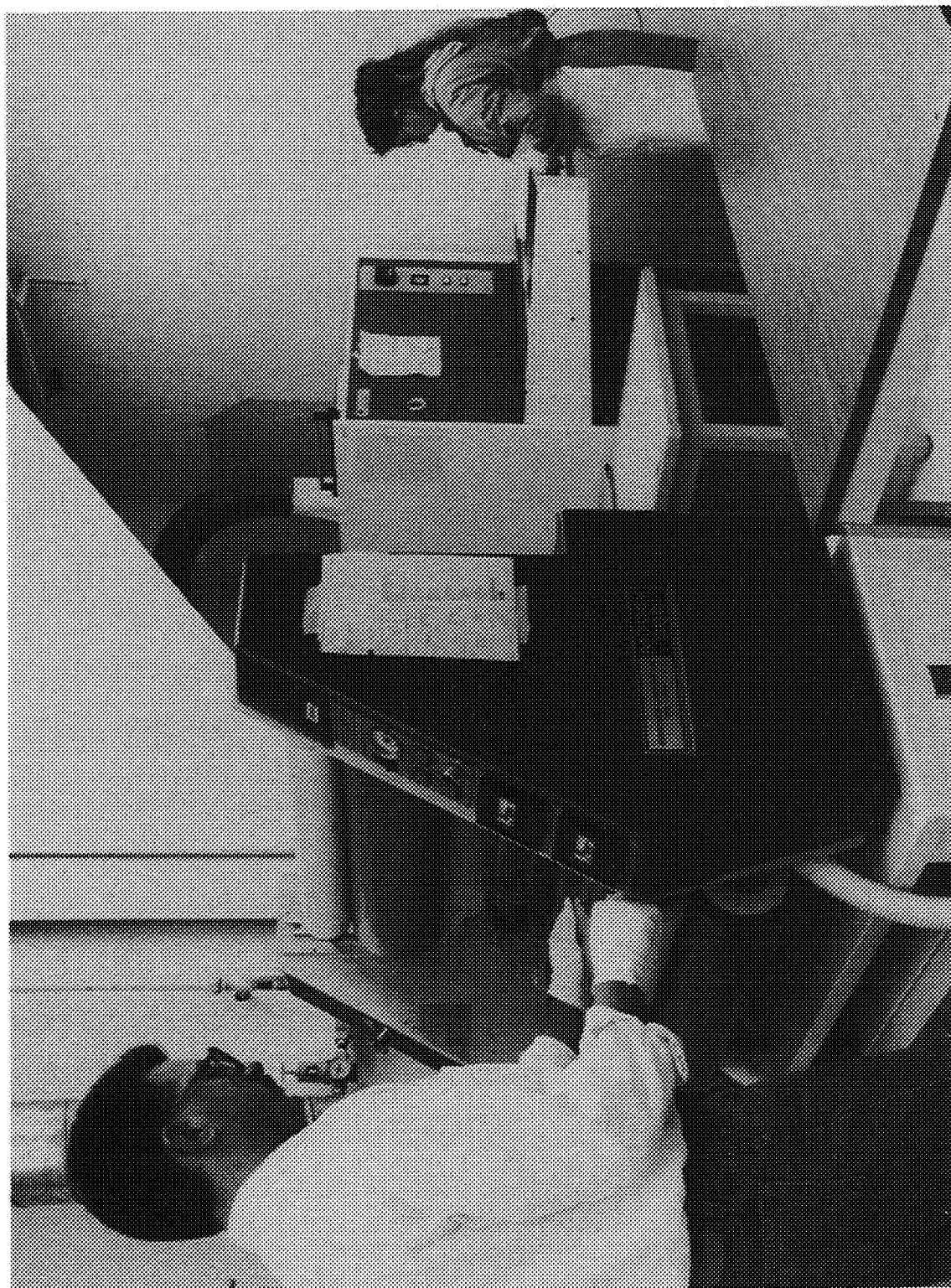


Figure A-7. Film Photo Resist

ORIGINAL PAGE
BLACK AND WHITE PHOTOGRAPH



Figure A-8. Both Sides of Prepared Platelets are Exposed

Exposed, developed platelets are supported horizontally on conveyor rollers in the etch machine (Figure A-9). Temperature and chemical concentration controlled acid sprays are applied to both sides of each platelet to maintain a uniform etching environment.

After forming all features platelets leave the etch machine and are rinsed to stop chemical action and remove residual photoresist. A partial set of completed formed platelet liner platelets are shown in Figure A-10. Platelets are then sent to the inspection station. Computer aided inspection techniques allows 100% inspection and measurement of critical features (Figure A-11).

After inspection completed platelets are cleaned, and if necessary flash-coated with a bond aid material (Figure A-12). Platelets are stacked under clean room conditions to prevent particle contamination of the intricate flow passages (Figure A-13). Stacked assemblies are then diffusion bonded under heat and pressure, either in a press (Figure A-14) or by hot isostatic press (HIP) techniques. Completed parts (Figure A-15) are post-processed to remove identification tabs, stacking pin holes and supporting flashing. Further processing may include additional machining, welding fittings or forming (Figure A-16).

ORIGINAL PAGE
BLACK AND WHITE PHOTOGRAPH

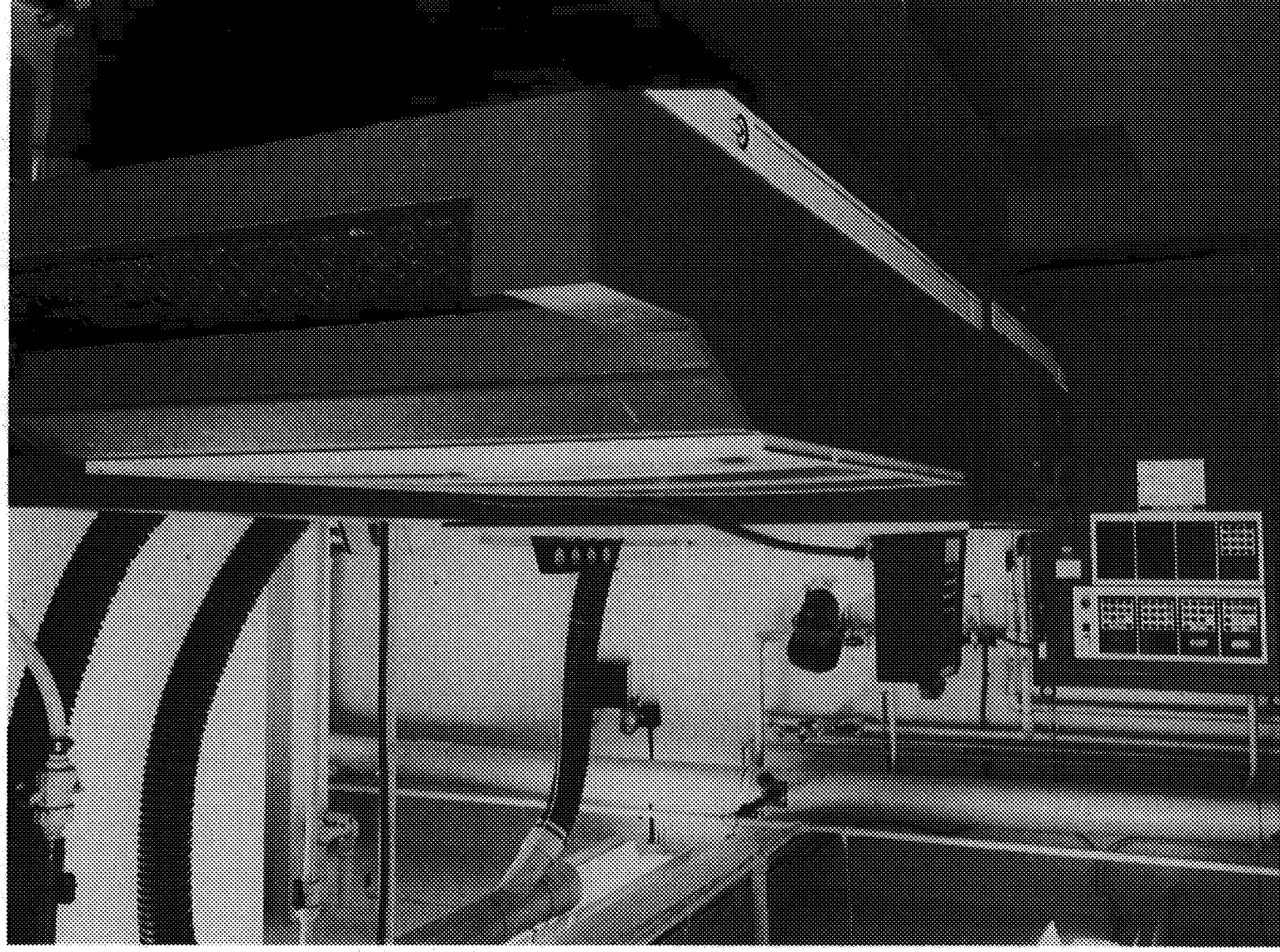


Figure A-9. Platelets are Supported Horizontally then Etched By Controlled Acid Sprays on Both Sides

ORIGINAL PAGE
BLACK AND WHITE PHOTOGRAPH

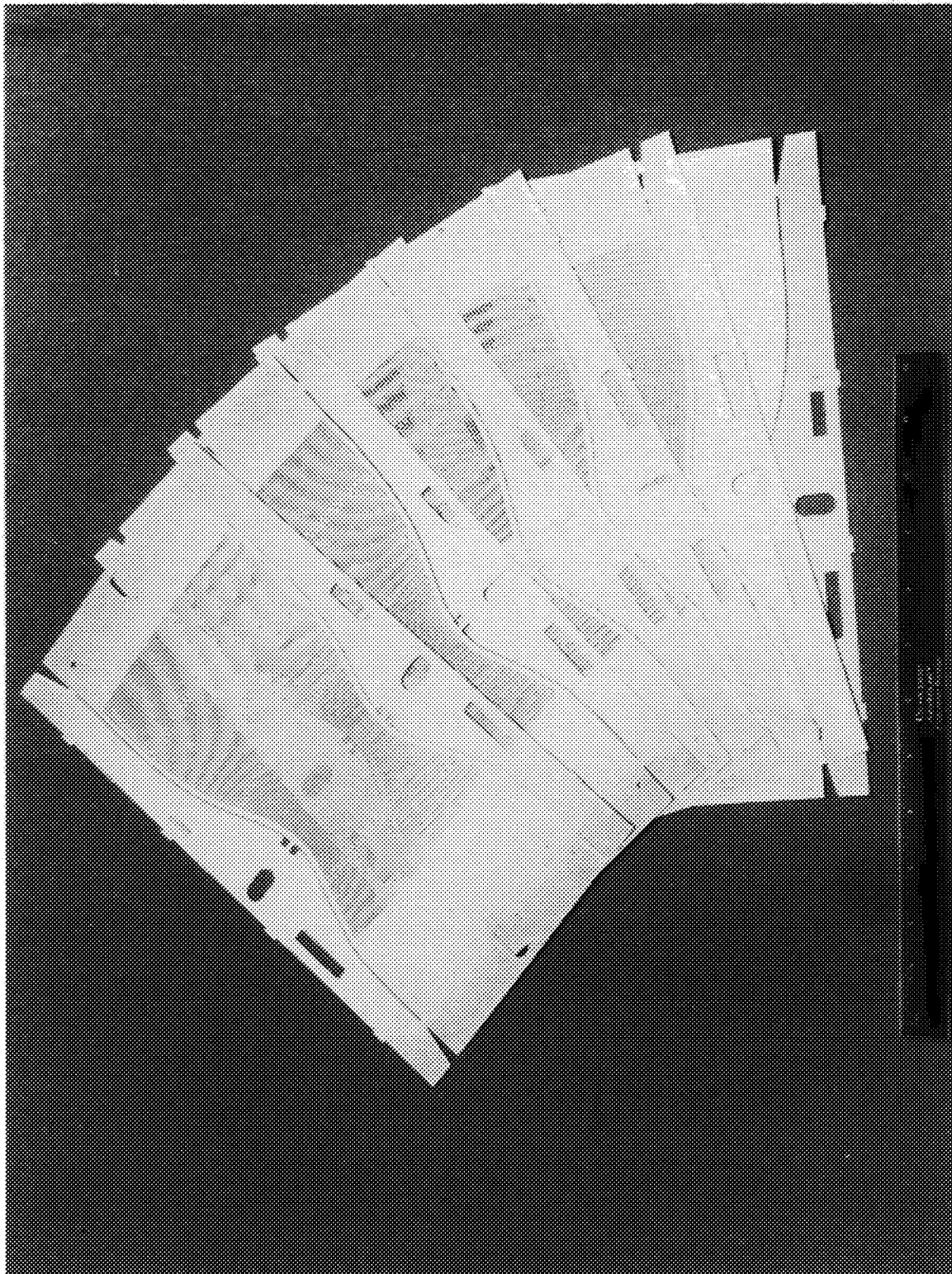


Figure A-10. Formed Platelet Combustor Liner Platelets and Panel

ORIGINAL PAGE
BLACK AND WHITE PHOTOGRAPH



Figure A-11. Computer Aided Inspection Techniques Allows 100% Inspection of Critical Dimensions

ORIGINAL PAGE
BLACK AND WHITE PHOTOGRAPH

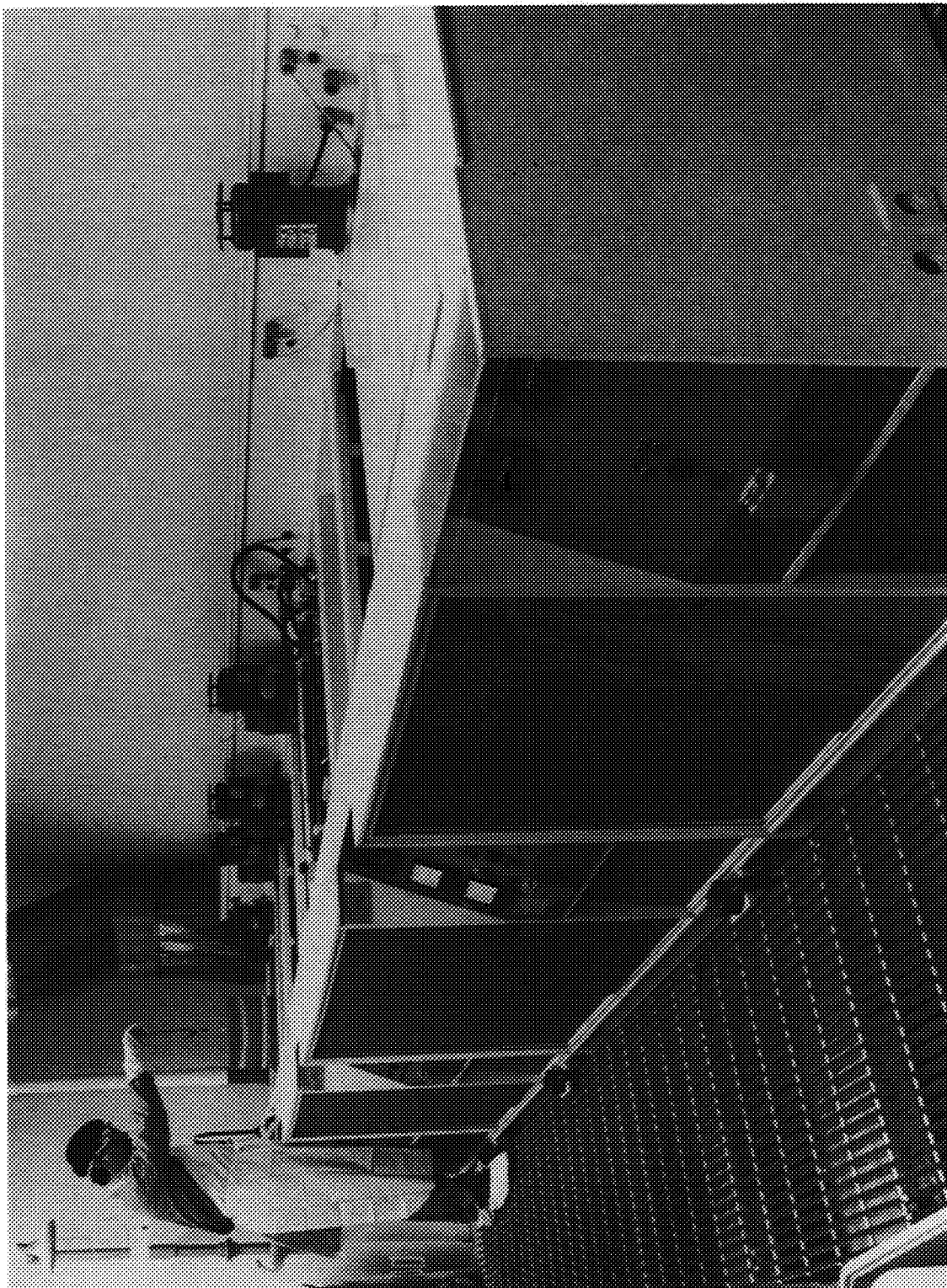


Figure A-12. Inspected Platelets are Cleaned Before Stacking

ORIGINAL PAGE
BLACK AND WHITE PHOTOGRAPH

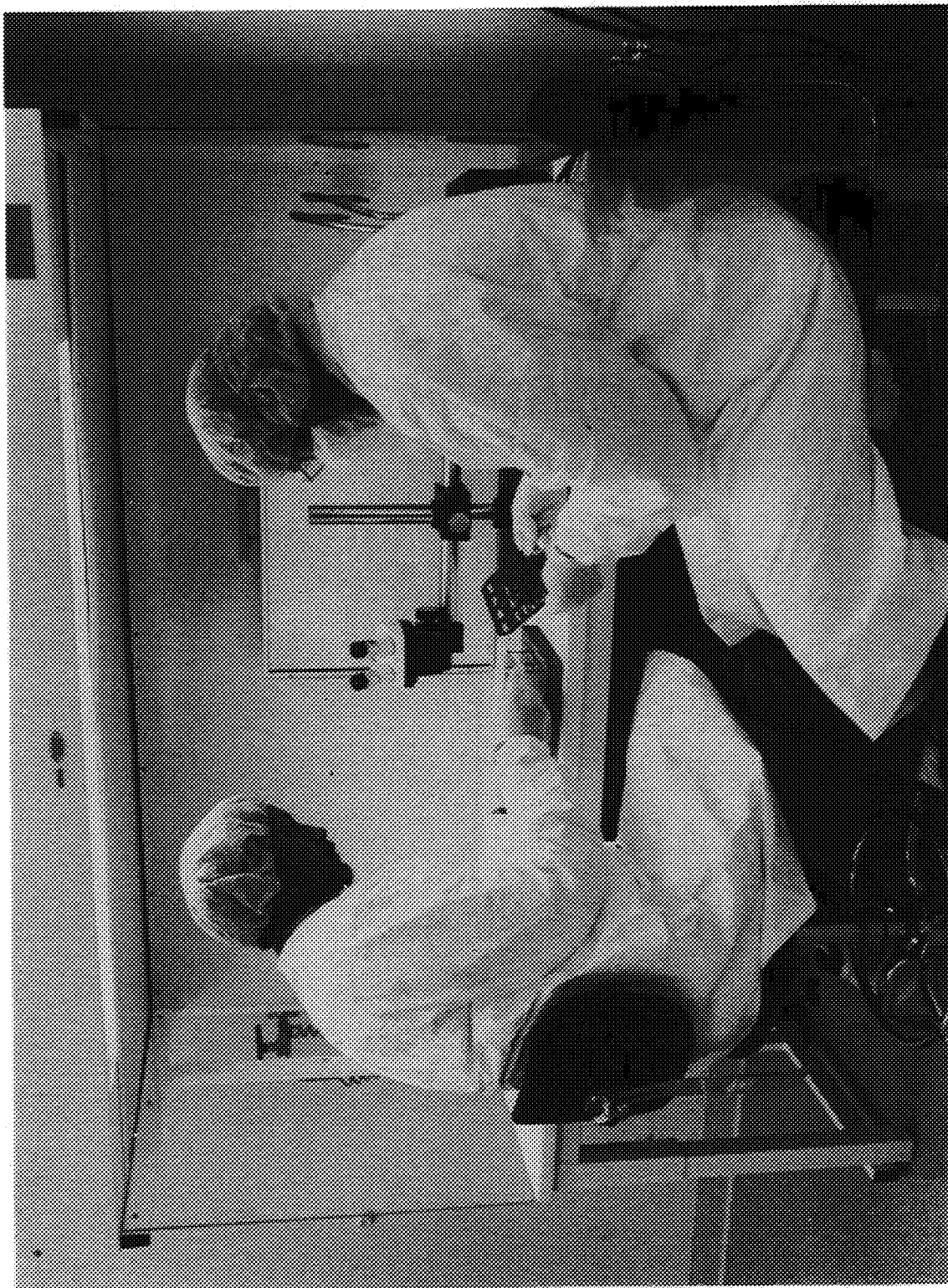


Figure A-13. Completed Platelets are Stacked Under Clean Room Conditions

ORIGINAL PAGE
BLACK AND WHITE PHOTOGRAPH

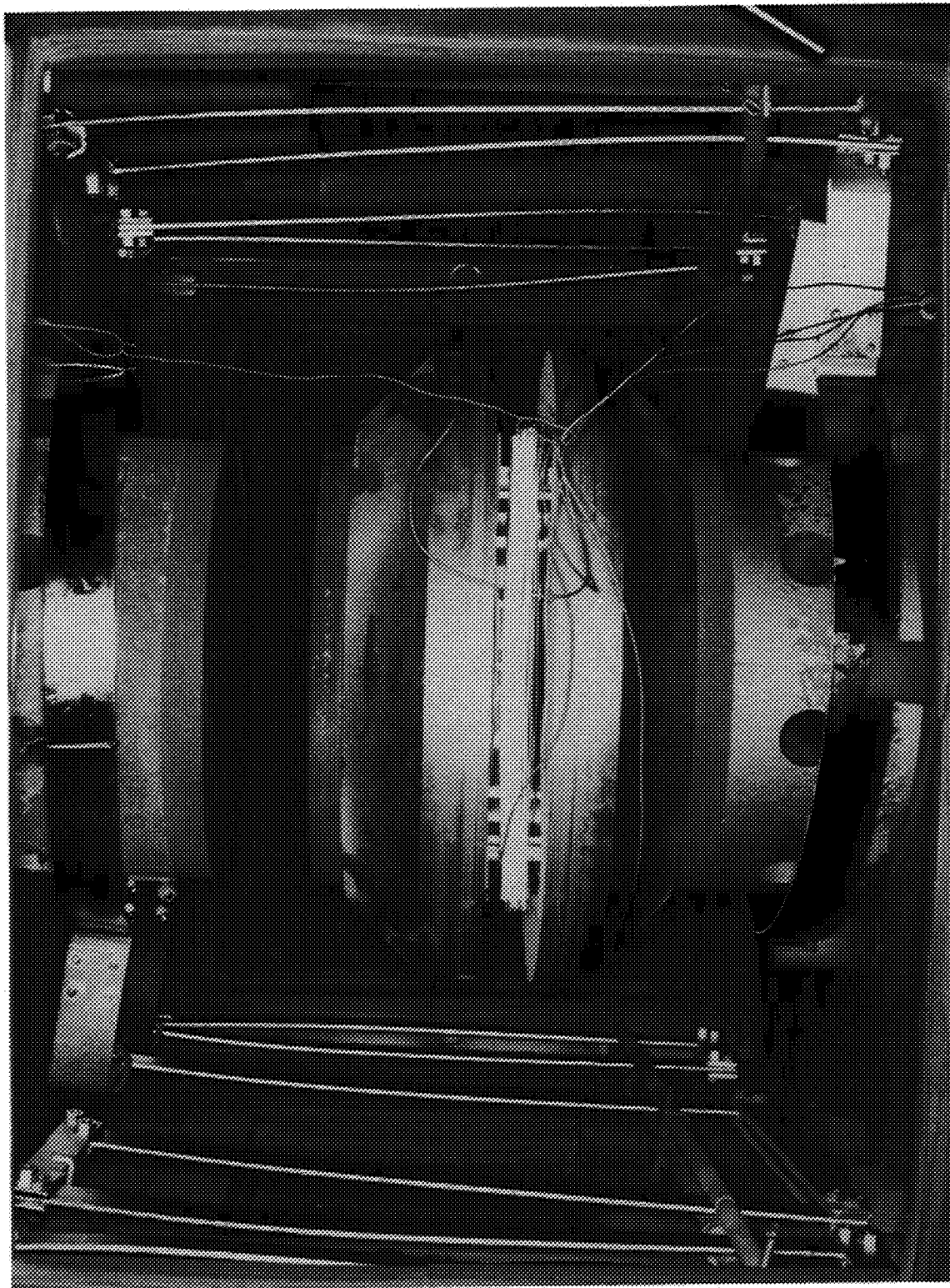


Figure A-14. Diffusion Bonding Furnace Applies Heat and Pressure to Platelet Stacks

ORIGINAL FILE
BLACK AND WHITE PHOTOGRAPH

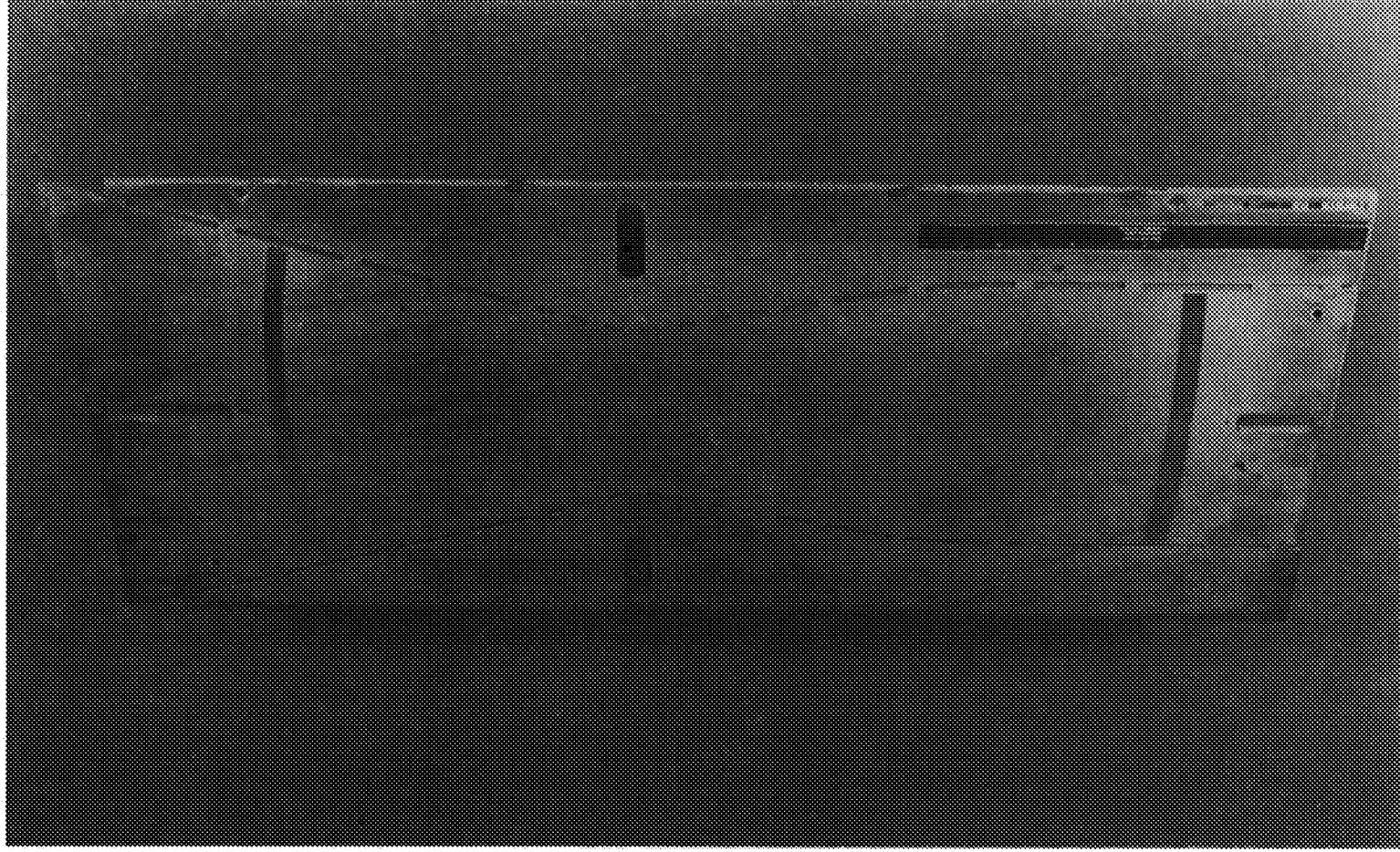


Figure A-15. Formed Platelet Combustor Liner Platelets and Panel

ORIGINAL PAGE
BLACK AND WHITE PHOTOGRAPH



Figure A-16. Completed Subscale Formed Platelet Liner

